UNIVERSITY OF LONDON THESIS

Degree PhD Year 2007 Name of Author JAIN, Shu

COPYRIGHT

This is a thesis accepted for a Higher Degree of the University of London. It unpublished typescript and the copyright is held by the author. All per consulting this thesis must read and abide by the Copyright Declaration below.

COPYRIGHT DECLARATION

I recognise that the copyright of the above-described thesis rests with the a and that no quotation from it or information derived from it may be published wi the prior written consent of the author.

LOANS

Theses may not be lent to individuals, but the Senate House Library may le copy to approved libraries within the United Kingdom, for consultation solely o premises of those libraries. Application should be made to: Inter-Library Lo Senate House Library, Senate House, Malet Street, London WC1E 7HU.

REPRODUCTION

University of London theses may not be reproduced without explicit w permission from the Senate House Library. Enquiries should be addressed t Theses Section of the Library. Regulations concerning reproduction vary acco to the date of acceptance of the thesis and are listed below as guidelines.

A. Before 1962. Permission granted only upon the prior written consent o author. (The Senate House Library will provide addresses where possible)

B. 1962-1974. In many cases the author has agreed to permit copying completion of a Copyright Declaration.

C. 1975-1988. Most theses may be copied upon completion of a Copy Declaration.

D. 1989 onwards. Most theses may be copied.

This thesis comes within category D.

☑ This copy has been deposited in the Library of University Col

☐ This copy has been deposited in the Senate House Library, Senate House, Malet Street, London WC1E 7HU.

Doctoral Thesis

Discovery and characterization of LRRK2: Gene Responsible for PARK8-linked Parkinson Disease

Shushant Jain

UNIVERSITY COLLEGE OF LONDON

January 2007

A thesis submitted to the University of London for the degree of Doctor of Philosophy

Institute of Neurology

Reta Lila Weston Institute Of Neurological studies

Laboratory of Neurogenetics

ProQuest LLC
789 East Eisenhower Parkway
P.O. Box 1346
Ann Arbor, MI 48106-1346

Declaration

I, Shushant Jain, confirm that the work presented in this thesis is my own. Where information has been derived from other sources, I confirm that this has been indicated in the thesis

ABSTRACT

Parkinson disease (PD) is an incurable movement disorder clinically characterized by resting tremor, bradykinesia and other cardinal features. A Japanese kindred with autosomal dominant PD showed linkage to a novel locus on chromosome 12p11.2-q13.1, subsequently given the designation PARK8. A British family showed linkage to the same region on chromosome 12, encompassing PARK8, with a maximal LOD score of 3.55. Genes within a 1-LOD support interval were subsequently prioritized for sequencing. A tyrosine to cysteine substitution at amino acid 1699 (Y1699C) that segregated with disease in the British family was discovered in the gene LRRK2. Subsequent studies demonstrated that mutations within LRRK2 are the most common genetic cause of PD, accounting for approximately 2-3% of apparently sporadic PD, 7-8% of familial PD and as much as 40% of PD in North African Arabic populations.

LRRK2 is large protein consisting of multiple protein interaction motifs as well as GTPase and kinase domains. Analysis of LRRK2 suggests it is largely cytoplasmic and mutations within LRRK2 increase aggregation formation, kinase activity and neuronal toxicity. Further investigation indicates LRRK2 is able to self interact, forming at least a dimer and may represent a potential mechanism for the aggregation of LRRK2.

LRRK2 also interacts with fasciculation and elongation factor zeta 2 (FEZ2), a mammalian orthologue of the Caenorhabditis elegans UNC-76 protein, which is involved in the axonal outgrowth and synaptic organisation. Although the function of LRRK2 is unknown, therapies directed towards LRRK2 are likely to have a great clinical impact and may bring us closer to understanding the pathogenic processes underlying PD.

TABLE OF CONTENTS

LIST OF FIGURES

LIST OF TABLES

LIST OF ABBREVIATIONS

3MT	3-METHOXYTYRAMINE
AD	ALZHEIMER'S DISEASE
ADE	ADENINE
ADP	ADENOSINE 5'-DIPHOSPHATE
ADY	ACTIVATION DOMAIN
AOO	AGE OF ONSET
AR	AUTOSOMAL RECESSIVE
ARJP	AUTOSOMAL RECESSIVE JUVENILLE PARKINSONISM
ARM	ARMADILLO
ATM	ATAXIA TELANGIECTASIA MUTATED
ATP	ADENOSINE TRIPHOSPHATE
ATR	ATAXIA-TELANGIECTASIA- AND RAD3-RELATED
BSA	BOVINE SERUM ALBUMIN
CAT	CHLORAMPHENICOL TRANSACETYLASE
CBD	CORTICAL BASAL DEGENERATION
CEPH	CENTRE D'ETUDES DU POLYMORPHISME HUMAIN
cM	CENTIMORGAN
CO-IP	CO-IMMUNOPRECIPITATION
COR	C-TERMINAL OF ROC DOMAIN
D2	DOMPAMINE RECEPTOR TYPE 2
DAT	DOPAMINE TRANSPORTER
dATP	2'-DEOXYADENOSINE 5'-TRIPHOSPHATE

DB	DNA BINDING DOMAIN
DLB	DIFFUSE LEWY BODY DISEASE
DMSO	DIMETHYL SULFOXIDE
DNA	DEOXYRIBONUCLEIC ACID
dNTPS	DEOXYNUCLEOTIDE TRIPHOSPHATES
DOPAC	DIHYDROXYPHENYLACETIC ACID
DTT	DITHIOTHREITOL
DZ	DIZYGOTIC
EBSS	EARLE'S BALANCED SALT SOLUTION
EDTA	ETHYLENEDIAMINETETRAACETIC ACID
EGF	EPIDERMAL GROWTH FACTOR
ETS	ELECTRON TRANSPORT SYSTEM
FCS	FETAL CALF SERUM
FRET	FLUORESCENCE RESONANCE ENERGY TRANSFER
GBA	GLUCOCEREBROSIDASE
GDP	GUANOSINE-5'-DIPHOSPHATE,
GDPβS	GUANOSINE 5'-O-2-THIODIPHOSPHATE
GPi	GLOBUS PALLIDUS INTERNA
GTP	GUANOSINE-5'-TRIPHOSPHATE,
GTPγS	GUANOSINE GAMMA THIO-PHOSPHATE
HIS	HISTIDINE
HWE	HARDY WEINBERG EQUILIBRIUM
IBR	IN BETWEEN RING FINGER DOMAIN

IN	INPUT
IP	IMMNUOPRECIPITATION
KD	KINASE DEAD
KDA	KILODALTON
LB	LEWY BODY
LD	LINKAGE DISEQUILIBRIUM
L-DOPA	LEVODOPA
LEU	LEUCINE
LIAC	LITHIUM ACETATE
LN	LEWY NEURITE
LOD	THE LOG OF THE ODDS RATIO
LRR	LEUCINE RICH REPEAT
LRRK2	LEUCINE RICH REPEAT KINASE 2
MAOB	MONOAMINE OXIDASE B
MB	MEGABASE
MPTP	1-METHYL-4-PHENYL-1, 2, 3, 6-TETRAHYDROPYRIDINE
MSA	MULTIPLESYSTEM ATROPHY
mtDNA	MITOCHONDRIAL DNA
MZ	MONOZYGOTIC
NaCl	SODIUM CHLORIDE
NADH	NICOTINAMIDE ADENINE DINUCLEOTIDE
NaF	SODIUM FLUORIDE
Na_3VO_4	SODIUM ORTHOVANADATE

NMR	NUCLEAR MAGNETIC RESONANCE
NP-40	NONIDET P-40
PBS	PHOSPHATE BUFFERED SALINE
PCR	POLYMERASE CHAIN REACTION
PD	PARKINSON DISEASE
PEG	POLYETHYLENE GLYCOL
PET	POSITRON EMISSION TOMOGRAPHY
PFA	PARAFORMALDEHYDE
PI3K	PHOSPHOINOSITIDE-3 KINASE
PMSF	PHENYLMETHYLSULPHONYLFLUORIDE
PSP	PROGRESSIVE SUPRANUCLEAR PALSY
RNA	RIBONUCLEIC ACID
ROC	RAS IN COMPLEX PROTEINS
ROCO	ROC (RAS OF COMPLEX PROTEINS)/COR (C-TERMINAL OF ROC
ROS	REACTIVE OXYGEN SPECIES
RT	ROOM TEMPERATURE
SDS	SODIUM DODECYL SULFATE
SN	SUBSTANTIA NIGRA
SNP	SINGLE NUCLEOTIDE POLYMORPHISM
SNpc	SUBSTANTIA NIGRA PARS COMPACTA
SNR	SUBSTANTIA NIGRA PARS RETICULATA
SUP	SUPERNATANT
TE	TRIS EDTA

TH	TYROSINE HYDROXYLASE
TRP	TRYPTOPHAN
tSNP	TAGGING SNP
UPS	UBIQUITIN-PROTEASOME SYSTEM
VTA	VENTRAL TEGMENTAL AREA
WD40	A PROTEIN BINDING MOTIF THAT CONTAIN ~7 REGIONS ~40 AA LONG CONTAINING A CONSERVED W & D

ACKNOWLEDGEMENTS

I am indebted to a number of people without whom this thesis would not have been possible.

First of all I would like to thank Professor Nicholas Wood, Professor Andrew Lees and Dr. Hardy for providing me with the opportunity to do my PhD.

I would like to thank Dr. Andrew Singleton and Dr. Mark Cookson, for teaching me the all that they know about neurogenetics and neuroscience. I am sorry for the pain I have inflicted over last 2 years and especially the last few months.

Thanks to all members of Reta Lila Western Institute of Neurological Studies; Dr. Rohan de Silva, Yvonne Welwa, Alan Pittman

Thanks to all members of the Molecular Neuroscience department at the Institute of Neurology especially Dr. Patrick Abou-Sleiman, Dr. Daniel Healy, Dr. Naheed Khan, Will Gilks for their help and company during the first part of PhD

Thanks to all members of the Laboratory of Neurogenetics, NIA, NIH; especially to Dr. Marcel van der Brug, Dr. Patrick Lewis, Jayanth Chandaran, Dr. Coro Paisan-Ruiz, Whitney Evans, Dr. Elisa Greggio, Alice Kaganovich, Janel Johnson, Dr. David Miller and Jeff Blackinton. Thank you all for your patience, friendship, knowledgeable discussions and making the lab an enjoyable place to be.

Finally I would like to thank my parents and sister for supporting me through my PhD and my life.

CHAPTER1: INTRODUCTION

Parkinson Disease (PD) was first described in 1817 by James Parkinson in his 'An Essay on the Shaking Palsy'[1]. In this paper, Parkinson described the clinical presentation of several individuals whose symptoms included shaking, slowness of movement and muscle stiffness [1]. In 1895, Brissaud reported lesions within the substantia nigra (SN) [2, 3] and, together with Meynert's previous observation [3, 4] that the basal ganglia is involved in abnormal movements, concluded that injury of this region was responsible for the motor symptoms of PD [3, 5]. This central observation was further emphasized by studies conducted by Tretiakoff, who discovered cellular damage in the SN of patients with post encephalitic parkinsonism [5, 6].

Nearly half a century later, in a co-operative effort between Carlsson, Ehringer and Hornykiewicz [7-11], dopamine was not only found to be a neurotransmitter within the brain, but deficient in the SN of PD patients. This led to the development of levodopa (L-dopa, metabolic precursor of dopamine) as a treatment for PD and this remains the most commonly used symptomatic treatment for PD.

PD affects approximately 5 million people globally [12-14], with a prevalence of 2% in persons older than 65 years of age. The primary risk factor for PD is aging, with incidence rising to approximately 4-5% by the age of 85 [15, 16, 17]. However, the contribution of other risk factors, such as environmental insults or genetic susceptibilities is less clear. For many years, it was believed that PD was primarily the result of environmental insult as several studies had recognized that individuals exposed to certain chemicals such as 1-methyl-4-phenyl-1, 2, 3, 6-tetrahydropyridine (MPTP) could develop a disease with parkinsonian features [18]. Further studies showed that a PD phenotype could arise from multiple different

etiologies including vascular insults, infections (Post-encephalitic parkinsonism caused by the influenza virus) and frontal lobe tumors [19, 20].

Research into PD was revolutionized when a genetic basis for PD was established with the identification of monogenic forms. Although genetic studies have highlighted biological pathways involved in PD, they have neither advanced our understanding of why the SN specifically degenerates, nor have they led to an effective treatment to halt the underlying progressive neurodegeneration.

CLINICAL CHARACTERISTICS OF PARKINSON'S DISEASE

PD belongs to a heterogeneous family of diseases referred to as parkinsonian syndromes [3, 21]. Within this group there are many diseases; progressive supranuclear palsy (PSP) [22, 23], diffuse Lewy body disease (DLB) [24, 25] and environmentally induced parkinsonism (exposure to MPTP and other pesticides) [18, 26]. A clinical diagnosis of PD requires the presence of tremor, rigidity and akinesia [27-29]. In addition, there are other criteria which must be fulfilled: i) No detectable cause (exposure to environmental toxins or infection) ii) No cerebella deficits iii) limited pyramidal signs iv) no lower motor dysfunction v) limited gaze palsy vi) minor autonomic deficits [28, 29]. The exclusion criteria limit the clinical diagnosis of PD and are meant to distinguish from other parkinsonian syndromes.

PD is a late onset disease, primarily occurring in the fifth or sixth decades [1, 3, 27], although some forms, particularly the recessive genetic diseases, can begin in childhood. Disease in individuals where a specific etiology is not known and where there is no clear family history of PD are classified as sporadic PD. The early symptoms of PD may be nonspecific, including mild depression and mood changes and subtle autonomic dysfunction.

Subsequently, an intermittent tremor can develop with asymmetrical rigidity, moving to the other side of the body within 3-5 years. Within five years, bradykinesia and postural instability ensue [30]. Many individuals also experience non-motor symptoms such as fatigue, depression, anxiety, sleep disturbances, constipation, bladder and other minor autonomic disturbances [3]. With prolonged disease duration there is a greater risk of dementia [31] perhaps reflective of the track and progression of neuronal loss in PD [32, 33]. At present, approximately 40% of patients experience cognitive impairment although the prevalence of dementia maybe underestimated [31, 34].

The average mortality rate in PD is approximately 1.5 times above the general population [35, 36]. On average, disease duration is 13 years, and the mean age at death is 73 years. The most common causes of death in PD patients are pneumonia through lack of activity, cardiovascular disease or severe injury through falling [30, 37].

PATHOLOGY OF PARKINSON'S DISEASE

The proximal cause for the movement disorder, and a pathological hallmark of PD, is the loss of neuromelanin-containing neurons in the substantia nigra pars compacta (SNpc) [32, 33] (Figure 1A). It is increasingly recognized that the pathology is not confined to the SNpc as non-dopaminergic systems, such as caudal brainstem nuclei (e.g., dorsal motor nucleus of the gloss-pharyngeal and vagal nerves) and anterior olfactory nucleus are also affected, perhaps significantly preceding dysfunction within the dopaminergic system [28, 32, 33].

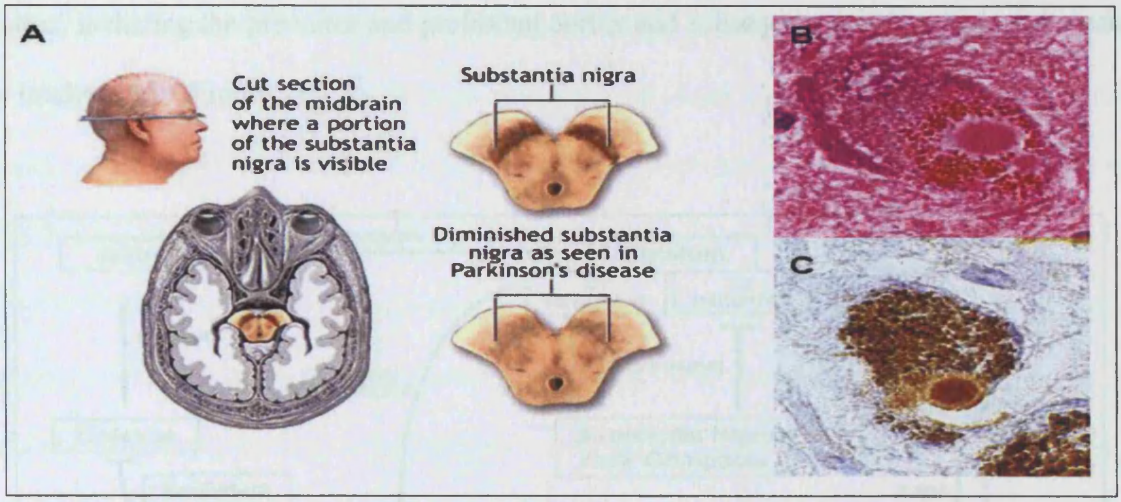

Figure 1: The pathological hallmarks of Parkinson disease: A) Loss of neurons in the substantia nigra underlies the clinical aspects of PD B) Typical Lewy body in PD: Hematoxylin and Eosin stain. C) Lewy body stained with anti-α-synuclein, the core component of Lewy bodies. (Pictures from (A) http://www.nlm.nih.gov/medlineplus and (B) www.saigata-nh.go.jp/.../neuropat/index.htm).

Release of dopamine from the nigral projections to the striatum [38-40] modulates activity by two pathways: the direct pathway mediated by the dopamine D1 receptor and the indirect pathway via the dopamine D2 receptor. The overall effect of striatal dopamine release is a reduction in basal ganglia output, leading to increased activity of thalamocortical projection neurons [40]. Voluntary movements are initiated at the cortical level of the motor circuit with outputs to brain stem, spinal cord, and multiple subcortical targets, including the putamen. Intermittent activation of the direct pathway by cortical inputs results in reduction of inhibitory basal ganglia output, disinhibition of thalamocortical neurons and facilitation of movement. By contrast, activation of the indirect pathway leads to increased basal ganglia output and to suppression of movement. In PD, loss of dopamine leads to increased activity of the subthalmic nucleus, with increased excitation of GPi/SNr neurons and greater inhibition of thalamocortical cells. This eventually leads to the decreases activation of the

cortex, including the premotor and prefrontal cortex and subsequent development of akinesia or bradykinesia (Figure 2) [41, 42].

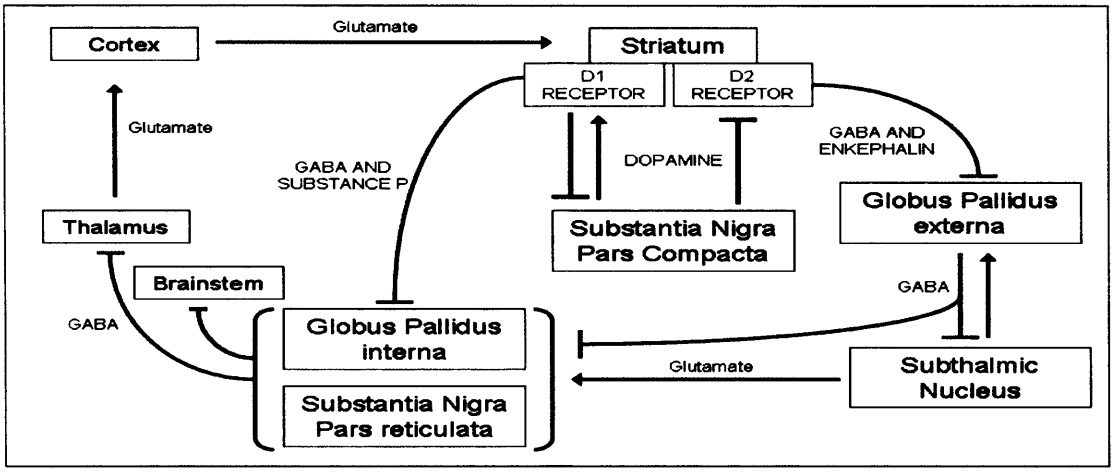

Figure 2: Neuronal pathways in the basal ganglia: The overall effect of striatal dopamine release is to decrease basal ganglia output, leading to increased activity of thalamocortical projection neurons. Lack of dopamine results in increased activity of globus pallidus interna and substantia nigra pars reticulate. This ultimately leads to disruption and inhibition of brainstem motor areas and thalamocortical motor system.

The dysregulation of the basal ganglia results in symptoms after 60-80% of the SN neurons are lost as remaining neurons are able to compensate by the sensitization of dopamine receptors and up regulation of various dopamine synthesizing enzymes, such tyrosine hydroxylase (TH) [43-45]. This implies that there is a substantial preclinical period in PD, perhaps of five to ten years, which is supported by functional imaging studies [45-49].

The second major pathological hallmark of PD are Lewy neurites (LN) or Lewy bodies (LB), discovered by Frederic Lewy in 1912 (Figure1B and 1C) [50]. These are insoluble inclusion bodies, which develop as spindle- or thread-like LNs in cellular processes, and in the form of

globular LBs in neuronal perikarya [51]. LBs are found in the surviving dopaminergic neurons of the SN, but can also be seen in noradrenergic neurons of the locus coeruleus, cholinergic neurons of the nucleus basalis of Meynert, dorsal motor nucleus of the vagus, spinal cord, and in the peripheral nervous system [33, 52]. LBs consist of a central dense core surrounded by a halo of 7-10-nm wide radiating fibrils, composed primarily of α-synuclein with various other proteins (e.g. ubiquitin, neurofilaments and heat shock proteins) [51].

Both of these key pathological hallmarks are important for the identification of PD and in the distinguishing of PD from other parkinsonian disorders. A pathological diagnosis of PD requires both loss of dopaminergic cells in the SN and the presence of LBs in surviving neurons in the presence of an intact striatum [30, 53, 54]. A term often used for a clinical syndrome that overlaps with PD but where there is no evidence of LBs, is parkinsonism.

ROLE OF ENVIRONMENT AND MITOCHONDRIA IN PD

There are different theories for the etiology of PD, which involves considering both environmental and genetic factors. Strong support for an environmental hypothesis of PD emerged in the 1980s, when drug addicts inadvertently self administrated MPTP [55]. This consequently led to a disease that was, apart from the age of onset, clinically indistinguishable from typical PD [55-58]. Pathological analysis revealed that these individuals developed pure nigral degeneration (preferential cell loss in the SNpc but relatively little loss of neurons in the locus coeruleus) without the formation of LBs [55, 59, 60].

As MPTP can induce clinical symptoms indistinguishable from PD, identifying its molecular target may provide an understanding of the molecular pathogenesis of the sporadic disease. MPTP is readily transported across the blood-brain barrier where it is converted to MPP^+ by

glial monoamine oxidase B (MAOB). MPP^+ is subsequently and specifically, taken up by the dopamine transporter (DAT) resulting in specific accumulation in DAT-positive SN neurons [26, 61, 62]. The mechanisms of MPP^+ toxicity primarily involves inhibition of the mitochondrial multi-enzyme complex I [59, 63], although adverse interactions between cytosolic enzymes and MPTP [61, 64] may also contribute.

Mitochondria are primarily responsible for the synthesis of adenosine triphosphate (ATP) via the electron transport system located in the inner membrane [65]. The electron transport system (ETS) is comprised of five complexes (Complex I-V) that transfer electrons between them to eventually reducing oxygen to form water. The reduction of oxygen also results in the production of excess protons in the cytosol, creating an electrochemical and pH gradient. Protons move from the cytosol into the mitochondria as result of the gradients, inducing the phosphorylation of adenosine diphosphate (ADP) to ATP via complex V of the ETS.

Complex I of the mitochondria is responsible for the transfer of electrons to ubiquinone and oxidation of NADH [65]. Inhibition of the process results in increased production of reactive oxygen species (ROS) [66] and decreased ATP production, which has several consequences for the cell:

1) ROS can lead to increased oxidative damage of both nuclear and mitochondrial DNA (mtDNA), as well as modification of multiple different proteins (e.g. DJ-1) [66], lipids and other biomolecules.
2) Lack of ATP may result in insufficient energy for essential cellular processes such as transcription, translation and protein turnover.

If the toxic insult continues, the cell is unable to repair itself and apoptosis can be induced by the formation of the mitochondrial permeability transition pores [65]. This leads to the loss of

mitochondrial membrane potential and release of factors such as Cytochrome C [65, 67] into the cytosol that can trigger caspase activation and apoptosis.

Many lines of evidence support a role of mitochondrial damage in the pathogenesis of PD. Complex I activity is systematically decreased in human PD brains [68, 69] and administration of MPTP to rats, mice and monkeys recapitulates many aspects of PD [61, 70]. Perhaps the most persuasive evidence comes from rats treated with rotenone, another complex I inhibitor [71]. These rats developed symptoms similar to PD and were responsive to L-dopa. Furthermore, they demonstrated selective neurodegeneration of the SN and formation of LB type pathology [71]. However, as complex I is reduced in several areas of the PD brain [68, 69, 72 73] and inhibition of complex I by rotenone is not specific to dopamine neurons, it is not clear if mitochondrial dysfunction alone is sufficient to cause nigral cell loss or PD [74-76].

Mitochondrial genome encodes for only 13 genes, with the remainder of mitochondrial components coming from nuclear encoded genes. Therefore, deficits in complex I and the selective vulnerability of SN neurons to mitochondrial toxins could potentially be explained by genetic mutations in nuclear and/or mitochondrial genes encoding mitochondrial components. A contribution of mtDNA mutations to the pathogenesis of PD has been suggested for several years [72, 77, 78]. Cells devoid of mitochondria (by exposure of host mitochondria to ethidium bromide) can be repopulated with mitochondria from PD patients to form cybrids (cytoplasmic hybrid) [77, 78] on a uniform nuclear background. This technique has demonstrated that the reduced complex I activity seen in PD can be transmitted stably into cybrid cell lines, which suggests that it may result from mutations in mtDNA [78]. Only recently have two studies implicated specific mutation of SN mitochondria as causes for impairment of cellular respiration, specific neuronal vulnerability and age dependent risk

associated with PD [79, 80]. Amplification of mitochondrial DNA revealed more somatic deletions within SN mitochondria than mitochondria from other brain regions [79, 80] and that deletions in SN mitochondria were higher in PD cases than controls [79]. By the age 70, nearly all the SN neurons had elevated levels of mtDNA deletions [79, 80], implying that these types of deletions might contribute to the age-dependent pathogenic processes seen in PD. However, why SN neurons have higher levels of mtDNA damage compared to other regions of the brain is unresolved. One hypothesis is the activities of TH, MAO and auto-oxidation of dopamine (formation of dopamine quinines) cause the formation of H_2O_2 [62, 81] (Figure 3). As a consequence, dopaminergic neurons have a higher basal oxidative burden than other neurons. This would cause higher levels of oxidative damage to biomolecules including mtDNA, thus increasing cellular susceptibility to toxic insults [82, 83 82] (Figure 3).

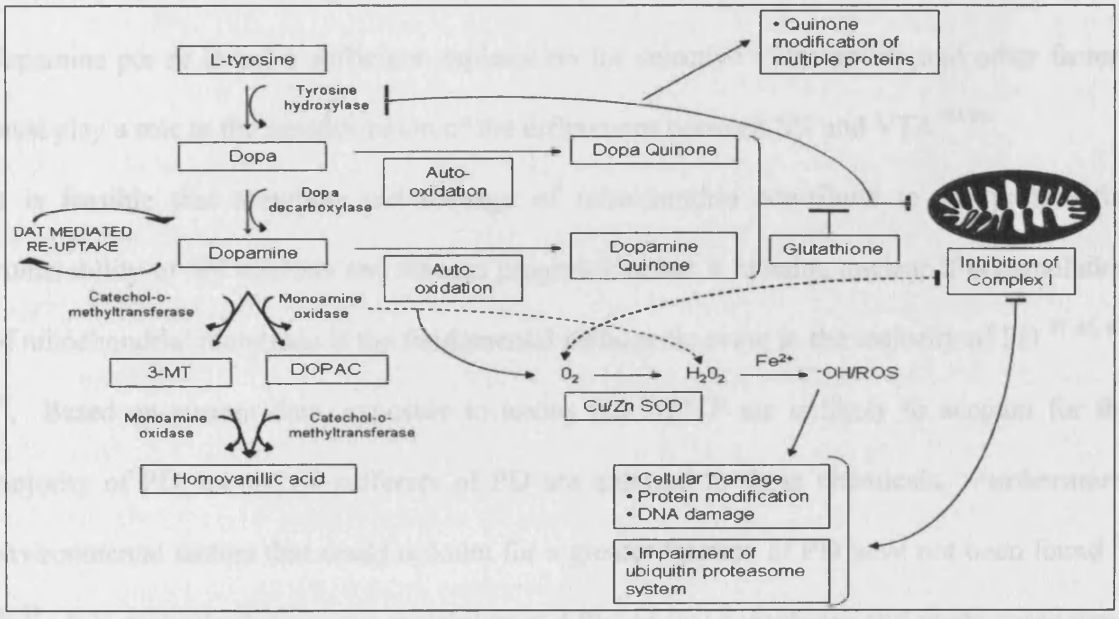

Figure 3 Mechanisms of neurotoxicity caused by dopamine synthesis and metabolism: Formation of dopamine quinones and breakdown of dopamine can lead to increased production of reactive oxygen species. Both free radicals and dopamine adducts can damage DNA, covalently modify proteins and

impair mitochondrial function leading to reduced ATP production and increased free radical formation. (ROS-reactive oxygen species, 3-MT-3-methoxytyramine, DOPAC-3, 4-dihydroxyphenylacetic acid, DAT-dopamine transporter)

There are several caveats to this hypothesis. Only one study [79] has shown an increase in SN mitochondrial deletions in cases compared to controls, thus larger studies are required are needed to determine if the difference is statistically significant.. From recent work, neuronal loss is not restricted to the SN [32, 33]. Therefore one needs to determine if mitochondria in other regions (e.g. caudal brainstem and anterior olfactory nucleus) suffer from significant levels of mitochondrial deletions. It is hypothesized that the environment created by dopamine synthesis and metabolism contribute to neuronal vulnerability. However, not all neurons of the dopaminergic system are affected in PD, with little or no neuronal loss observed in the ventral tegmental area (VTA) or retro-rubral field [32, 33, 62]. Therefore, dopamine per se is not a sufficient explanation for selective vulnerability and other factors must play a role in the determination of the differences between SN and VTA [84-86].

It is feasible that mutation and damage of mitochondria contribute to the preferential vulnerability of SN neurons and disease progression, but it remains unclear if accumulation of mitochondrial mutations is the fundamental pathogenic event in the majority of PD [87 65, 67, 88]. Based on current data, exposure to toxins like MPTP are unlikely to account for the majority of PD, as not all sufferers of PD are exposed to these chemicals. Furthermore, environmental factors that could account for a greater fraction of PD have not been found [61 20, 89]. It is probable that genetic variability at different loci contributes and predisposes some individuals to accumulating higher levels of mitochondrial mutations and damage, thus

leading to sufficient neuronal loss and clinical manifestation of disease. As a consequence, various strategies have been employed to identify the genetic causes of PD [90].

GENETICS OF PARKINSON'S DISEASE

Many diseases have a genetic component, whether it is due to inherited mutations or as a result of genetic variation controlling the response to environmental stresses such as viruses or toxins. The identification of the genetic causes of a disease allows one to isolate the primary pathogenic mechanism and/or contributors to a disease. The ultimate goal is to use this information to identify and develop new ways to treat, cure or even prevent the disease. Twin studies are a common method used to determine the relative contribution of genetics to disease in a population. This is performed by comparing concordance of disease in monozygotic (MZ) twins (who share all autosomal genes) and dizygotic (DZ) twins (who share, on average, 50% of autosomal genes). The theory of this technique is that if genetic factors are the primary cause of disease then concordance in MZ pairs will be higher, and on average double, when compared to DZ twins. Several PD twin studies have shown similar rates of concordance in MZ and DZ twin pairs, suggesting genetic predisposition plays a relatively minor role in disease [91-96]. However, there were many aspects of these studies that were criticized [47, 97-99]. Most of these studies were cross-sectional and did not follow individuals over time to exclude the possibility that disease may develop at a later date in individuals who were scored initially as unaffected. Recent evidence, based on positron emission tomography (PET) studies measuring [^{18}F]-6 fluorodopa (^{18}F-dopa) uptake, indicate that there may be decreased dopaminergic function even in the absence of signs and symptoms of parkinsonism in the asymptomatic twin of a PD patient [43-45, 48, 100]. Indeed

concordance rates have been reported to be three times higher in monozygotic compared to dizygotic twins using this outcome measure (58% vs. 18% respectively) [46]. These data indicate that the initial twin concordance studies may have underestimated the role of genetics in PD, but also suggest genetics is not the sole determinant of disease. These data are consistent with the more prevalent hypothesis, that the majority of typical PD cases are a result of a complex interplay between genetic variability, environmental exposures and stochastic factors [101]. However, it should be noted that there is a lack of definitive evidence for this model of disease risk as no environmental or genetic factors have been unequivocally established as underlying the majority of typical PD.

In contrast to twin studies, the analysis of multiple nuclear families or isolated populations has led to the identification of multiple genes and loci that cause Mendelian PD (autosomal recessive or dominant) or increase risk for PD (Table 1).

Locus	Protein Name	Inheritance pattern	Phenotype
PARK1 PARK4	*α-SYNUCLEIN*	AD	AOO ~ 40-50 years Features of dementia with Lewy bodies
PARK2	*PARKIN*	AR	AOO ~35 years Slow disease progression L-dopa responsive No Lewy bodies
PARK3	*UNKNOWN*	AD WITH REDUCED PENETRANCE	AOO~50 years Typical PD L-dopa responsive No pathology available
PARK5	*UCHL-1*	AD	AOO ~50 years Typical PD L-dopa responsive No pathology available
PARK6	*PINK1*	AR	AOO ~35-45 years Slow disease progression L-dopa responsive No pathology available
PARK7	*DJ-1*	AR	AOO ~ 30-40 years Slow disease progression L-dopa responsive No pathology available
PARK8	*LRRK2*	AD	AOO ~50 years Typical PD L-dopa responsive Variable pathology
PARK9	ATP13A2	AR	AOO ~ 16 years Levodopa-responsive parkinsonism with pyramidal degeneration, supranuclear gaze palsy, and dementia
PARK10	UNKNOWN	RISK FACTOR	AOO~50-60 years Typical PD No pathology available
PARK11	UNKNOWN	RISK FACTOR	AOO~50-60 years Typical PD No pathology available
PARK12	UNKNOWN	RISK FACTOR	AOO~50-60 years Typical PD No pathology available
Chromosome 5 (5q23)	UNKNOWN	RISK FACTOR	AOO~50-60 years Typical PD No pathology available

Table 1 Genetic Loci implicated in Parkinson's disease. Abbreviations: AOO; Average age of Onset, AR; autosomal recessive, AD; autosomal dominant

I. SNCA (PARK1; PARK4; α-synuclein)

The role of SNCA in PD became evident in 1997 when a mutation (A53T) within a Greek kindred was shown to cause autosomal dominant PD [102]. Subsequently, two additional missense mutations (A30P and E64K) [103, 104] have been identified as rare causes of disease, as have multiplications of the genomic segment containing the gene encoding α-synuclein [105-107].

Soon after the discovery of mutations in SNCA as the first genetic cause of PD, this protein was found to be the major component of LBs, the pathological hallmark of PD [108]. The study of this rare familial form of PD has relevance to idiopathic PD because the major deposited protein species in typical PD is encoded by a gene that when mutated results in PD. However, the pathology in individuals with SNCA mutations is not typical of idiopathic PD and is usually more widespread with LBs not only in the SN but throughout the cortex [109, 110]. Several patients have been described whose presentation is similar to diffuse Lewy body disease (DLB). The parkinsonian associated with SNCA mutations presents at a relatively early age (30s to 50s) and is rapidly progressive. In many cases, the disease in patients with SNCA mutations, progresses to include prominent dementia and hallucinations[111], likely a reflection of the extensive cortical pathology noted in these patients [111, 112].

Aggregates of α-synuclein define a series of disorders collectively referred to as synucleinopathies (e.g. DLB, multiple system atrophy (MSA) and Hallervorden-Spatz disease) [113-115]. Clinically these diseases can be distinguished from PD although they can present with parkinsonian features, such as rigidity [113]. Pathologically, the location and distribution of α-synuclein aggregates differs in each of these diseases [113]. For example, the primary aggregates in MSA are glial cytoplasmic inclusions [116]. The clinical and

pathological (α-synuclein positive aggregates and dysregulation of the basal ganglia–thalamocortical circuitry) overlap between these diseases may represent a spectrum of the same underlying patho-physiological mechanism. As a consequence, understanding how α-synuclein causes neuronal degeneration may aid our understanding of all these different diseases.

Much speculation remains about the physiological function of α-synuclein with many hypotheses regarding its role in the pathogenesis of PD. α-synuclein is part of a gene family including β and γ synuclein [117] [118-120], characterized by an imperfect 11-amino acid repeat of the consensus sequence KTKGEV at the N-terminus of the protein. Following this repetitive region, there are more variable regions in α-synuclein, such as a central hydrophobic core region and a negatively charged acidic carboxyl terminal [121]. α and β-synuclein are expressed at high levels in the brain [122] [123] while γ-synuclein is more abundant in the peripheral nervous system [120].

α-synuclein was initially cloned as a protein that was located at the presynaptic nerve terminals and therefore a role in maintaining or contributing to synaptic function was hypothesized [119, 122, 124]. This hypothesis was strengthened by the observation that α-synuclein can bind to acidic phospholipids [119, 125] at the synaptic junction, but its function at the synapse is not fully understood [126-128] [129]. In α-synuclein knockout mice there is a decrease in the numbers of undocked synaptic vesicles [127-129], suggesting a role in vesicle maintenance. α-synuclein may also be required for pre-synaptic activity dependent negative regulation of dopamine neurotransmission [127]. α-synuclein knockout mice show impairment of synaptic response to a prolonged train of repetitive stimulation capable of depleting docked and reserve pool vesicles [128]. However these deficits are generally small and in other

respects knockout mice develop normally, indicating α-synuclein is not critical for synaptic formation or function. However, since there is significant homology between the synuclein family members, functional compensation by β and γ synuclein may occur and knockout of all three might be required to define the endogenous functions of this protein family.

Because SNCA was the first gene implicated in PD and because its protein product is the major deposited species in the hallmark lesion of the sporadic disease, considerable efforts have been made to understand the pathophysiological process that results from mutation of α-synuclein. Initially, this work focused on the consequences of qualitative changes in α-synuclein (i.e. missense mutations A53T and A30P); however, with the discovery that overexpression of the wild-type α-synuclein, in the form of genomic multiplication, can result in PD [130], this has grown to include analysis of how quantitative changes in this protein can lead to disease. There are several lines of thought on the pathogenicity of α-synuclein mutations. Firstly, α-synuclein can aggregate under a number of different conditions [131]; α-synuclein can aggregate into oligomers that can then further develop into fibrils [131, 132]. The end product of α-synuclein aggregation is the formation of insoluble polymeric fibrils, which are thought to be the species that are deposited as LBs. This process is promoted by both the A53T mutation and overexpression of α-synuclein (Figure 4) [133, 134]. Fibrillar-aggregates of α-synuclein may themselves be directly toxic to cells, either inhibiting normal cellular processes such as protein trafficking and/or protein degradation by the proteasome and lysosome [112, 135]. Conversely, A30P slows the rate of fibril accumulation but increases the rate of α-synuclein oligomer (protofibril) formation [121, 136, 137]. Because of this and other data [137-140, 133] it is has been suggested that an oligomeric species, which are themselves relatively soluble, are the toxic species [121, 137, 140, 141].

The role of protein deposition into inclusion bodies in disease processes is unclear but may in fact represent a protective mechanism. Evidence for this hypothesis is emerging from recent work involving the Huntington (HTT) protein and P301L MAPT transgenic mice. As with α-synuclein, mutant forms of HTT aggregate but surviving neurons contain inclusion bodies, suggesting the formation of these structures aids in cell survival [142]. In P301L MAPT transgenic mice, induction of mutant TAU expression causes neuronal loss and behavioral impairment. When mutant TAU expression is turned off, cognitive abilities improve and no further neuronal loss is observed. However TAU continues to accumulate suggesting that soluble TAU aggregates do not result in neuronal cell death [143]. Animal models of α-synuclein support the hypothesis that fibrillisation of α-synuclein may actually protect against PD [133, 144]. In transgenic mouse models over-expressing or mutant (A30P or A53T) human α-synuclein, do not contain fibrillar α-synuclein inclusions [145, 146] and exhibit neuronal loss, while fibrillar inclusion formation can occur in transgenic Drosophila, without neuronal cell loss [144, 147 148].

α-synuclein inclusion formation is associated with phosphorylation at Ser-129 and it is this species that is primarily deposited in LBs [149]. Altering this residue to either prevent or mimic phosphorylation, suppresses or enhances α-synuclein toxicity respectively in Drosophila transgenic models [150]. The phosphorylation status of α-synuclein is not only correlated with its toxicity, but appears to prevent its aggregation. As increased toxicity appears to be associated with reduced numbers of inclusion bodies, this observation also suggests that inclusion formation may be protective [150, 151].

As the formation of α-synuclein fibrillar-aggregates may be protective, other mechanisms of cell death mediated by mutation and over-expression of α-synuclein intermediates [152 153 154]

have been suggested. α-synuclein protofibrils have the ability to form pores-like structures [133] which can cause leakage of vesicles [141] . Furthermore, PD associated mutations are able to increase the permeabilizing activity of α-synuclein by increasing protofibril formation. The subsequent binding and formation of pores in the mitochondrial or vesicular membranes [155] or at the cell surface, could lead to disruption of numerous cellular activities and cell death [135, 155-157,] .

Mutation or overexpression of α-synuclein may also impair the 26S proteasome [158-160 161, 162]. The 26S proteasome is part of the ubiquitin-proteasome system [163 160], responsible for the intracellular degradation of ubiquinated proteins. The proteasome itself is a barrel shaped multi-protein complex, composed of a 20S core protease unit and two 19S regulatory units. Ubiquinated proteins dock on the 19S cap and unraveled in an ATP-dependent process. Once unraveled, proteins are degraded into 3-25 amino acid peptides which are subsequently released. Mutant forms of α-synuclein are more resistant to degradation by the 26S proteasome [164, 165] and thus impairment of the proteasome by too much or mutant α-synuclein [166] could result in the accumulation of potentially cytotoxic abnormal proteins [162, 165]. The accumulation of these proteins could subsequently lead to mitochondrial damage, up-regulation of pro-apoptotic factors [167] and impairment of other crucial cellular processes [155, 156, 158, 166].

The potential mechanisms of α-synuclein toxicity described above may not be mutually exclusive. Damage to cellular membranes, such as the mitochondrial membrane may result in the increased production of ROS and decrease in ATP production. As a consequence, α-synuclein may be modified, which promote its aggregation [66, 150, 153, 168-170], and impairment of the proteasome through lack of ATP [163, 171, 172]. Conversely, α-synuclein may impair the

proteasome, leading to the accumulation of cytotoxic proteins, mitochondrial damage and general perturbation of cellular processes. Further work is needed to discern how α-synuclein causes toxicity.

II. PRKN (PARK2; PARKIN)

The gene (PRKN) encoding PARKIN was the first to be identified with mutations that underlie autosomal recessive juvenile parkinsonism (ARJP) and represents the most common known cause of early onset parkinsonism [173]. PRKN mutations account for approximately 50% familial cases where the age of onset is below 40 years [174, 175] but are less common in patients with older ages of onset.

The clinical picture of PRKN linked disease is distinct from typical PD, as patients commonly present with young age of onset (<40 years), dystonia, hyper-reflexia, slow progression, more symmetrical onset and early complications from L-dopa treatment [21, 176 177]. The symptoms associated with PRKN linked disease may represent a separate clinical entity from typical PD [178, 179]. However, an accurate diagnosis of PRKN linked disease cannot be based only clinical manifestation of the disease [180], as affected individuals can present with symptoms clinically indistinguishable from idiopathic PD in cases with a later age of onset [181]. Patients survive an average of 10 to 20 years [182, 183].

Despite the relative abundance of PRKN linked cases, there is a paucity of neuropathological data from patients with disease unequivocally caused by PRKN mutation. A key question is the role of LB pathology in PRKN linked disease. While the majority of reports indicate a lack of LB pathology, more recent studies have suggested α-synuclein positive LBs may be a feature of this disease [184, 185 181]. Despite the questions remaining about LB pathology in

PRKN linked disease, there is certainly degeneration and dysfunction of the dopaminergic neurons and as such, establishing the mechanism of the preferential vulnerability of this neuronal system in PRKN linked disease is likely to be directly relevant to typical PD [184, 185].

PARKIN contains an N-terminal ubiquitin-like homology (UBL) motif and two RING finger motifs separated by an in-between RING (IBR) finger domain at the C terminus [178, 186]. The presence of these motifs, suggested PARKIN was a component of the ubiquitin proteasome system. Further work confirmed and identified PARKIN specifically as an E3 ubiquitin ligase [187], which is responsible for the addition of ubiquitin molecules to specific target proteins, that are subsequently recognized by the proteasome and degraded [188, 189].

The ubiquitin-proteasome (UPS) mediated degradation pathway is involved in a variety of important intracellular processes such as cell cycle progression, removal of damaged/misfolded proteins and signaling cascades [160]. Ubiquitylation and the subsequent degradation of proteins, require the actions of three enzymes. Ubiquitin is initially activated in an ATP-requiring step by an activating enzyme, E1. Once activated, ubiquitin binds to E1 and transferred to the next enzyme, E2. These two proteins are essential in transfer of active ubiquitin to the final enzyme class E3, which is responsible for catalyzing (directly or indirectly) the transfer of ubiquitin to Lys residues on the target protein and is thus critical for substrate specificity. Polyubiquitin chains are formed by repeated cycles of ubiquitin addition and are usually degraded by the 26S proteasome complex (Figure 4) [160, 163].

As a consequence of the large deletions and multiple mutations throughout the gene, decreased PARKIN activity [121, 178, 186, 190] may lead to the accumulation of one or more of its substrates and subsequently to nigral cell death via impairment of the mitochondria [172, 191] and/or proteasome [152, 171]. Support for this hypothesis has come from transgenic flies over-

expressing PAEL-R and rats over-expressing CDCrel-1 [192, 193], both PARKIN substrates, where specific degeneration of dopamine neurons was noted [193, 194]. The phenotype could be rescued by over-expression of wild type but not mutant PARKIN [193, 194]. However, there is no accumulation of PAEL-R or other PARKIN substrates [195, 196] in PARKIN knockout mice. This is perhaps due to the redundancy in the ubiquitin proteasome system or may be because the substrates identified are not in vivo substrates [197]. In fact, PARKIN null mice show very mild impairments in behavior and dopaminergic transmission and metabolism [195, 196]. Further work is required to confirm PARKIN substrates in vivo and if they contribute to neurodegeneration in PD.

Although PARKIN null mice do not show accumulation of any of the identified substrates, they do show reduced levels of proteins involved in mitochondrial oxidative phosphorylation and protection from oxidative stresses [198, 199]. Knockout of PARKIN homologues from both mice and Drosophila cause decreases in mitochondrial respiratory capacity [198, 200] demonstrated by reduced lifespan, locomoter defects due to apoptotic cell death [191, 201] and male sterility due to spermatid individualization defects. It is unknown if PARKIN prevents apoptosis by inhibiting the release of cytochrome C [65, 191] apoptosis or indirectly, as PARKIN may ubiquinate and degrade components of the pro-apoptotic signaling cascade [202] (e.g. BAG5) and/or intracellular apoptotic stimuli (e.g. PAEL-R). How PARKIN maintains mitochondrial function and protects neurons is a critical question that remains unresolved. However, this is especially interesting as other genes mutated in PD (PINK1 and DJ-1) directly link mitochondria to neuronal loss.

III. DJ1 (PARK7)

DJ-1 mutations are found in young-onset autosomal recessive parkinsonism [203] but are the rarest known genetic cause of parkinsonism (<1-2% of familial PD) [204, 205]. Given the rarity of DJ-1 mutations there is limited clinical data and no pathological data available in DJ-1 linked patients [206] but DJ-1 does appear to localize to small percentage of LBs [207, 208]. The two families originally shown to have disease caused by DJ-1 mutation were from an isolated population in the Netherlands and a small family from Italy with consanguineous parents. The patients in these families presented with PD at a very early age and followed a relatively benign course [203]. Consistent with loss of function, DJ-1 is recessively inherited and one of the original families possessed a large deletion encompassing the start codon of DJ-1. Subsequently, multiple point and splice mutations have been described within DJ-1[206]. Although the current function of DJ-1 is unclear [121, 209-211], some mutations (e.g. L166P) destabilize DJ-1 [212-214] thus leading to increased degradation by the proteasome [212, 213, 215-217]. As a consequence there is insufficient DJ-1 which is hypothesized to increase neuronal vulnerability to toxic insult and apoptosis [215, 218-220].

Several hypothesizes exist as to how DJ-1 protects cells from toxic insult [87, 221]. DJ-1 is a 189 amino acid member of the ThiJ/PfpI/DJ1 super family, ubiquitously expressed [207, 222] and localizes to both the cytosol and mitochondria [215, 223] as well as the nucleus in dividing cells. Under oxidative stress conditions, such as exposure to paraquat or MPTP, DJ-1 undergoes an acidic shift in pI by modifying the side chain of cysteine 106 to form a sulfinic acid [215, 224]. This is correlated with the protein relocating from the cytosol to the outer mitochondria membrane [215, 219]. In support of this hypothesis overexpression of DJ-1 in culture can decrease sensitivity to specific stressors, such as paraquat and MPTP [215, 220, 225]. Conversely,

loss of DJ-1 in mice, cell culture and Drosophila models leads to increased sensitivity to oxidative stresses [219, 225-227]. Mutation (C106A) of the cysteine residue primarily modified in the presence of oxidative stresses [215] leads to the loss of protection conferred by DJ-1. Thus, oxidation of DJ-1 is an essential part of its protective function. In addition, increased oxidation of C106 has been confirmed in animal models exposed to oxidative stresses [219] and in sporadic PD patients [228] suggesting modification of this residue may also be related to disease pathogenesis.

DJ-1 only has a weak ability to scavenge free radicals and thus, DJ-1 is unlikely to primarily function as an anti-oxidant protein. Consequently, a role for DJ-1 as an oxidative stress sensor has been suggested [220, 224, 226]. DJ-1 may have an analogous role to the DNA damage sensing enzymes (e.g. ATM, ATR and RAD proteins) where specific enzymes recognize different types of DNA damage and are able to mediate the appropriate response (e.g. apoptosis, cell cycle arrest, transcription) [82]. As DJ-1 was cloned as part of a RNA protein binding complex [211, 213, 229], it is postulated that DJ-1 may control transcription and/or translation of particular RNA species in response to oxidative stress [230].

Alternatively DJ-1 has been shown to bind to numerous proteins [209-211, 222] such as DAXX [231], preventing it from activating the apoptotic pathway and decreasing cell sensitivity to oxidative stresses. However, many of these DJ-1 interactors still require validation in vivo, both to confirm the interaction and to establish that they play specific roles in DJ-1 mediated cell survival.

IV. PINK1 (PARK6; PTEN induced kinase 1)

Mutations in the gene PINK1, encoding PTEN induced kinase 1, were identified in four Italian families with recessive early onset PD [232]. Initial screens for PINK1 mutations in early-onset familial cases revealed that PINK1 mutations are a more common cause of young onset PD than DJ-1 mutations, but not as prevalent as PRKN mutations. PINK1 mutations are estimated to cause 4% of familial recessive PD [233-239].

The clinical course of individuals with PINK1 mutations resembles that of typical PD, except the age of onset is earlier (approx 35 - 45 years of age) and disease progression is slower. Similar to PRKN linked disease, dystonia at onset appears to be more frequent in individuals with PINK1 mutations [237, 240-242]. No pathology data is available from any PINK1 mutated cases [206] but PINK1 can localize with a small proportion (5-10%) of LBs in sporadic cases [243].

PINK1 is predicted to be a serine-threonine kinase that is targeted to the mitochondria [232]. Once PINK1 enters the mitochondria, the N-terminal mitochondrial targeting motif is cleaved. There is some evidence that the mature kinase can be redirected to the cytosol, although this data is largely derived from overexpression studies in cell culture and it is not clear if this is true in more physiologically relevant systems [244].

Although no substrates of PINK1 have been identified, the recessive nature of the disease and the presence of truncating mutations in PINK1-linked cases [232], suggest loss of kinase activity may result in cell loss [244, 245]. As PINK1 is a mitochondrial kinase and can protect cells against oxidative stresses such as paraquat and MPTP [232, 244] (Figure 4), PINK1 may phosphorylate multiple proteins to maintain mitochondrial function and inhibit apoptosis. In support of this observation, knockout of Drosophila PINK1 results in male sterility, apoptotic

muscle degeneration, defects in mitochondrial morphology and increased sensitivity to oxidative stress [246, 247].

As the phenotype associated with PINK1 knockout Drosophila is very similar to PARKIN knockout Drosophila [148, 201], Drosophila over expressing PARKIN were crossed with PINK1 knockout Drosophila [246, 247]. Surprisingly, PARKIN transgenic flies are able to rescue PINK1 null flies but the reverse is not true. Moreover, removing both PINK1 and PARKIN, results in identical phenotypes as PINK1 null flies, suggesting that PARKIN is downstream of PINK1. How PINK1 and PARKIN co-operate in the same pathway is unknown. Potentially, PINK1 may phosphorylate activators of PARKIN or may co-operate with PARKIN in clearance of particular substrates [218, 246-248]. Precedence for this idea is shown by the observations that phosphorylation of the amino terminus of p53 reduces its affinity for MDM2, an E3 ligase, thus decreasing the degradation of p53.

As mutations within PINK1 were only recently identified in PD, more work is needed to determine what the endogenous function of PINK1 is and how mutations within PINK1 can cause selective degeneration of the SN.

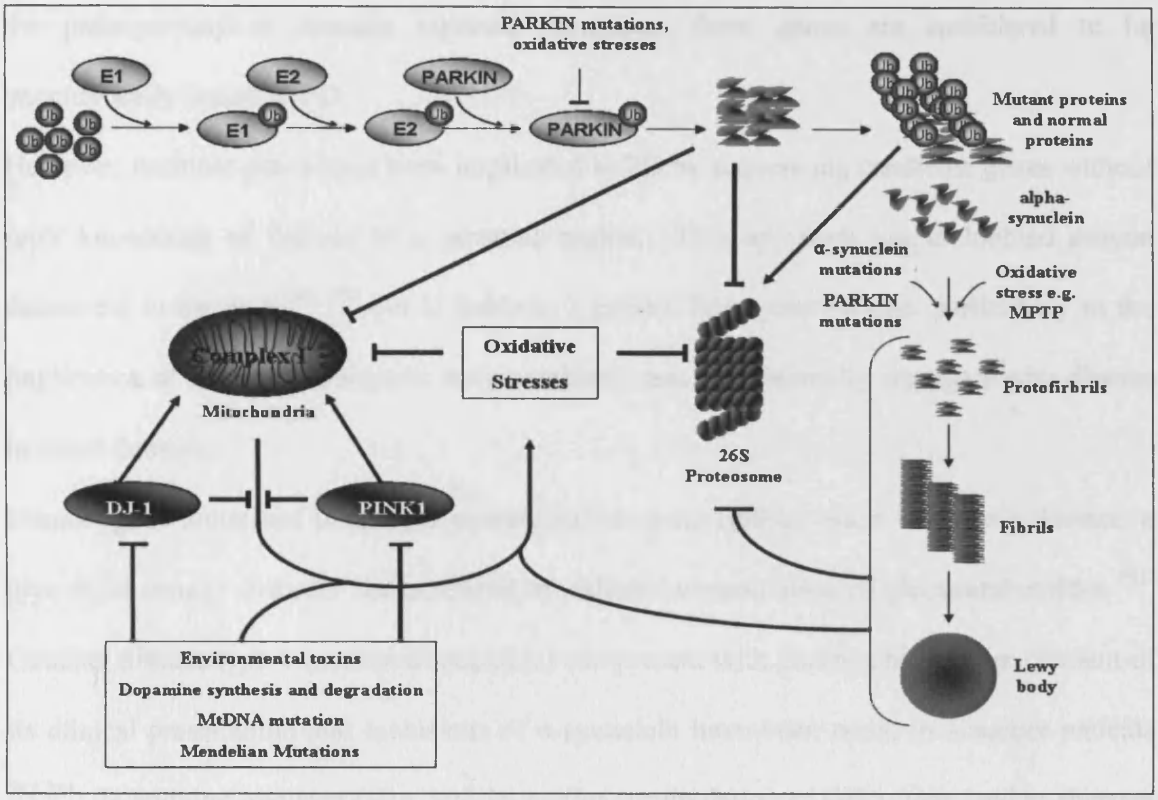

Figure 4: A proposed model for mechanisms of cellular toxicity in PD. PRKN mutations and oxidative stress can inhibit PARKIN mediated ubiquitination of specific substrates leading to their accumulation. These substrates may inhibit both the proteasome and mitochondria. The formation of α-synuclein protofibrils and aggregates can be toxic to both the mitochondria and proteasome. PINK1 and DJ-1 promote cell survival, either directly or indirectly by protecting mitochondria from oxidative stress.

V. NR4A2, SYNPHILIN-1, GLUCOCEREBROSIDASE (GBA), UBIQUITIN C-TERMINAL HYDROLASE L1 (UCHL1), OMI/HTRA2 AND PARK9: THEIR POTENTIAL ROLE IN PD

SNCA, PRKN, PINK1 and DJ-1 were identified through linkage analysis and subsequent sequencing of candidate genes within the linked region. Although questions remain about

the pathogenicity of specific reported mutations, these genes are considered to be unequivocally linked to PD.

However, multiple genes have been implicated in PD by sequencing candidate genes without prior knowledge of linkage to a genomic region. This approach has undoubted proven successful in the past [249, 250] but is liable to a greater false positive rate, particularly in the implication of rare non-pathogenic polymorphisms that coincidentally segregate with disease in small families.

Homozygous mutations in the glucocerebrosidase gene (GBA) cause Gaucher's disease, a glycolipid storage disorder characterized by cellular accumulation of glucocerebrosides [251]. Gaucher disease type-1 (non-neuronopathic) can present with parkinsonism as an element of its clinical presentation and inclusions of α-synuclein have been noted in Gaucher patients [252-254]. In addition, reduced GBA activity and/or accumulation of GBA, may lead to aberrant protein degradation by the lysosomal pathway, specifically α-synuclein [255], as it too can be degraded by the lysosome.

Thus GBA was screened for six common gene mutations in 99 Ashkenazi Jewish patients with PD and 1543 controls. 31% of the PD group carried mutations (almost all were heterozygous) compared to 6% of controls [256-259]. The authors concluded that heterozygous mutations in this gene predisposed individuals of Ashkenazi Jewish population to PD. This finding has not been consistently replicated in the general population therefore the relevance to PD is questionable [260, 261]. GBA mutations within the Ashkenazi Jewish population probably arose as a founder event and as this population was relatively isolated and homogeneous, these variants have been enriched leading to their increased prevalence. Thus, it is possible that GBA is a risk factor for PD in the general population but at a much lower

frequency compared to Ashkenazi Jews. Larger case control studies would therefore be required to detect a significant genetic affect [262].

Mutations in UCHL-1, PARK5, were initially described in single affected German sib pair with a family history compatible with autosomal dominant PD, although the transmitting father was asymptomatic, suggesting incomplete penetrance of the mutation [263]. The clinical features were typical of idiopathic PD, however, the age of symptom onset (49 and 51 years) was marginally younger [263]. UCHL-1 has a plausible biological role in PD as it is a neuron specific protein that may have dual functions as an ubiquitin hydrolase and an ubiquitin protein ligase [264-266], potentially placing UCLH-1 in the same pathway as PARKIN [264]. Despite extensive screening, no further mutations in UCLH-1 have been described [264, 267-271]. Several groups have also analyzed a S18Y polymorphism within UCHL-1 as a risk factor for sporadic PD. Initially, this polymorphism appeared to be protective against PD as it was over-represented in controls compared to PD cases [272]. In support of this finding, S18Y appeared to enhance the hydrolase activity of UCHL-1 increasing the availability of ubiquitin for proteolytic degradation of substrates [273] and preventing the accumulation of potentially toxic proteins. However genetic studies of the S18Y polymorphism in PD patients have been inconsistent [90, 264]. Some of the studies that suggested a positive effect of the S18Y polymorphism did not correct for population allelic frequency differences and deviations from Hardy Weinberg equilibrium [272, 274-279]. In addition the increased hydrolase activity associated with the S18Y polymorphism could not be replicated [280]. Therefore, the role of UCHL-1 in either sporadic or familial PD remains ambiguous.

Recently, a heterozygous mutation within OMI/HTRA2 (G399S) has been described in four individuals with PD and a polymorphism (A141S) has been associated with increased risk for

PD [281]. OMI/HTRA2 is a serine protease which can induce apoptosis by binding to inhibitor of apoptosis (IAP) proteins [282, 283]. OMI/HTRA2-knockout mice display parkinsonian phenotypes, including rigidity and tremor [284]. Striatal neurons are most susceptible but neurodegeneration progresses to the brain stem and spinal cord, including motor neurons [284]. OMI/HTRA2 does map to a locus implicated in PD (PARK3, Table 1) but no mutations were found in the original PARK3-linked families [285] and another mouse model harboring a point mutation (S276C), perhaps a better model of the heterozygous mutations observed in PD patients, has a more severe phenotype with weight gain, followed by ataxia, repetitive movements and akinesis [285]. Further work is needed to determine if mutations within OMI/HTRA2 are a cause and/or a risk factor for PD.

Heterozygous mutations have been described in both NURR1 [286] and SNCAIP1[287]. NURR1 is a transcription factor required for the differentiation of the midbrain neurons [288] and SYNPHILIN-1 may interact with both α-synuclein and PARKIN [289, 290]. Although both proteins may be involved in SN function or interact with other proteins implicated in PD, there have been no additional mutations discovered, leaving their pathogenicity uncertain.

For all five genes (UCHL-1, NURR1, SNCAIP1, OMI/HTRA2 and GBA) there has been no replication of the original study in independent populations and thus evidence for association is limited to the original families or populations. These genes may be involved in the SN function and/or regulation, but it is unclear if any of the genes have a genetic involvement in PD.

Kufor-Rakeb syndrome was originally described in an Arabic family [291] inheriting an autosomal recessive disease and subsequently given the designation, PARK9 [292]. This syndrome has many of the features associated with parkinsonian disorders, including

bradykinesia and response to L-dopa. However, the disease also has several other features such as spasticity, vertical gaze deficits and an early dementia that is distinct from the dementia seen in late PD patients. Therefore it has been suggested that Kufor-Rakeb syndrome is a disease where parkinsonism is part of the clinical spectrum [293] and that is not true PD.

The gene underlying PARK9 was recently cloned as the lysosomal ATPase, ATP13A2 [294] and together with the clinical overlap with Niemann-Pick disease Type C, suggest Kufor-Rakeb syndrome may be a lysosomal storage disorder [293]. As Kufor-Rakeb disease can present with parkinsonian features, it is unclear if it should be regarded as part of PD. It is not until pathological data is available that can one classify this disease, thus its relevance to the molecular pathways involved in PD are uncertain.

VI. RISK FACTOR LOCI

Immense progress has been made in the last eight years to understand and identify the genetic factors contributing to PD. Nevertheless, they account for <2% of total PD and therefore the etiology of the majority of PD remains elusive. To discover additional loci that either cause or contribute risk for disease, numerous population based approaches have been used.

Affected Sib pair analysis [295, 296] has implicated the presence of several loci contributing to genetic risk for PD. This method looks for genomic regions which are shared between affected siblings at an increased rate relative to the background sharing of alleles between siblings. The linkage peaks of two loci (on chromosome 2p13 – PARK3 and chromosome 5q23) have overlapped in at least three independent sib pair studies and merit further study

[297-303]. PARK11 and 12 [300, 304] have also been identified using this methodology, but linkage of these regions with increased risk for PD have yet to be replicated in independent PD populations [301, 305, 306]

An alternative approach to the affected sib-pair design is to use small genetically isolated populations. The principle is that individuals who have PD and are distantly related will share smaller chromosomal regions compared to individuals without disease and are closely related. This has been used very effectively by the biopharmaceutical company deCODE, who traced the genealogy of over 100,000 individuals from Iceland and identified a susceptibility locus for late onset PD on chromosome 1p32 (PARK10) [307]. This locus has been subsequently replicated in a different population [306, 308] suggesting that this susceptibility factor is not unique to PD patients of Icelandic origin, but the identity of the underlying gene change has not been resolved, leaving the locus uncertain [306, 309, 310].

VII. PARK8

In 2002, autosomal dominant PD within a large Japanese kindred from Sagamihara was linked to the pericentromeric region of chromosome 12 [311]. This region was given the designation PARK8. Further linkage of autosomal dominant PD in two families to PARK8 confirmed the locus and suggested that the gene could be a common cause of PD [312-314]. The aims of the studies reported in this thesis were to identify the gene responsible for PARK8 and, once identified, begin biological characterization of the protein product to understand its pathological role in PD.

CHAPTER 2: IDENTIFICATION OF GENE UNDERLYING PARK8-LINKED PD

INTRODUCTION

The PARK8 locus was originally described in a large multi-generational pedigree from Japan with autosomal dominant parkinsonism [311, 315]. Affected members from this family presented with a clinically typical L-dopa responsive PD, with an age at onset of approximately 50 years [315]. Neuropathologically, individuals exhibited pure nigral degeneration in the absence of LBs. Genome-wide linkage analysis in this family, provided evidence for a novel locus on chromosome 12 segregating with disease, with a maximal parametric two point LOD (log of odds ratio) score of 4.32 at marker D12S435 (12p11.2). Haplotype reconstruction and analysis limited the disease interval to a 13.6cM interval, between markers D12S1631 and D12S339. Several unaffected individuals shared the disease-carrying haplotype which suggested the possibility of incomplete penetrance of the mutation. A subsequent report identified two additional families with autosomal dominant PD [316, 317] with a maximal LOD score of 3.33 on chromosome 12 (D12S1701). Clinical features in this family included bradykinesia, rigidity, resting tremor and good response to L-dopa but pathological analysis yielded variable findings, with some individuals showing TAU pathology [317].

As disease within multiple independent families had shown significant linkage to a region encompassing the PARK8 locus, there was sufficient evidence to reliably link this area to PD. Therefore, I undertook genetic analysis of a family from Lincolnshire [313] with autosomal dominant PD to identify the gene underlying PARK8-linked PD

MATERIALS AND METHODS

Family information: Lincolnshire Kindred

All subjects gave informed consent. The study was approved by the Ethics Committees of the National Hospital for Neurology and Neurosurgery (NHNN). A pathological diagnosis of PD was made using the UK PD society brain bank criteria [318]. A clinical diagnosis of PD required two of the three cardinal signs; tremor, rigidity and bradykinesia; responsiveness to L-dopa; unilateral/asymmetric symptoms at onset and no atypical features. One affected member was scanned using ^{18}Fdopa and PET.

Linkage analysis of chromosomal 12 markers:

Linkage of this family to other regions of the genome implicated in PD (Table 1) had been excluded [319]. Whole genome linkage analysis had previously been completed [313] and suggested segregation of disease with a region on chromosome 12 with a maximal LOD score of 3.55 at marker D12S364. Additional markers (Table 2) were run in the region to confirm and refine the genomic disease interval.

Marker Name	cM position	Forward Primer	Reverse Primer	Fragment length
D12S98	27.51	5' FAM - TATAGTGACTGGCTGCCCAA	CAAAGCCTGACGTAGAAGCA	217
D12S1580	30.91	5' FAM - GCATGTGGATGGATGGATTT	GACTCTCAACCCACTGCTGG	345
D12S1630	35.25	5' FAM - GATGTGTTTAGATGCTTGGAAGG	GCTCATCAGTGAGTTGACCTGT	270
D12S1654	39.55	5' FAM - TCAAATGGCTGTGCTCTCAA	GATCTGTGGAGTTATTTGGGAGAG	253
D12S1606	42.85	5' FAM - ATGGACTTAAGAGTGCATTGACTAC	TTGTGTCAGGGTCACTGATTT	184
D12S1640	49.54	5' FAM - GAAAGAGGACATCTTAAGGGAGG	TTTGCAATGTTCATTCCTGG	170
D12S1681	53.43	5' FAM - CTGGTCCATTCCCAACTGAG	AACCCTTGGTGTCCCTTACC	271
D12S85	60.49	5' FAM - TTTCTGGCACCTCTCACTCC	GCACTCTACATGTGCAAAGTCAA	158
D12S1590	63.23	5' FAM - CACCATGCTCAGCCTCTATTT	GCTGCAGTGAGCCATGAT	206
D12S347	65.16	5' FAM - TATTGACTGCCACTGCTGCT	GCTCCATCCATTACTTAATGACTCT	379
D12S1724	69.88	5' FAM - CGCACCCAGCCAACTATTA	CCGTGCTGGTTCTATCTGTG	276
D12S1644	72.76	5' FAM - CTGTCCAGCGAGTTCAAGG	AGGGACCTGGGTAGAAGGAG	201

Table 2 Additional linkage markers run on chromosome 12 to confirm and delineate chromosomal region linked to disease

PCR mix for amplification of linkage markers:

Component	Amount per reaction
10x buffer	2.5µl
dNTPs (25mM each dNTP)	0.4µl (Final concentration of each dNTP – 200µM)
$MgCl_2$ (25mM)	1.5µl (1mM)
Forward Primer (10µM)	1µl
Reverse Primer (10µM)	1µl
Taq (Applied Biosystems)	0.15µl
DNA (50ng/µl)	1µl
ddH_2O	17.45µl

PCR cycling conditions for amplification of linkage markers:

1 cycle: 95°C – 2 min

35 cycles: 95°C – 30secs

	60°C – 30secs
	72°C – 30secs
1 cycle	4°C - HOLD

Products were diluted 1:100 with ddH_2O and 1µl of diluted PCR products were combined with 12µl of formamide and 0.3µl of 400HD ROX size standard (Applied Biosystems). Samples were heated at 95°C for 5 minutes and run on ABI PRISM 3100 Genetic Analyzer. All runs included CEPH1331-1 DNA to correct for inconsistencies between runs.

After electrophoresis, results were analyzed using GeneScan v3.6 and Genotyper v3.7 software (Applied Biosystems). Following data analysis, all genotypes and pedigree data was exported and managed in Cyrillic v2.1 software.

Statistical Analysis of chromosomal 12 markers:

Parametric 2–point LOD score calculations were performed using the MLINK program of the LINKAGE package [320-324]. The disease allele frequency was set to 0.001 and the model used for the disease assumed an autosomal dominant trait. Penetrance was set at 70% as the largest family with PARK8-linked disease [311] demonstrated a penetrance of approximately 70%.

Multipoint linkage analysis was performed using SIMWALK2 [325] with the above parameters. SIMWALK2 was also used to reconstruct haplotypes with the minimum number of recombinations and verify marker inheritance patterns to identify marker typing incompatibilities.

Allelic frequencies for each marker were obtained from public databases (http://www.gdb.org; http://www.cephb.fr/). Genetic distances were obtained from the Marshfield sex averaged linkage map (http://research.marshfieldclinic.org/genetics).

Candidate gene sequencing:

Genes within a 1-LOD support interval of the maximal two point LOD score (D12S1640 to D12S85) (Table 3) were considered as candidate genes. Variants that were identified within coding regions and splice sites of each gene were compared with those listed on the NCBI SNP database (http://www.ncbi.nlm.nih.gov/entrez/query.fcgi?CMD=search&DB=snp). Variants that were not listed on the NCBI SNP database were genotyped in the family to confirm segregation with the disease haplotype.

Genomic primer design for all genes was performed using Exon-primer (http://ihg.gsf.de/ihg/ExonPrimer.html). Each exon and at least 100bp of flanking intronic sequences was amplified. PCR amplification for all the sequenced genes except for LRRK2 was performed using a standard reaction mixture (pg 54-55) although conditions for individual exons varied with respect to annealing temperature, primer and $MgCl_2$ concentration.

Chr position (bp) start	Chr position (bp) stop	Gene Name	Chr position (bp) start	Chr position (bp) stop	Gene Name	Chr position (bp) start	Chr position (bp) stop	Gene Name
30753754	30798715	C1QDC1	33486879	33499660	LOC390301	41139341	41269745	PRICKLE1
30810101	30844209	LOC400019	34070139	34072501	ALG10	41316885	41317210	LOC390308
30861088	30906379	LOC390299	34081640	34100942	LOC144631	41734153	41734454	MRPS36P5
30996973	31032485	LOC390300	34208975	34211156	LOC260338	42007112	42010592	LOC400025
31118077	31148992	DDX11	36758977	36768884	LOC401715	42034279	42231991	ADAMTS20
31155860	31163465	DKFZp434C0631	36881636	36883817	LOC121014	42249839	42271090	LOC400026
31296164	31297990	LOC387850	36886300	36904590	LOC390305	42340088	42341171	LOC401717
31324785	31370340	C12orf14	36996645	37004051	LOC144245	42408758	42438817	DKFZP434G1415
31368517	31370146	FLJ13224	37332269	37585687	CPNE8	42439047	42468166	IRAK4
31428985	31635219	MGC24039	37674838	37751521	LOC121216	42473793	42486445	PTK9
31521677	31522058	MRPL30P2	37973297	38123185	KIF21A	42516229	43069808	DKFZp434K2435
31641308	31641610	LOC341356	38146513	38164195	LOC390306	42687843	42690385	ZNF75B
31658655	31660757	LOC387851	38232814	38300237	ABCD2	43188332	43556405	NELL2
31703388	31713168	MGC50559	38306287	38588369	FLJ40126	43742668	43745461	FKSG42
31715343	31773697	LOC196394	38438831	38785928	SLC2A13	43853114	43896056	LOC51054
31798920	31799484	LOC144383	38905080	39049354	DKFZp434H2111	43896170	44112401	DKFZp313M0720
31835854	31836367	LOC400022	39073517	39224969	LOC441636	44405781	44407955	LOC400027
32029259	32037306	FLJ10652	39222629	39250821	MUC19	44409887	44586590	ARID2
32151452	32422078	BICD1	39588426	39750361	CNTN1	44601462	44610015	SFRS2IP
32546361	32684940	FGD4	40117841	40254659	PDZRN4	44867833	44948824	SLC38A1
32723491	32788621	DNM1L	40761917	40826522	LOC283464	45038238	45052814	SLC38A2
32788348	32800080	CGI-04	40840421	40918264	YAF2	45063727	45332625	LOC387853
32835055	32940957	PKP2	40966980	40968629	LOC400024	45444811	45506006	SLC38A4
32941351	33031271	LOC283343	40992156	41006174	MADP-1	45584459	45637559	LOC390310
33419615	33484021	SYT10	41006214	41128690	PPHLN1	45755756	45759915	AMIGO2

Table 3: List of candidate genes within a 1-LOD support interval of the maximal multi-point LOD score (between markers D12S1640 and D12S85). Abbreviations: Chr-Chromosomal

PCR mix for candidate gene amplification:

Component	Amount per reaction
10x buffer	2.5µl
dNTPs (25mM each dNTP)	0.4µl (Final concentration of each dNTP – 200µM)
$MgCl_2$ (25mM)	1.5µl (1mM)
Forward Primer (10µM)	1µl
Reverse Primer (10µM)	1µl
Taq (Applied Biosystems)	0.15µl

DNA (50ng/µl)	1µl
ddH_2O	17.45µl (total volume 25µl)

PCR cycling conditions for candidate gene amplification:

1 cycle:	95°C – 2 min
35 cycles:	95°C – 30secs
	60°C – 30secs
	72°C – 30secs
1 cycle	4°C - HOLD

General PCR product purification protocol:

1. Add ddH_2O to PCR mixture with 100µl total volume.
2. Place in MultiScreen $PCR_{\mu 96}$ Filter Plate (Millipore)
3. Vacuum for 10min at 20 inches Hg
4. Add 20ul of water and place on plate shaker for approximately 10min.
5. Remove resuspended purified products and place in PCR plate for sequencing reaction.

DNA Sequencing Reaction Mix Protocol:

1. 50ng of DNA (generally, 2.5µl of purified PCR product)
2. 1µl of 3.2 pmol primer
3. 0.5µl Big Dye (Applied Biosytsems)
4. 2µl 5x Sequencing Buffer
5. Enough ddH_2O to make total volume 10µl/well

Sequencing cycling reactions:

1 cycle:	96°C – 2min
25 cycles:	96 °C – 10seconds
	50 °C – 5secs
	60 °C – 4min
1 cycle:	4 °C – HOLD

Purification of Sequencing PCR products:

1. Resuspend sequencing products to 20ul with ultrapure water
2. Place in MultiScreen $PCR_{\mu 96}$ Filter Plate (Millipore)
3. Vacuum for 5min at 25 inches Hg
4. Remove from vacuum and add a further 20ul of ultrapure water
5. Re-vacuum for 5min at 25 inches Hg
6. Add a further 20ul of water and place on plate shaker for approximately 10min.
7. Remove resuspended and purified products and place in plate.

Purified sequencing products were run on an ABI3100 Genetic Analyzer and analyzed with Sequencher software (Genecodes, VA).

LRRK2 exon amplification reaction:

In the case of LRRK2, the PCR amplification was performed using Abgene 1.1x Thermo-Start PCR Master Mix. Thermo-Start DNA Polymerase is a chemically modified Taq Polymerase, which requires activation for fifteen minutes 95°C incubation. The amplification mixture contains:

Component	Amount per reaction
Thermo-Start PCR Master Mix1.1x	13μl
Primers F/R (10μM)	1μl
DNA (50ng/μl)	1μl

PCR cycling conditions are the same as those described above (PCR cycling conditions for candidate amplification, pg 55) except for a 15 minute incubation at 95°C.

Assay of control subjects for LRRK2 mutation within Lincolnshire kindred

The variant (Y1699C) identified in the British family was screened in the CEPH Human Genome Diversity Panel Cell Line (http://www.cephb.fr/HGDP-CEPH-Panel/), which is made up of 1051 samples from different populations, many of which are European [326]. A further 650 control subjects from North America were screened for the mutation.

Assay of LRRK2 in PD cases with familial history of PD:

All 51 exons of LRRK2 were sequenced in a total of 117 pathological cases with one or more affected first-degree relatives. A pathological diagnosis of PD was made using the UK Brain Bank criteria [318]. One proband was also included with prominent postural tremor with a family history of parkinsonism (Figure 11; II.2, Family 4). An autosomal dominant mode of inheritance (one or more affected first-degree relatives across two generations) was present in 60 patients. The remaining 57 subjects were sibling-pairs.

RESULTS

Clinical and pathological description of Lincolnshire kindred:

The mean age of onset of PD was 57 years of age (range 40-75) with affected individuals initially presenting with unilateral leg tremor. All reported hemi-parkinsonism symptoms typical of progressive parkinsonism. Cognition was not significantly abnormal despite lengthy disease duration in some subjects. All affected individuals demonstrated a good and sustained response to L-dopa with minimal development of L-dopa induced dyskinesia. Behavioral alterations, such as anxiety, depression and paranoia were observed in total of seven patients [313]

PET imaging showed a pattern of nigrostriatal dysfunction (presynaptic reduction of putamenal ^{18}F-dopa uptake with relative sparing of the caudate) similar to idiopathic PD [327]. Pathological examination of an individual after 20 years of disease duration revealed no evidence of brain atrophy. There was severe pallor of the SN and the locus coerulus was indiscernible. Histological examination showed severe loss of pigmented neurons in the dorsal and ventral tiers of SN with marked gliosis. LBs and LNs were present in the locus coerulus and olfactory bulb. Cortical LBs were observed with a frequency corresponding to brainstem predominant Lewy body disease. Neurofibrillary tangles (NFTs) were also present in the hippocampus, subiculum, entorhinal and transentorhinal cortices corresponding to Braak and Braak stage II [313].

Linkage analysis of chromosome 12 markers in Lincolnshire kindred

As mentioned above, all known PD genetic loci had been excluded from this family [319]. In addition, whole genome linkage analysis provided significant evidence (LOD score of 3.55 θ= 0.00 at marker D12S364) to chromosome 12 [313]. Thus, I focused on decreasing the disease linked interval by typing an additional 12 markers around D12S364 (Table 2, Figure 5).

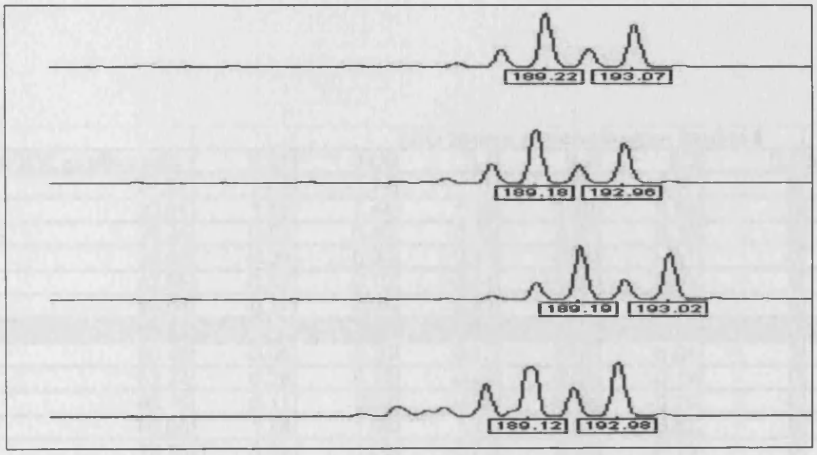

Figure 5: Example of a dinucleotide marker D12S1606. Allele size scored using the program Genotyper.

All data was corrected to CEPH control and exported to Excel (Microsoft) where the data was formatted for the linkage programs MLINK and SIMWALKv2. Multipoint linkage analysis using SIMWALK 2 gave a maximal LOD score of 2.2 between markers D12S85 and D12S1590 (Figure 6). Two point LOD scores were calculated using MLINK which gave a maximal LOD score of 2.04 at marker D12S1681 (Table 4)

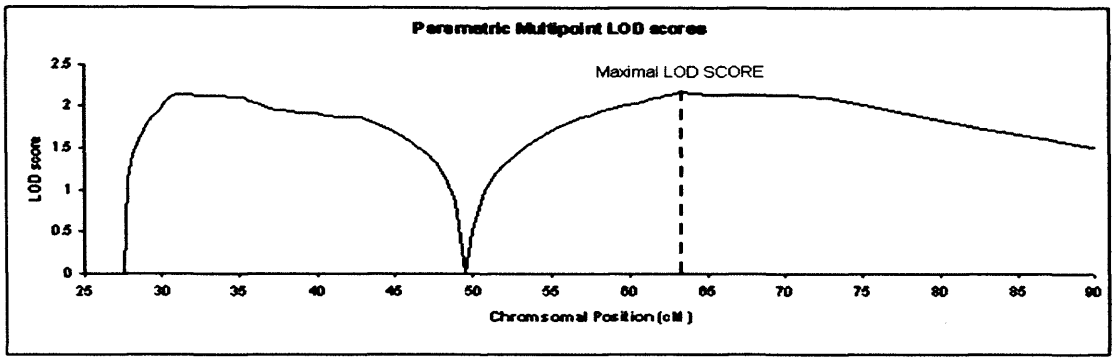

Figure 6: Multipoint linkage analysis results. Maximal LOD score of 2.2 was observed between markers D12S85 and D12S1590.

			LOD Scores at recombination fraction θ					
Markers	deCODE position (cM)	0.01	0.05	0.1	0.2	0.3	0.5	Max Lod score
D12S98	27.51	-1.4	-1.14	-1	-0.7	-0.37	0	0
D12S1580	30.91	1.56	1.44	1.28	0.92	0.54	0	1.59
D12S1630	35.25	0.53	0.46	0.39	0.27	0.16	0	0.55
D12S1654	39.55	-0.28	-0.32	-0.33	-0.23	-0.1	0	0
D12S1606	42.85	-0.63	-0.19	-0.04	0.03	0.02	0	0.03
D12S1640	49.54	-0.31	0.26	0.43	0.45	0.32	0	0.47
D12S85	60.49	-0.86	-0.35	-0.17	-0.07	-0.04	0	0
D12S1590	63.23	0.29	0.15	-0.02	-0.22	-0.19	0	0.32
D12S347	65.16	0.11	0.02	-0.08	-0.18	-0.16	0	0.13
D12S1724	69.88	1.78	1.65	1.46	1.06	0.63	0	1.81
D12S1644	72.76	-1.32	-1.05	-0.72	-0.33	-0.13	0	0

Table 4: MLINK two point LOD score results. Maximal two point LOD score was observed at marker D12S1681.

Haplotypes were reconstructed using SIMWALK2, in order to refine the disease interval (Figure 7). No recombination events were observed in affected individuals. Individuals who carried portions of the disease haplotype (e.g. Figure 7, individuals IV: 3 and IV: 11), did not present with any symptoms but were still below the average age of onset. Thus genes within a 1-LOD support interval of the maximal two point LOD score were prioritized for sequencing.

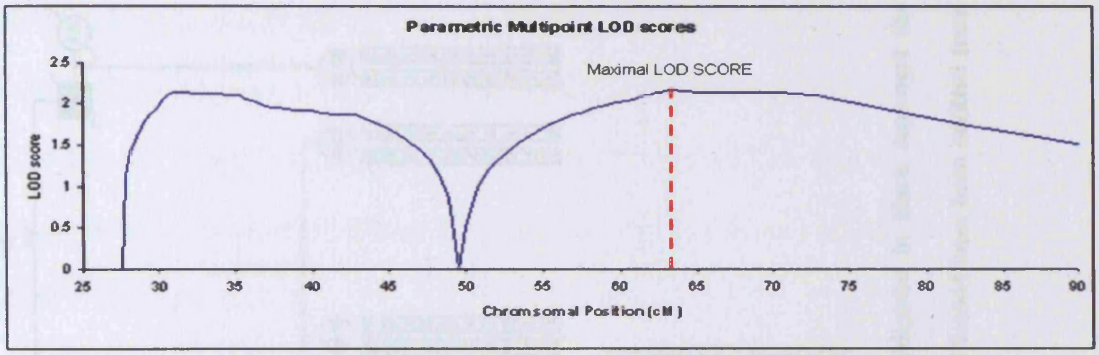

Figure 6: Multipoint linkage analysis results. Maximal LOD score of 2.2 was observed between markers D12S85 and D12S1590.

				LOD Scores at recombination fraction θ				
Markers	deCODE position (cM)	0.01	0.05	0.1	0.2	0.3	0.5	Max Lod score
D12S98	27.51	-1.4	-1.14	-1	-0.7	-0.37	0	0
D12S1580	30.91	1.56	1.44	1.28	0.92	0.54	0	1.59
D12S1630	35.25	0.53	0.46	0.39	0.27	0.16	0	0.55
D12S1654	39.55	-0.28	-0.32	-0.33	-0.23	-0.1	0	0
D12S1606	42.85	-0.63	-0.19	-0.04	0.03	0.02	0	0.03
D12S1640	49.54	-0.31	0.26	0.43	0.45	0.32	0	0.47
D12S1681	53.43	2	1.86	1.66	1.24	0.76	0	2.04
D12S85	60.49	-0.86	-0.35	-0.17	-0.07	-0.04	0	0
D12S1590	63.23	0.29	0.15	-0.02	-0.22	-0.19	0	0.32
D12S347	65.16	0.11	0.02	-0.08	-0.18	-0.16	0	0.13
D12S1724	69.88	1.78	1.65	1.46	1.06	0.63	0	1.81
D12S1644	72.76	-1.32	-1.05	-0.72	-0.33	-0.13	0	0

Table 4: MLINK two point LOD score results. Maximal two point LOD score was observed at marker D12S1681.

Haplotypes were reconstructed using SIMWALK2, in order to refine the disease interval (Figure 7). No recombination events were observed in affected individuals. Individuals who carried portions of the disease haplotype (e.g. Figure 7, individuals IV: 3 and IV: 11), did not present with any symptoms but were still below the average age of onset. Thus genes within a 1-LOD support interval of the maximal two point LOD score were prioritized for sequencing.

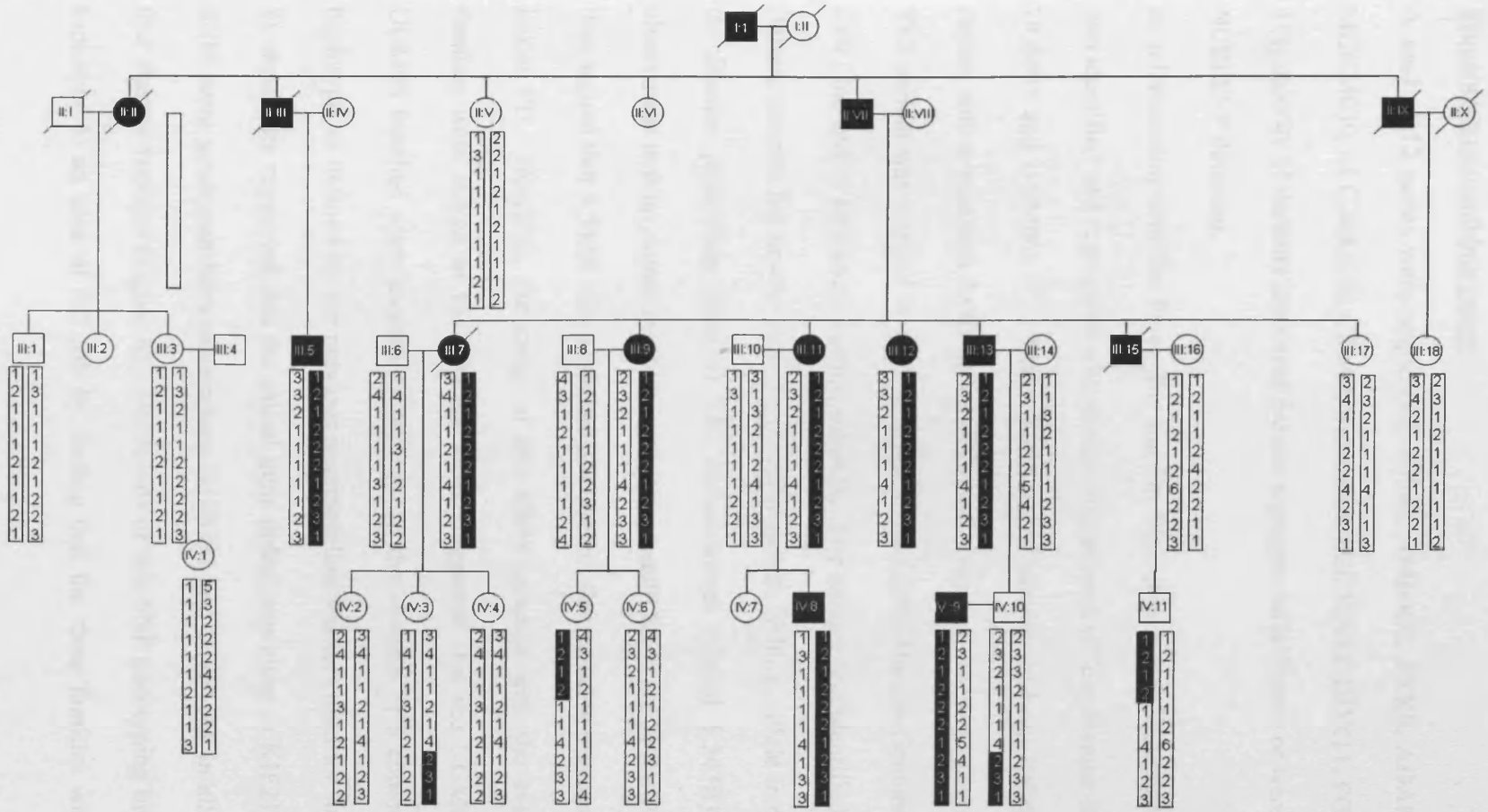

Figure 7: Pedigree of Lincolnshire Kindred. Affected individuals are denoted by filled symbols. Haplotypes highlighted in black represent the predicted disease haplotype. Marker order is as chromosomal order (Table 3 and 17) but markers D12S1654 and D12S1644 have been omitted from the pedigree as neither was informative.

Sequencing of candidate genes:

A total of 12 genes were sequenced; CPN8, AMIGO2, PTK9, ADAMTS20, CNTN1, MGC24039, SLC38A1, SLC38A2, SLC38A4, SLC38A12, DDX11, FGD4 and KIF21A. The majority of variants identified did not segregate with disease or were not listed on the NCBI SNP database.

In collaboration with Dr. Perez-Tur and Dr. Singleton, a K543R variant within KIF21A was identified and segregated with disease in three out of four Basque families (UGM03, UGM05 and UGM06) [328]. These families had previously been linked to the PARK8 region with a maximal LOD score of 3.21 for marker D12S345 (family UGM05) [328]. This variant was assayed in 1039 samples of the CEPH Human Genome Diversity Panel Cell Line and in 58 Basque control subjects. The variant was identified in two of the 58 Basque samples but absent from the diversity series. With an allele frequency of 0.01 in the Basque population (two of 116 chromosomes carried K543R) and the added observation that no mutations within this gene could be found in the British family, the data argued that K543R was a rare variant and not the mutation responsible for PARK8-linked PD. However, the rarity of this allele, coupled with the evidence that these families were linked to the PARK8 locus, suggested that the UGM03, UGM05 and UGM06 families were ancestrally related. In the absence of a common inter-kindred haplotype, as defined by the previous microsatellite markers used for linkage [328] (Figure 8), these data suggested that the causal gene defect was close to KIF21A. A further 23 SNPs were genotyped between markers D12S331 and D12S1668 in all members of the four Basque families (Figure 8). The results of this SNP genotyping limited the disease haplotype to an area of 3.2 Mb by finding that the three families who contained the

KIF21A variant did not share the same genotype for rs10876410 (Figure 8). Secondly, the data verified that all four Basque families shared a smaller inter-kindred disease haplotype, which was flanked by rs4548690 and D12S1653 marker, further reducing the linkage area further to a region of 2.6 Mb (Figure 8 and 9).

			BASQUE FAMILY ID			
IDENTIFIER	bp	CONSENSUS	UGM3	UGM4	UGM5	UGM6
D12S1698	30855986	-	122	126	118	124
D12S1621	31754700	-	191	191	191	191
rs1523118	37515966	-	T	T	C/T[a]	T
D12S331	37547321	-	177	177	177	177
rs11169992	37603474	-	C		C	C
rs10876410	37708557	-	T	A/T[a]	T	A
rs10876646	37887093	-	T	T	T	T
rs10747736	37912177	-	T	C	T	T
rs10747736	37912177	-	T		T	T
rs10876876[b]	38011263	-	A	-	A	A
rs11171789[b]	38024258	-	T	C	T	T
K543R[b]		-	G	A	G	G
rs10876886[b]	38035530	-	C	A/C[a]	C	C
rs11172282	38161804	-	G	C/G[a]	G	G
rs11172541	38229025	-	A	-	A	A
rs10877201	38298564	-	C	T/C[a]	C	C
rs4548690	38475137	-	T	C	T	T
rs7294916	38494630	T	T	T	T	T
rs4423249	38554997	T	T	T	T	T
rs515205	38689229	A	A	A/G[a]	A	A
rs937110	38815159	C	C	C/G[a]	C	C
SNP1	38815163	T	T	T	T	T
rs4768224	38947670	T	T	T	T	T
IVS13-54[c]	38943803	C	C/G[a]	C	C	C
IVS13+68[c]	38944038	G	G/A[a]	G	G	G
R1398G[c]	38990503	C	C	C	C	C
M1601T[c]	39011294	G	G	G	G	G
rs12423567	39063583	G	G	-	-	G
rs12423567	39063583	G	G	G	G	G
rs10784616	39117987	C	C	C	C	C
rs11612876	39256712	T	T	-	T	T/C[a]
rs10784800	39386364	C	C	C	C	C
rs10879192	39471471	C	C	C/T[a]	C	C
D12S1668	39489795	235	235	235	235	235
D12S1653	41093581	-	215	215	203	215

Figure 8: Markers used to fine-map the candidate interval and determine Basque interfamily shared haplotype and the boundaries of this haplotype. The K543R variant that did not segregate with disease in all three families is highlighted in yellow box. The black outline indicates the extent of the haplotype common between the Basque families. [a] Phase not determined; [b] Within KIF21A; [c] Within DKFZp434H111

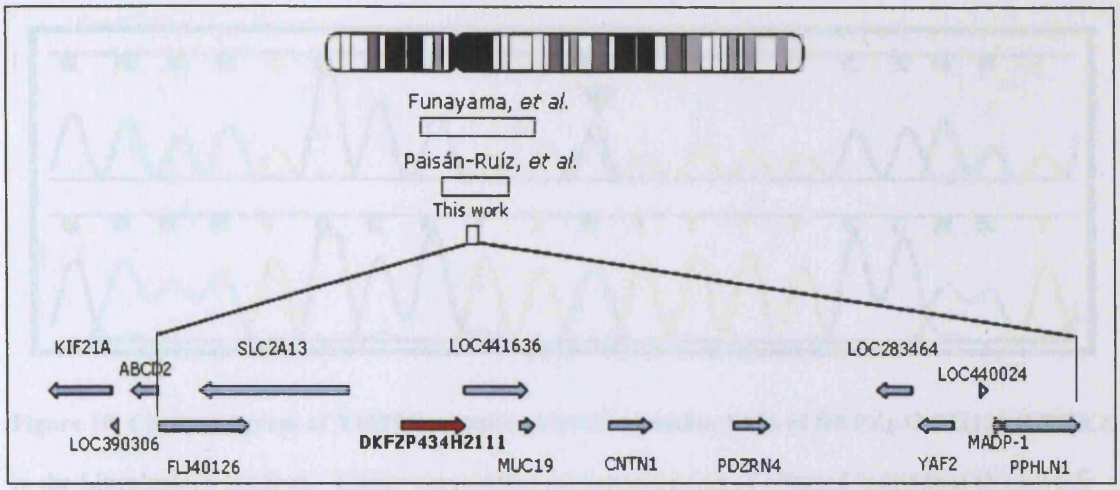

Figure 9: Ideogram of chromosome 12 showing the linked areas defined by Funayama et al. in 2002, the refined area, and the region shared by all four Basque families.

(B) Schematic representation of the known genes and predicted transcripts in the area shared by the Basque families. Highlighted gene (red) represents the putative transcript where mutations in PARK8-linked families were identified.

Identification of a mutation within LRRK2 in the Lincolnshire kindred:

All genes and predicted open reading frames (Figure 9b) were sequenced in two affected and unaffected members from UGM03 and UGM05 families. Only one of them, LOC441636, was not analyzed as it was similar to submaxilary apomucin, MUC19 and unlikely to play a role in neurodegeneration. Mutations in one predicted transcript, DKFZP43H2111, were identified (Figure 10) in both the Basque (R1441G) and Lincolnshire kindred (Y1699C). Both mutations segregated with disease and neither variant were present in Basque (80 control patients), 650 North American controls or 1039 controls from the diversity series. Thus it was highly likely we had identified the gene responsible for PARK8-linked PD.

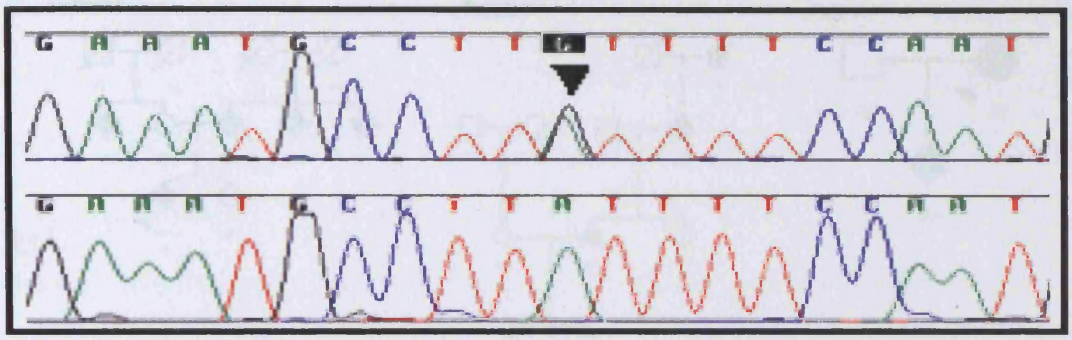

Figure 10: Chromatogram of Y1699C mutation identified within Ex35 of DKFZp434H2111 (LRRK2) in the Lincolnshire kindred. Upper chromatogram is sequencing of affected individual IV: 9 while lower chromatogram is sequencing of an unaffected individual.

Identification of additional LRRK2 mutations

Out of a series of 117 patients with a family history of PD, 5 (4 autosomal dominant, 1 sib pair) LRRK2 substitutions were identified. A G2019S mutation was identified in three patients (Family 1, 2 and 5; Figure 11), R1941H in one subject (Family 3; Fig. 11) and T2356I mutation in another (Family 4; Fig. 11). Overall, mutations were found in 5.1% of the 118 families screened. In addition, healthy subjects with LRRK2 mutations were also identified: III.3, aged 55 years (Family 4; Fig. 11) and II.5, age unknown (Family 5; Fig. 11). These mutations were not found in a total of 1438 control chromosomes.

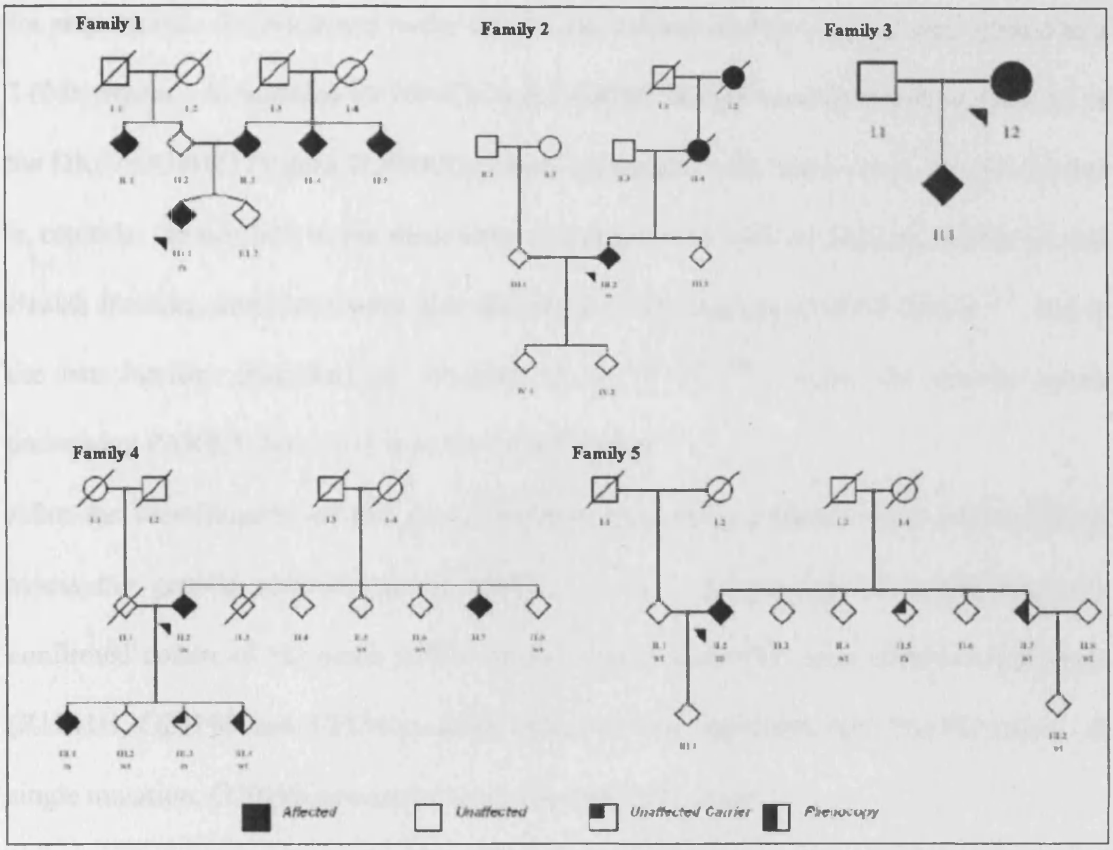

Figure 11 Families in which LRRK2 mutations were identified; Family 1 2 and 5 had the G2019S mutation. Family 3 had a R1941H mutation and Family 4 had a T2356I mutation. LRRK2 mutations were also identified in asymptomatic individuals; Family 4-III.3 and Family 5 – II.5

DISCUSSION

As the family showed significant linkage (LOD score 3.55; θ=0.00) to chromosome 12 [313], further markers were genotyped to both confirm disease haplotype segregation and to refine the disease interval. No affected individuals possessed a recombination which reduced the disease interval, so based on both multi-point and two points LOD scores (2.2 and 2 respectively), genes between markers D12S1640 and D12S85 were prioritized

for sequencing. As discussed in the results, the critical disease interval was refined to a 2.6Mb region. A mutation (Y1699C) in the British family was identified in exon 35 of the DKFZp434H2111 gene (LRRK2), which segregated with disease and was not present in controls. In addition to the discovery of mutations in both the Basque (R1441G) and British families, mutations were also described in the original PARK8 family [329] and in the two families described by Wszolek et al [316, 317, 330]. Thus, the genetic lesion underlying PARK8-linked PD is in the LRRK2 gene.

After the identification of the gene, multiple sequencing projects were undertaken to assess the genetic contribution of LRRK2 to PD. Sequencing of a pathologically confirmed cohort of PD cases with a family history identified three different mutations (R1941H, G2019S and T2356I), which accounted for approximately 5% PD cases. A single mutation, G2019S accounted for 2.5% of the PD cases.

In terms of genetic testing, LRRK2 is the most important gene linked to PD discovered to date, as sequencing has yielded multiple mutations [331-333], with one single mutation (G2019S) accounting for 1-2% of sporadic PD and 5-6% of familial European PD [334-337]. In addition, the G2019S mutation is present at much higher rates in other populations (11% Portuguese cohort; 23% Ashkenazi Jewish population; 40% North African Arab population) [335, 338, 339].

The clinical presentation associated with the G2019S LRRK2 mutation is similar to idiopathic PD; with asymmetric presentation of bradykinesia, rigidity, tremor, L-dopa responsive and the absence of major cognitive abnormalities [313, 340, 341]. However, the age of onset associated with the G2019S is extremely variable, ranging from 28-88 although collectively, the mean age of onset is approximately 56 years of age [334, 337, 338, 342-344]. The

penetrance associated with LRRK2 mutations is also extremely variable, as current estimates for the G2019S mutation are close to 30% [339, 345, 346] while other mutations such as, Y1699C, appear to be 100% penetrant [313, 330]. The penetrance associated with the G2019S mutation is highly age dependent, increasing from 21% at the age of 50 years to 81% at the age of 70 years [343].

Not only is there variability in the clinical presentation but also in the pathology associated with LRRK2 mutations. The pathology in the British family is similar to idiopathic PD [313] as both LB and cell loss in the SN were present. However, in the original description of the Japanese kindred, nigral degeneration without LBs was reported [347]. Two other LRRK2 kindreds also have diverse pathologies. Histopathology from patients in Family D (R1699C mutation) [317, 330], is more consistent with diffuse LB, nigral degeneration and PSP-like pathology. A second family, Family A, has clinical and pathological features consistent with a motor neuron disease where anterior horn cell degeneration and gliosis were observed [313 317, 330]. Interestingly, this family shares the same Y1699C LRRK2 mutation as the Lincolnshire kindred whose phenotype, pathology and functional imaging is strikingly similar to idiopathic Parkinson's disease [317, 330]. The heterogeneous pathology, which includes LBs, TAU and amyloid, raises the possibility that LRRK2 may interact directly or indirectly with other pathways that lead to neurodegeneration or the pathology observed may simply be co-incidental. It should be noted that limited sequencing of LRRK2 in other neurodegenerative diseases has not identified any mutations [344]. More extensive sequencing of LRRK2 is needed to determine if mutation of LRRK2 is involved in other neurodegenerative diseases.

The variability in the disease occurrence, presentation, progression and endpoint suggests that there are other genetic, environmental or stochastic events that modulate the disease process caused by LRRK2 mutation. Unlike mutations in other genes that cause PD, the frequency with which mutations in LRRK2 occur, affords us the opportunity to investigate these specific modulators of disease, and one would hope these will also be relevant to idiopathic PD [348].

CHAPTER 3: ASSEMENT OF COMMON VARIATION WITHIN LRRK2 AND THEIR CONTRIBUTION TO SPORADIC PD IN EUROPEAN POPULATIONS

INTRODUCTION

It has been suggested that PD is a complex disease and is the result of intricate interactions between the environment, genes and stochastic factors [12]. Much of the research aimed at identifying genes associated with typical PD has focused on the role of common variation in modulating lifetime risk for disease. This often involves a candidate gene association analysis, where a gene is typically chosen based on its function, expression or genomic position, common variants are assayed within the gene and the frequency of these variants are compared between cases and controls [296, 349]. The ease and low cost of this approach has resulted in hundreds of candidate gene association studies being published in PD, many of which have not been consistently replicated [350, 351].

There are many possible reasons for the poor reproducibility of association studies in PD, and in other disorders. Firstly, PD is almost certainly a heterogeneous group of disorders that may have the same, different or overlapping susceptibility factors [177, 352]. This is analogous to the heterogeneity observed in Mendelian PD where a phenotype associated with a particular genetic mutation may not be distinguishable from the phenotype of other genetic forms [89]. A second problem is inadequate study design, which can involve

several factors. Many studies involve small sample sizes (greater false negative/positive rate) [349], poor selection of control populations (increased false positive rate), failure to correct for population stratification [350] and multiple testing (increased false positive rate) [353, 354] and failure to utilize linkage disequilibrium patterns (LD) to track and distinguish the true causative mutation (failure to replicate association in other populations) [355, 356].

An ideal case control study needs statistical power and hence a large sample size. Cases and controls should be matched for age and ethnicity to avoid population stratification bias, whereby subgroups have allele frequency differences. For example if one population subgroup has a higher disease prevalence, then alleles more frequent in that population will tend to be associated with disease, even if they do not influence it. Study design such as the use of unlinked genetic markers (genomic control) or a longitudinal analysis of healthy individuals may help resolve this, although these strategies are technically difficult.

For all statistical approaches that use multiple tests, the appropriate p value correction (e.g. Bonferroni correction), should be applied to protect against a false positive result. A caveat is that if the correction is too conservative it is possible to miss a true positive. This is particular pertinent in the current climate of genome wide searches, where thousands of comparisons are often made. Replication of a positive association is essential and will dissect a true positive [349, 357, 106].

Two well characterized genes in terms of genetic association with typical PD are those encoding SNCA and MAPT. When the α-synuclein triplication was discovered [106] a logical question that arose was whether smaller increases in α-synuclein could increase the risk for sporadic disease. Many studies have attempted to address this question but,

as with most studies looking at risk factors in complex diseases, they have been largely inconclusive. Even though a polymorphic multi-allelic repeat in the promoter of α-synuclein (Rep1) can negatively regulate α-synuclein expression, genetic analysis of this marker has produced mixed results as to whether variation at this locus affects risk for sporadic PD [358-363]. Examination of common variability in other genes involved in monogenic forms of PD has failed to reveal a consistent association with sporadic PD [90], although a recent meta analysis has suggested that individuals with a 263bp Rep1 allele are approximately 1.5 times at greater risk of developing PD [363].

Perhaps the most robust genetic association with increased risk for PD comes from analysis of the microtubule associated protein, TAU. Mutations in the MAPT gene cause Frontotemporal Dementia and Parkinsonism linked to chromosome 17 (FTDP-17) [364]. The TAU protein forms NFTs in many diseases, collectively referred to as tauopathoies such as Alzheimer's Disease (AD), progressive supranuclear palsy (PSP) and corticobasal degeneration (CBD) [365]. Consequently, MAPT was considered as a candidate gene for these diseases [366] and a specific haplotype (referred to as the H1 haplotype) has been consistently associated with increased risk for PSP and CBD [367-369]. As PSP and CBD can often present with parkinsonian features [370], and PD can present with TAU pathology [317, 330, 371], a role for MAPT in PD has been evaluated. Thus far, numerous studies demonstrate that individuals that are homozygous for the H1 haplotype are approximately 1.5 times at greater risk of developing PD [177].

Although MAPT and SNCA have been extensively investigated, the role of common genetic variability in these genes in risk for PD is still debatable [90]. The advent of the HapMap project (www.hapmap.org) and the availability of technology for genome wide

association studies promise a more complete genetic analysis of PD. These data should reveal common genetic variability underlying disease and, in the absence of association, give a reasonable indication of a lack of a single common genetic variant underlying disease [372]. This latter point leads to another reason why there has been a general failure to identify common genetic risk variants for disease; namely that perhaps there are no common variants that individually confer a detectible risk. There is preliminary evidence for the lack of a single strong genetic risk factor in PD from the first whole genome association study carried out in this disease [306]. By its very nature, high-density genome-wide SNP association results in many false positives. Where the genetic variability underlying disease is only of minor to moderate effect, the level of "noise" and true signals will be about equivalent, and the former will outweigh the latter [354]. This was the case in this study and while the absence of a single overwhelming positive in the initial experiments may at first be disappointing, this misses the advantage of this relatively unbiased type of experiment. With some caveats, these data tell us not only what might be there, but also what is not there. It suggests that in PD there is not a single common variant of large effect, such as the effect of ApoE alleles in AD. This is invaluable data when we come to consider and design experiments [306].

Even though common variation (allele frequency >5%) has not been found to increase risk for PD, recently, heterozygous mutations within PINK1 and PRKN have been suggested to act as risk factors for disease development [182, 238, 240, 241, 373], as unaffected carriers can present with a sub-clinical phenotype. There is also significant over-representation of heterozygote mutation carriers in PD cohorts compared to controls [240, 374, 375]. PET imaging of heterozygous PINK1 and PRKN patients suggests a degree of

dopaminergic dysfunction as they showed a significant decrease in ^{18}F-dopa uptake [373] [376-378]. It remains unclear if and how heterozygous mutations within PRKN or PINK1cause a disease with a later age of onset [379] [380] [180, 381] when the Mendelian forms of these two genes cause a recessive disorder with early onset.

The studies discussed above suggest that common variants in genes associated with Mendelian forms of PD might contribute to the risk of sporadic disease but that the effects may be small. To assess if common variation within LRRK2 could contribute to risk of PD, a rigorous case-control association study was performed that included multiple populations to address the issue of independent replication.

MATERIALS AND METHODS

Clinical description of Finnish and Greek cohorts:

A case-control study was performed in order to evaluate association with risk for PD and common variants within the LRRK2 locus. Two different European cohorts, from Finland and Greece were used for this study.

The Finnish cohort consists of 283 subjects, 147 patients (87 men, 60 women) with sporadic PD and 136 controls (50 men, 86 women). The mean age at examination of the patients was 67.2 years (range 38–88) and mean age of controls was 65.8 years (range 37–87). The PD diagnoses were verified with a clinical follow-up for at least 4 years or, alternatively, clinical follow-up for at least 2 years plus ^{123}I-β-CIT-SPECT findings supporting idiopathic PD. Patients with dementia or patients who reported first-degree

relatives with parkinsonism were excluded. Controls were neurologically normal subjects living in the same geographical area.

The Greek cohort consists of 217 PD patients and 221 healthy controls age, gender and ethnicity-matched. The mean age of examination was 69.8 ± 8.7 years (range 44-95); while their mean age at onset of disease was 68.3 ± 12.8 years (range 32-93). The diagnosis of PD was based on established criteria [28]. Controls were neurologically normal subjects living in the same geographical area. Experienced neurologists performed all clinical assessments. Informed consent was obtained from all subjects.

Identification of tagging SNPs for LRRK2:

Linkage disequilibrium (LD) is the non-random association between two or more alleles such that certain combinations of alleles (haplotypes) are more likely to occur together than other combination of alleles. The strength of LD between SNPs is eroded over time due to genetic recombination. This process leads to discrete blocks of sequences, within which SNPs are in strong LD with each other and are flanked by recombination hotspots. SNPs between LD blocks are generally not in LD. LD can be measured by two different methods D' [382] and R^2 [383]. When D' is equal to 0, then the two markers are completely independent; when D' is equal to 1.0, then one maker is able to completely predict the genotype of the other. R^2 is a stricter measure of LD and can only equal 1 when marker loci have an identical allele frequency and every occurrence of an allele at each marker perfectly predicts the other marker. When SNPs are in LD with each other and form haplotypes, there is redundant information contained within the haplotype. One can predict the state of one marker knowing information about another. Thus, one can infer

within a region of reasonable LD (D' and R^2>0.5), a large proportion of the variation by typing a small number of key 'tagging' SNPs (tSNPs). tSNPs can only effectively and reliable infer genetic variation where the minor allele frequency (MAF) of the SNP is greater than 5% [384].

tSNPs were selected from 215 SNPs across the LRRK2 locus, identified from the HapMap Project (www.hapmap.org). SNPs with a minor allele frequency <0.05 were excluded from the analysis. A total of 31 tSNPs were identified using TagIT v2.03 [384], which selects tSNPs using a criteria based on the R^2 measure of association and allows analysis of trio and population data [384]. First, the LRRK2 haplotype structure was characterized, and the tSNPs that represented the most common haplotypes, were identified. A further five potentially functional SNPs, of which four are non-synonymous changes (rs7308720, rs10878307, rs71339914, rs11564148) and one in the predicted promoter region (rs2201144) of LRRK2, were genotyped. The tSNPs and the five potentially functional SNPs were structured in three different LD blocks, containing 17, 7 and 7 tSNPs respectively. Finally all tSNPs, spanning 0.13 Mb were typed in idiopathic PD patients and control subjects in order to screen for association with risk for PD.

Genotyping for all the samples was performed using Assays-by-design Service-SNP Genotyping (Applied Biosystems). All genotype data obtained from the Finnish and Greek cohorts were stored and analyzed using the GERON genotyping database (http://neurogenetics.nia.nih.gov/index.html).

Genotyping of tSNPs:

SNP genotyping was performed using Assays-by-Design Service-SNP Genotyping (Applied Biosystems). PCR amplification was performed in 5ul reaction, which contains the following PCR reagents:

Component	Amount per reaction
TaqMan mix	2.5µl (TaqMan, Universal PCR Master Mix, Applied Biosystems)
ddH_2O	0.875µl
Probe (20µM)	0.125µl
DNA (10ng/µl)	1.5µl

Thermo cycling parameters were:

1 cycle:	50°C	2min
40 cycles:	95°C,	10min
	95°C,	15secs
	60°C,	1min
1 cycle:	4°C,	HOLD

In allelic discrimination assays, the PCR included a specific, fluorescent, dye-labeled probe for each allele at the 5' end. During the PCR amplification, each probe anneals specifically to the complementary sequence and the fluorescence generated, indicating which alleles are present in the sample. Fluorescence is detected using the ABI Prism 7900HT sequence detection system and analyzed with SDS software (Applied Biosystems).

Statistical analysis of tSNPs and risk for PD

In order to compare allelic and genotypic distribution between case and control populations the Pearson chi-square (χ^2) test using GERON genotyping (http://neurogenetics.nia.nih.gov) was performed. P-values were corrected for multiple testing using the Bonferroni correction (P=0.05/n where n is the number of tests). Haplotype construction and tests of haplotype association were performed using the program Genecounting in association with the module Genecounting Permute [385]. Genecounting implements the expectation-maximization (EM) algorithm for haplotype analysis of unrelated individuals. Genecounting Permute performs permutation tests for global association and significance of specific haplotypes using Freeman-Tukey and proportion tests [385]. One thousand replications were performed for each analysis using a random number seed. Haplotype associations were performed individually for each of the three previously identified blocks of LD except for block 1, which had to be split into 2 overlapping sections, 1a (rs2201144 to rs2723264) and 1b (rs2046928 to rs4272849), in order to reduce computation time.

RESULTS

No association between common variation in LRRK2 and risk for PD:

A total of 36 SNPs, 31 tSNPs identified from the Caucasian HapMap data using TagIT v2.03 and five potentially functional SNPs (Table 5), were typed in idiopathic PD patients and control subjects. The selected SNPs captured and predicted 95% of the

identified genetic variation across the gene. These variants were distributed in three blocks of LD (Figure 12).

SNP	rs number	Contig position	Minor Allele (Frequency)	Tagging/Coding
1	rs2201144	38897130	C (0.093)	promoter
2	rs1491941	38907082	C (0.373)	tSNP
3	rs10878244	38917875	A (0.134)	tSNP
4	rs10878245	38918058	T (0.492)	tSNP; L153L
5	rs10878247	38918367	T (0.321)	tSNP
6	rs10878258	38927959	G (0.229)	tSNP
7	rs1491938	38931897	T (0.489)	tSNP
8	rs10784451	38936155	A (0.183)	tSNP
9	rs2046928	38938661	G (0.059)	tSNP
10	rs2723264	38938787	T (0.250)	tSNP
11	rs4293189	38943492	A (0.427)	tSNP
12	rs10784661	38943804	G (0.192)	tSNP
13	rs7308720	38943967	G (0.088)	N551K
14	rs4768224	38947670	A (0.369)	tSNP
15	rs11564207	38950910	A (0.107)	tSNP
16	rs7308193	38951494	G (0.347)	tSNP
17	rs10878299	38953142	G (0.058)	tSNP
18	rs7971935	38956661	A (0.051)	tSNP
19	rs4272849	38957068	C (0.483)	tSNP
20	rs10878307	38958256	G (0.061)	I723V
21	rs4318033	38967208	G (0.067)	tSNP
22	rs7957754	38972305	G (0.449)	tSNP
23	rs7966550	38974962	C (0.150)	tSNP; L953L
24	rs10784498	38983701	A (0.287)	tSNP
25	rs7133914	38989178	A (0.092)	R1398H
26	rs11564148	39000168	A (0.324)	S1647T
27	rs10878386	39012195	G (0.069)	tSNP
28	rs2404834	39015274	T (0.096)	tSNP
29	rs1427273	39018997	C (0.296)	tSNP
30	rs11564147	39025760	A (0.069)	tSNP
31	rs10878405	39028521	A (0.324)	tSNP; E2108E
32	rs4768235	39030353	A (0.127)	tSNP
33	rs7303525	39031042	C (0.196)	tSNP
34	rs7132187	39031075	A (0.298)	tSNP
35	rs7307310	39031448	T (0.092)	tSNP
36	rs890575	39034662	G (0.117)	tSNP

Table 5: List of tSNPs and coding polymorphism genotyped in both the Finnish and Greek populations to assess if common variation within LRRK2 contributes risk for PD. Regions highlighted represent the LD block in which each SNP is located in. Five non-synonymous and promoter SNPs were not part of the tagging set. Minor allele frequency and chromosomal position are based on NCBI reference sequence build 124.

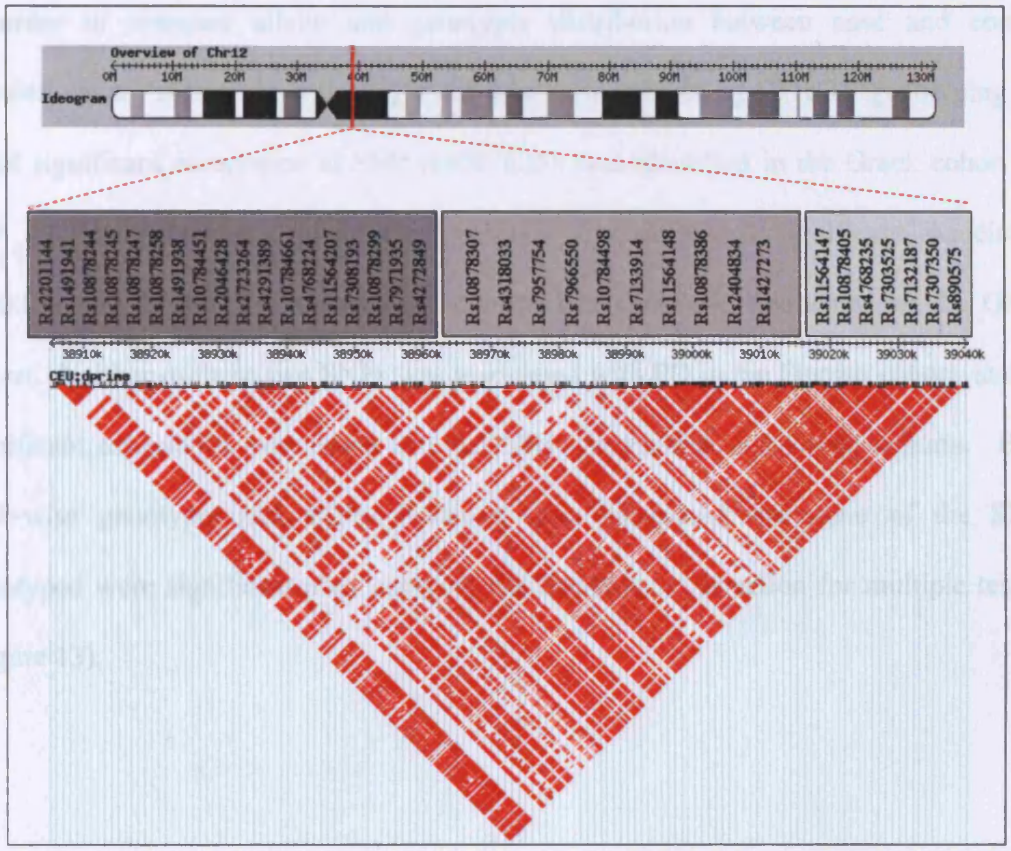

Figure 12: SNP locations and LD structure for LRRK2 and approx 20kb upstream of LRRK2. The triangle plot is constructed by connecting every pair of SNPs along lines at 45 degrees to the horizontal track line. The colour of the diamond at the position that two SNPs intersect indicates the amount of LD: more intense colours indicate higher LD. LRRK2 LD structure demonstrates 3 blocks of high LD separated by relatively well-defined boundaries of low LD, denoted by the three differentially shaded boxes above the triangle LD plot.

Of the 36 SNPs genotyped in the Greek and Finnish cohorts, three SNPs deviated from Hardy Weinberg equilibrium (HWE) and were subsequently excluded from the appropriate analysis. Rs10878247 deviated from equilibrium in both Greek case and control cohorts, rs7132187 deviated only in the Greek control cohort and rs4293189 was broke HWE in both Finnish and Greek control cohorts

In order to compare allelic and genotypic distribution between case and control populations, a Pearson chi-square (χ^2) test was performed using GERON genotyping. A small significant association at SNP rs10878258 was identified in the Greek cohort for both allelic (p=0.05) and genotypic (p=0.013) frequencies. A significant association (p=0.03) at SNP rs2723264 was also identified in genotypic frequency for the Greek cohort. Neither of these two SNPs was associated with PD in the Finnish cohort, and no significant association was found at other SNPs in Finnish and Greek cohorts. Both SNP-wise genotypic and allelic P-values were calculated and none of the SNPs genotyped were significant after applying the Bonferroni correction for multiple testing (Figure 13).

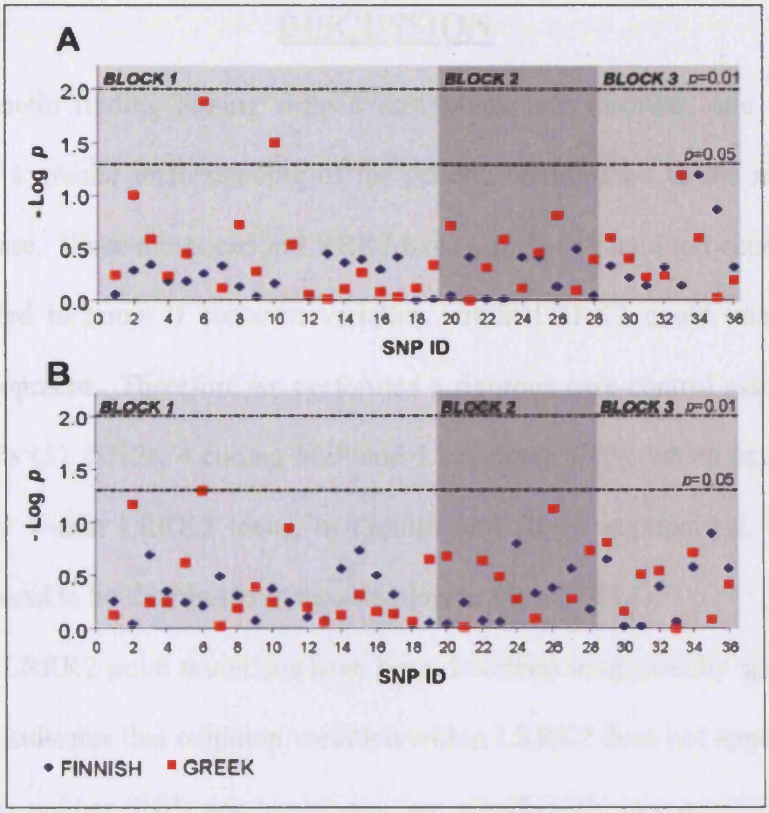

Figure 13: A) Genotypic and B) Allelic –log P values for single SNP association between LRRK2 and PD. P-values are not adjusted for multiple testing.

There was no association in any of the three haplotype blocks extending over the LRRK2 region, in either the Finnish or Greek populations (Table 6).

	Greek				*Finnish*			
	χ^2	DF	P value	Standard error	χ^2	DF	P value	Standard error
Block 1a	84.30	1013	0.685	0.014	30.96	1013	0.826	0.011
Block 1b	51.90	502	0.285	0.014	38.86	502	0.240	0.013
Block 2	41.18	1013	0.588	0.015	30.22	1013	0.370	0.015
Block 3	38.48	120	0.599	0.015	11.92	120	0.863	0.010

Table 6: Results of association analysis between LRRK2 haplotypes and PD.

DISCUSSION

With any genetic finding arising from a rare Mendelian disorder, one hopes it will translate into a greater understanding of the genetic contribution to the more common sporadic disease. Since mutations in LRRK2 have also been found to occur in idiopathic PD, we wanted to know if common variation within LRRK2 could increase risk for disease development. Therefore we performed a rigorous case-control association study using 36 SNPs (31 tSNPs, 4 coding SNP and 1 promoter SNP), which captures 95% of the variability within LRRK2 locus, in Finnish and Greek populations. The analyzed SNPs were found to be distributed in three haplotype blocks of LD.

Even though LRRK2 point mutations have been described in apparently sporadic PD [334-337], our work indicates that common variation within LRRK2 does not appear to increase risk for PD as neither SNPs nor haplotypes, are significantly over-represented in a PD population [386, 387]. This work has been replicated in a larger (340 cases) independent population [388], where a total of 121 SNPs (81 tSNPs and 40 coding SNPs) were genotyped, thus representing a more comprehensive analysis of the genetic variability within LRRK2.

One group has reported a significant association between LRRK2 (driven by the SNP rs10506151) and increased risk for PD in a Chinese population [389]. This study represents the largest cohort analyzed to assess if common variation within LRRK2 affects risk for PD (446 cases and 486 controls). However, the associated SNP in this population was not identified as a tSNP in either of the two European population studies, reflecting the genetic diversity between European and Asian populations and the need to design different tSNPs sets for independent ethnic populations. Furthermore, as this study was

conducted within a Chinese population, it may represent a true genetic risk factor within this population and not in others, as may be the case may be for GBA [256, 257, 259-261, 390] (pg 43-44). Other studies have demonstrated that rare variation within LRRK2, G2385R (MAF~3%), is significantly over-represented in the Chinese population [391-393]. The G2385R variant may be a population specific variant and analogous to the G2019S variant, which is rare in the Chinese population [394].

The ability of tSNPs to capture genetic information decreases dramatically as the marker allele frequencies decreases [262, 383], thus if a variant within LRRK2 that contributes to risk of PD is rare (MAF<5%), as is the case for the G2385R variant in the Chinese population [391, 393], then none of the studies conducted to date would be able to reliably detect them. To detect these variants, systematic sequencing of all exons in large PD cohorts is needed. In addition, neither of the two cohorts used are sufficiently powered to detect risk factors with modest allelic odds ratio (2<OR<3). This statement strictly depends on several factors including disease and marker allele frequencies, strength of LD and the allelic odds ratio of the disease gene (for review see [262]).

The contribution of common genetic variation to sporadic PD is unknown [351] but one can almost be certainly sure that no risk factors such as APOE exist in PD [395]. As APOE ε4 homozygotes have an odds ratio of approximately 3, one can detect its effect with as few as 150 cases and 150 controls [395]. At best, common variation within LRRK2, only has a modest effect on risk for PD (1<OR<2), therefore case control series of 500 to 1000 cases are needed to discern a true effect of LRRK2 on risk for PD [262]. At present there is no evidence for common variation within the LRRK2 locus influencing risk for PD in a European population but larger studies are required to confirm or refute this finding.

CHAPTER 4: CLONING AND PRELIMINARY BIOLOGICAL ANALYSIS OF LRRK2

INTRODUCTION

Prior to the identification of PD-causing mutations in LRRK2, the gene had been annotated as part of the kinase super family and was named for leucine-rich repeats and the kinase domain [396] [397, 398] (LRRK2). LRRK2 belongs to a newly identified family of proteins referred to as ROCO proteins [399, 400] that contain two conserved domains i) a ROC (Ras in complex proteins) domain that belongs to the Ras GTPase super family and ii) a COR domain (C-terminal of ROC). In addition, LRRK2 contains multiple protein interaction motifs such as HEAT/ARMADILLO (ARM) [401], WD40 [402] as well as the leucine rich repeats (LRR) [403, 404]. Very little is known this family of proteins, with only three members having being investigated [403]; human DAPK [405], and the Dictyostelium GbpC [406] and Pats1 [407].

Although LRRK2 belongs to this family of proteins, its primary amino acid sequence and the motifs suggest that it has unique properties [400]. The closest homolog of LRRK2 is LRRK1, but this protein differs significantly, lacking approximately 500 amino acids from the N-terminus that includes the HEAT/ARM repeat motifs while the remainder of the protein domain structure is similar [403]. As LRRK2 is a unique protein and mutations have been identified in all predicted domains of LRRK2 [408], it is difficult to predict how mutations in LRRK2 might affect its function. Therefore, in the present study, wild type

and mutant versions of LRRK2 were created and expressed in mammalian cells to determine how mutation of LRRK2 might alter function.

MATERIALS AND METHODS

RNA isolation for LRRK2 cDNA synthesis:

RNA was isolated from BE (3)-M17 dopaminergic neuroblastoma using Trizol reagent (Invitrogen) according to the manufacturer's instructions. However, after sequencing of cloned fragments, multiple mutations were present within all the different clones chosen. As a result, total brain RNA (Ambion) was purchased cDNA was prepared using SuperScript III First Strand Synthesis System for RT-PCR (Invitrogen). Manufacturer's protocol for Oligo dT reverse transcription were followed

Amplification of LRRK2 cDNA:

Overlapping cDNA fragments of LRRK2 were amplified using the primer pairs shown in Table 7.

Fragment (bp position)	Forward Primer	Reverse Primer
Amplicon 1 (1-1261)	ATGGCTAGTGGCAGCTGTCA	CATTCGCAGATGCCTGGAAA
Amplicon 2 (1107-3094)	CGCATGCTGGGCACTAAATA	CACATAGCTGTTGTGGAAAGC
Amplicon 3 (2385-4717)	CCTGGATGTGGCCAACAATA	CTGCGTGAGGAAGCTCATTT
Amplicon 4 (3373-4717)	CCCTTGAGACTGAAGGAACT	CTGCGTGAGGAAGCTCATTT
Amplicon 5 (4337-6227)	CTGTGATTCTCGTTGGCACA	CCCTCTACTATTCTACCTCC
Amplicon 6 (5041-7584)	GAGCTTCCCCATTGTGAGAA	ATGAGACGAACATCTGTTGAGTAA

Table 7: Primers used to amplify portions of LRRK2 cDNA

PCR mix for amplification of LRRK2 cDNA fragments:

Component	Amount per reaction
ddH_2O	40.6ul
10x cloned Pfu reaction buffer	5.0ul
dNTPS (25mM each dNTP)	0.4ul (Final concentration of each dNTP – 200μM)
cDNA template (10ng/ul)	1.0ul
Forward Primer (10μM)	1.0ul (Final concentration of Primer 200μM)
Reverse Primer (10μM)	1.0ul (Final concentration of Primer 200μM)
PfuTurbo DNA polymerase (2.5U/ul)	1.0ul
Total Reaction volume	50ul

LRRK2 cDNA PCR cycling conditions and cloning:

1 cycle	95°C	2mins
4cycles	94°C	30secs
	60°C	30secs
	72°C	1min/kb
16cycles	94°C	30secs
	60°C (-0.4°C/cycle)	30secs
	72°C	1min/kb
4cycles	94°C	30secs
	50°C	30secs
	72°C	1min/kb
1cycle	4°C	HOLD

Amplified fragment were run on 1% agarose gels and bands matching expected sizes, were extracted using a gel extraction kit (Qiagen) as per manufacturer's instructions. Isolated fragments were A-tailed using the following procedure:

1. 7µl of purified PCR product
2. 1ul 2mM dATP
3. 1ul 10x PCR buffer
4. 1ul Taq DNA polymerase (Qiagen:1U/µl)
5. Products were incubated at 70°C for 30 minutes

A-tailed PCR products were cloned into the pGEM-T easy vector system (Promega) as per manufacturer's instructions. Disruption of the LacZ reporter gene was used to identify insert positive clones. Clones were subsequently grown in ampicillin -containing media and plasmids extracted using the plasmid extraction kit (Qiagen) as per manufacturer's instructions. Plasmids were sequenced (General sequencing protocol pg 55-56) with appropriate primers (Table 8) in addition to M13 forward and reverse primers.

A non-synonymous change was introduced into Amplicon 2 (1107bp-3094bp) to remove an MscI site and aid in the cloning protocol. The plasmid was subsequently re-sequenced in its entirety to ensure no additional mutations were created. A variety of different primers were designed to sequence LRRK2 cDNA (Table 8).

	Forward	Reverse
cDNA1	CGAAGAGGACGAGGAAACTCT	TCGCGACTCTCATATAGGAG
cDNA2	CCTCCAAGTTATTTCAAGGC	TGGTGAACACCAAGGACTTC
cDNA3	GTGGGTTGGTCACTTCTGT	GTTAGGAGGAGATCTAAGGTC
cDNA4	GCCAGTGTAAACTTGTCAGTG	TGGCTGGAAATGAGTGCATG
cDNA5	TGCCATGCACTCATTTCCAG	GTAAGCCTATGGAGCAAACAGC
cDNA6	GTGGAAGTCCTCATGAGTG	CTGCAATGCTGCATTCTCTG
cDNA7	CGAAGTCCATGAGTTTGTGG	TTTGTAACAGGCTTCCAGCC
cDNA8	GGCTGGAAGCCTGTTACAAA	GGCCATCTTCATCTCCAATC
cDNA9	CGCATGCTGGGCACTAAATA	CATTCGCAGATGCCTGGAAA
cDNA10	GCTCATAGGGAAGTGATGCT	ACAGCCACTTTCAGCCACTT
cDNA11	TGAAGTGGCTGAAAGTGGCT	GCTGCACTGGTAATGATGTC
cDNA12	CCCTGGATATAATGGCAGCA	CCTGTTCAAAGCTGCTAGGA
cDNA13	CCAGGGAGGATACAGAAT	GGATACATCTGCAGTGTG
cDNA14	TATCCCTGGAAGGTGCTATG	CAGCAGATGTCCAGTTCCTA
cDNA15	ATAGGAACTGGACATCTGCTGG	GAATGATGCACCAGCAGCTTAG
cDNA16	CTAAGCTGCTGGTGCATCATTC	GAAGATCCCTCCTTTGCTTG
cDNA17	TGCTAGAGAGAGCGTGTGAT	TATTGTTGGCCACATCCAGG
cDNA18	CCTGGATGTGGCCAACAATA	GAGCAAACACACTGTCCATAG
cDNA19	GTGCTGTGGAAGAAGGAACA	GGTGAGCAACGCTGTAATAC
cDNA20	GTATTACAGCGTTGCTCACC	CACATAGCTGTTGTGGAAAGC
cDNA21	CCCATATGAGGCATTCAGAC	AAACCACTGAGGGTCCAATG
cDNA22	ATGACATTGGACCCTCAGTG	CTCTCCACTTTAGGACAAGC
cDNA23	CCCTTGAGACTGAAGGAACT	GAGGCAAGAAAGGCATAGCA
cDNA24	TGCTATGCCTTTCTTGCCTC	CAAAGATTTCCAGTGTGCGG
cDNA25	CCGCACACTGGAAATCTTTG	ACAGCCAATCTCAGGAGGAA
cDNA26	TCCTCCTGAGATTGGCTGT	CCCACACATTTAGGACGAGA
cDNA27	GCATAGATGTGAAAGACTGGCC	TGAAGAGCCAAGGCTTCATG
cDNA28	GAGCATTGTACCTTGCTGTC	GTGGTAATCTCGTATGGCAG
cDNA29	CTGTGATTCTCGTTGGCACA	CTGCGTGAGGAAGCTCATTT
cDNA30	TCAGCTTGTTGTTGGACAGC	TGCAGTGCTGGGTCTTGAAA
cDNA31	GGAACCCAAGTGGCTTTGTA	CGCGAAATAATGCCCTTAGG
cDNA32	CCTAAGGGCATTATTTCGCG	GTTCTCACAATGGGGAAGCT
cDNA33	GAGCTTCCCCATTGTGAGAA	GACAATAAGCTTCAGGAGACC
cDNA34	GGTCTCCTGAAGCTTATTGTC	AATCTCCAGCAACCCAGGAA
cDNA35	TTCCTGGGTTGCTGGAGATT	TTCTAGGCAGGTCAGCCAAA
cDNA36	GATCAACCAAGGCTCACCAT	TTCTCCTTCATAGGCTGCTC
cDNA37	GAGCAGCCTATGAAGGAGAA	TTTGTCCTGCTGAAGCAGG
cDNA38	GATATCTTTGCTGGCAGCTG	CAATGCCGTAGTCAGCAATC
cDNA39	GATTGCTGACTACGGCATTG	CCCTCTACTATTCTACCTCC
cDNA40	CCTGAAGTTGCCAGAGGAAA	TTCTCAACCATAGGCCATGG
cDNA41	CCATGGCCTATGGTTGAGAA	CCCAGCCAAAATGCTTGCATT
cDNA42	GGAATGCAAGCATTTGGCTG	CTTCGGTATTGATGACCAGG
cDNA43	ATTGTGTCTGGGACACAGTC	CTAACTTGCCATCAGCGGTT
cDNA44	GAACCGCTGATGGCAAGTTA	AATCTTTGTGCCACATCCTCCC
cDNA45	GGGAGGATGTGGCACAAAGATT	GTGCACGCAGTCTATTAGTC
cDNA46	GTGGACTAATAGACTGCGTG	GCTGTGCTGTCATCATGACT
cDNA47	GCTCTTTGGATAGGAACTGG	TTCCGGTTGTAGCCCAATAC
cDNA48	GTATTGGGCTACAACCGGAA	CGACAAGCAATAGTCCTGTC
cDNA49	TGTAAAACGACGGCCAGT	CAGGAAACAGCTATGACC

Table 8: List of primers used to sequence LRRK2 cDNA. M13 primers were also used to sequence 5' and 3' ends of the cDNA. All non-synonymous sequence differences between cDNA cloned and published sequence (NM-198578) were confirmed as polymorphisms and not altered.

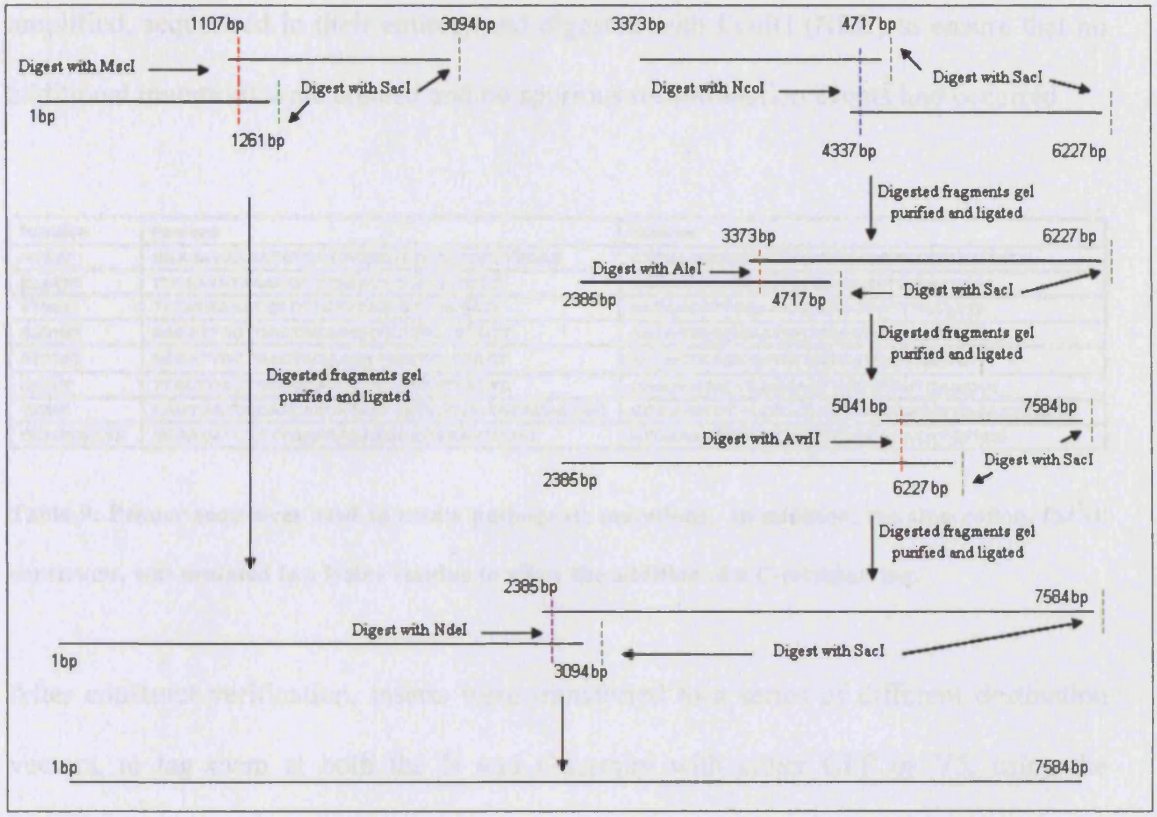

Figure 14: Schematic representation of cloning strategy employed to clone LRRK2 cDNA. All fragments were TA cloned into the pGEMT easy vector. This was done to use the unique SacI site (----) in the poly-linker of pGEMT easy vector.

Once the cDNA was constructed in the pGEM-T easy vector (Figure 14), the cDNA was re-amplified using primer cDNA1 forward and cDNA49 reverse (Table 8; LRRK2 cDNA PCR cycling conditions and cloning, pg 87) and ligated into the pCR®8/GW/TOPO vector (Invitrogen). Once positive clones were identified, the insert was sequenced (General DNA sequencing reaction, pg 55-56) for orientation (5'-3') and for the presence of additional mutations. After the identification of a correct clone, a series of mutagenesis reactions were performed using XL-site directed mutagenesis kit to remove the stop codon and introduce various mutations (Table 9). Clones with mutations were

amplified, sequenced in their entirety and digested with EcoRI (NEB) to ensure that no additional mutations were created and no spurious recombination events had occurred.

Mutation	Forward	Reverse
I1122V	GGAAATAAAATATCAGGGGTATGCTCCCCCTTGAG	CTCAAGGGGGAGCATATCCCCGATATTTTATTTCC
R1441C	TTCAATATAAAGGCTTGCGCTTCTTCTTCCC	GGGAAGAAGAAGCGCAAGCCTTTATATTGAA
Y1699C	TATATGAAATGCCTTGTTTTCCAATGGGATT	AATCCCATTGGAAAACAAGGCATTTCATATA
G2019S	AAGATTGCTGACTACGGCATTGCTCAGTACT	AGTACTGAGCAATGCTGTAGTCAGCAATCTT
G2019D	AAGATTGCTGACTACGACATTGCTCAGTACT	AGTACTGAGCAATGTCGTAGTCAGCAATCTT
I2020T	TTGCTGACTACGGCACTGCTCAGTACTGCTG	CAGCAGTACTGAGCAGTGCCGTAGTCAGCAA
T2356I	CAGTGATTCCAACATCATAATAGTGGTGGTAGACACTGC	GCAGTGTCTACCACCACTATTATGATGTTGGAATCACTG
OCH2528LYS	CGAACATCTGTTGAGAAAAAGGGCGAATTCGAC	GTCGAATTCGCCCTTTTTCTCAACAGATGTTCG

Table 9: Primer sequences used to create pathogenic mutations. In addition, the stop codon, for all constructs, was mutated to a lysine residue to allow the addition of a C-terminal tag.

After construct verification, inserts were transferred to a series of different destination vectors, to tag them at both the N and C-termini with either GFP or V5, using the Gateway LR clonase reaction (Invitrogen) using the manufacturer's protocol. Mutations (Table 9) were also created on a 'kinase dead' background in which three critical residues within the kinase domain had been mutated to theoretically make a non-functional kinase (K1906A, D1994A and D2017A).

Mammalian cell expression of LRRK2:

For mammalian cell transfection, prepare full length LRRK2 using the Endofree maxi kit (Qiagen). Modifications to manufacturer's protocols are as follows. Treat LRRK2 plasmids as low copy plasmids:

1) Grow plasmids in a overnight culture volume of 300ml
2) After the protein precipitation step, spin lysates at 4500*g for 10 mins prior to loading onto QiaFilter cartridge.

3) Warm DNA elution buffer to 55°C prior to DNA elution

Measure the DNA concentration and purity. Only use plasmids with an A^{260}/A^{280} above 1.8 for transfections.

Mammalian cell transfections

Mammalian cell transfections were carried out in COS-7, HEK and SY5Y cells. Cells were maintained in Opti-MEM I (Invitrogen) supplemented with 10% fetal bovine serum and grown with 5% CO_2. Transfections were performed using Fugene transfection reagent (Roche).

Plate cells at $1x10^6$ cells per $10cm^2$ cell culture dish in serum containing media. The following day, replace media with serum free media and transfect as per manufacturer's recommendations. The ratio of transfection agent to DNA to use is 3:1. Add transfection agent/DNA mix to the cells and replace the media the following day, with serum containing media. Harvest cells 48hrs post transfection to run on SDS page and western blot.

Protein Extraction from mammalian cells:

Solutions:

Wash Buffer

TBS (used ice cold)

- 137mM NaCl 8g/litre
- 2.7mM KCl 0.2g/litre
- 25mM Tris Base 3g/litre

Extraction Buffer:

- 10mM Tris.HCl pH 7.4; 2% SDS; Protease Inhibitor

Method:

1. Wash each cell line twice with 4ml of cold wash buffer.
2. Add 1ml wash buffer and scrape cells from flask into microfuge tube.
3. Pellet 5000g, 5min 4°C.
4. Resuspend pellet in 50µl of extraction buffer and sonicate 10sec (1second pulses).
5. Store at –80°C following the removal of an aliquot for BCA protein assay (PIERCE) as per manufacturer's protocol.

Western blot protocol:

Solutions for western blotting:

- Tris-Glycine SDS sample buffer Laemelli (2x). Add 5% (v/v) β-mercaptoethanol (Sigma) to an aliquot immediately before use.
- Tris-Glycine SDS running buffer: dilute 1:10 from stock (Biosource)
- 10x transfer buffer: 100 mM CAPS, pH 11.0: 22.13 g CAPS (Sigma) in approx. 800 ml water, pH to 11.0 with 1M NaOH, make up to 1 liter and store at 4°C.
- Transfer buffer: 10 mM CAPS (SIGMA), 10% methanol.
- TBS-Tween (TBS-T) (20 mM Tris.HCl, pH 7.6, 137 mM NaCl, 0.1% Tween). Dilute 10x TBS (Biosource) and add 1mL Tween 20 (Sigma) per liter.
- Block buffer: 5% dried skimmed milk powder in TBS-T
- ECL + reagents (Amersham)

Method for Western blotting:

1. Mix protein extracts in a ratio of 1:2 with 2x sample buffer (plus β-mercaptoethanol) and heat 65°C, 15 mins (or 90°C, 5 mins).
2. Assemble sufficient 4-20% Tris-glycine gel(s) (Biorad Ready Gels) in 1x Running buffer.
3. Load 10μg total protein per lane. Load stained biotinylated markers.
4. Run gel(s) at 120V constant till sufficient separation of ladder and loading dye front has migrated out of the gel.
5. Towards the end of the gel run: pre-wet PVDF membrane (Millipore, Immobilon P) with methanol (~30s), then water (~2 min) then 1x Transfer buffer. Soak two pieces of filter paper per gel in 1x transfer buffer. Once the gel has run, also soak this in 1x transfer buffer for approx 5 min.
6. Assemble the transfer stack with the membrane towards the positive electrode.
7. Transfer overnight at 30V.
8. Remove membrane from transfer tank. Rinse in TBST once.
9. Block in block buffer - 1h.
10. Primary antibody: Appropriate antibody (generally 1:2000) in block buffer for 1hr.
11. Wash TBST, 3x5 min.
12. Appropriate secondary antibody: anti-mouse Ig, HRP conjugated (Jackson labs) 1:5000 in block buffer. Also incubate markers with Streptactin (BioRad) 1:1500 in TBST. 1h at room temperature.
13. Wash TBST, 3x5 min.

14. Mix ECL+ reagents 1+2 together according to product insert (Amersham).

    Incubate blot in this 5 min.

15. Expose blot to BIOMAX film (KODAK) for appropriate amount of time.

    Develop film in the automatic developer.

Preparation of Primary Rat Cortical Neurons

Solutions for the preparation of primary rat cortical neurons:

Papain solution

- 250µl of 0.1% DNAase (Worthington Biochemical Corp)
- 500µl of EBSS (Sigma)
- Papain (Worthington – 199 units)

STOP solution

- 250µl of 0.1% DNAase (Worthington)
- 0.6mg of Papain Inhibitor (Worthington)
- 5.4ml of EBSS (Sigma)

10/10

- 10ml EBSS (Sigma)
- 0.1g BSA (Sigma)
- 0.1g Trypsin Inhibitor (Sigma)

Modified neurobasal Media

- Neurobasal Media (Invitrogen)
- 10ml 200mM stock Glutamine (Sigma)
- 10ml B27 (Invitrogen)
- Filter sterilize media

Method for the preparation of primary rat cortical neurons:

Dissected rat brain from E18 pups was kindly provided to us by Dr. Kesavapany.

1. Coat plates/coverslips (22mm) with poly-L-lysine (Sigma, 2mg/ml) either at room temp overnight or in 37 °C incubator for 1-2 hours.
2. Wash with distilled water and leave to dry
3. Place cortex in papain solution and triturate with 5ml pipettes 10 times. Incubate solution for 40 minutes at 37°C with mixing every 10 minutes
4. Triturate the sample a further 10 times with a 5ml pipette
5. Centrifuge for 5 minutes at 1000rpm
6. Remove supernatant and discard
7. Add 3ml of STOP solution and triturate a further 2-3 times. Incubate at room temp for a further 10 minutes
8. Gently pipette supernatant into 10/10 solution
9. Centrifuge at 800rpm for 10 minutes
10. Add modified neurobasal media and count cells.
11. Plate $5x10^5$ neurons per 22mm coverslip

Transfection of Primary Rat cortical neurons

Allow neurons to attach to cover slips and recover for 3 days before proceeding to transfection. On the third day, remove neurobasal media from neurons (conditioned media) and store at 37 °C. Add fresh modified neurobasal media. Add DNA to Lipofectamine 2000 (Invitrogen) as per manufacturers' instructions. Add DNA/Lipofectamine complex to neurons for 6 hours before replacing with conditioned media. Fix cells after 72 hours.

Immunocytochemistry of mammalian cells and rat primary cortical neurons

Solutions:

•PFA recipe: Heat 50 ml distilled water in a fume cupboard to about 50°C. Add 4g paraformaldehyde with stirring. As it stirs in, add a few drops of 1M NaOH until the solution clears. Remove from the heat and allow to cool. Add 10 ml of 10x PBS. Check the pH (should be 7.2 – 7.4, adjust with HCl if needed) and make up to 100 ml with water. Store at 4°C for up to a week. Before use, allow to come up to room temperature.

Method:

1. Fix with 4% PFA in PBS, pH 7.2 –7.4 for 30min RT
2. Wash out excess fixative with PBS (3 times)
3. Permeabilize with 0.1% (w/v) saponin in PBS, 10 minutes
4. Quench excess fixative by incubating with 0.1M Glycine in PBS, 20 min, RT
5. Block buffer with 5% FCS, 5% Goat serum in PBS 1hr

6. Primary antibody; Monoclonal antibody/s 1:200 (Anti-GFP or Anti-MYC – ROCHE) and/or Rabbit polyclonal anti-p139 TAU - O/N 4°C.

7. Wash cells with PBS, 3x5 minutes

8. 2° antibody e.g., Goat anti-mouse IgG/AlexaFluor 568 or Goat anti-rabbit IgG/AlexaFluor 488, 1:200 in block buffer, 1h RT

9. Wash cells with PBS, 3x5 minutes and counterstained with 1μM TO-PRO3 (Molecular Probes).

10. Mount under ProLong antifade kit (Molecular probes)

11. Slides examined using a Zeiss LSM510 META confocal microscope

Confirmation of LRRK2 self interaction:

From yeast two hybrid results, LRRK2 was also able to bind to itself. Differentially tagged versions of LRRK2 were co-transfected into COS-7 cells and immunoprecipitated (Co-immunoprecipitation protocol, pg149-153) to determine if LRRK2 could bind to itself in mammalian cells.

RESULTS

Cloning and mammalian cell expression of LRRK2 cDNA:

At the onset of this study, LRRK2 was only a predicted gene with short cDNA expression clones as evidence. To confirm and construct the full transcript length of LRRK2, several overlapping fragments were amplified from brain cDNA. Sequencing of the cDNA fragments yielded a transcript with an open reading frame of 7584bp encoding a

2527 amino acid protein (Figure 15). One deviation in the LRRK2 amino acid sequence from (XP-935913) was found at position 150bp (A50H). This nonsynonomous change is a reported polymorphism (db SNP accession no. rs2256408) so was therefore not altered.

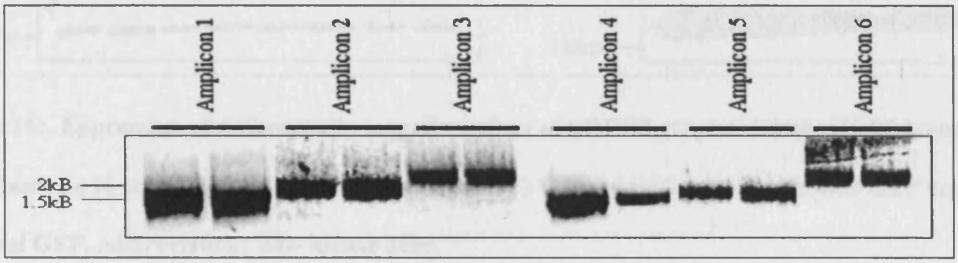

Figure 15: PCR products of overlapping fragments for LRRK2. Table 7 shows primer sequences used for each amplicon.

The complete LRRK2 cDNA was cloned into several gateway entry vectors, various mutations were created (Figure 14, Table 9) and subsequently transferred into mammalian expression plasmids with a GFP or V5 tag either at the N or C - terminus. Verified constructs were transiently transfected into COS7, HEK 293 and SY5Y cells (Figure 16; data not shown for HEK and SY5Y cells) and analyzed by western blotting using antibodies directed against the appropriate tag.

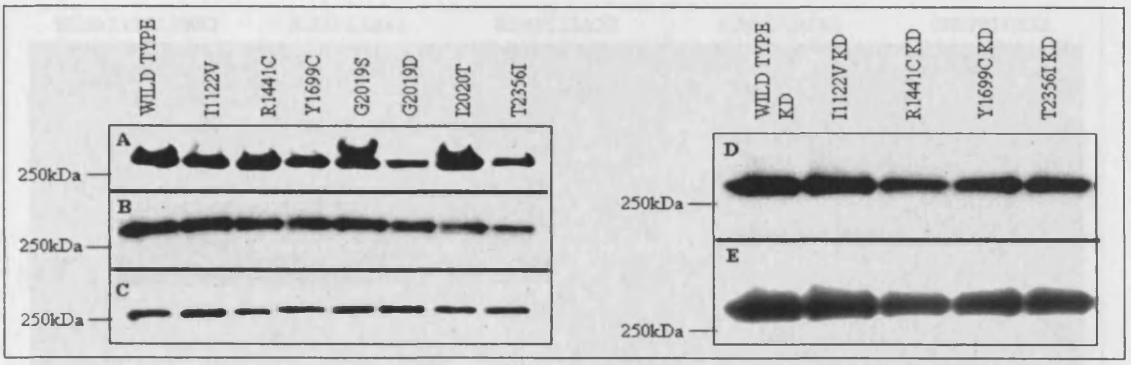

Figure 16: Expression of differentially tagged versions of LRRK2 extracted from COS7 mammalian cells. Panel A) N-terminal GFP, B) C-terminal GFP, C) C-terminal V5, D) N-terminal GFP and E) C-terminal GFP. Abbreviation: KD- kinase dead.

All forms of tagged LRRK2 (GFP or V5; Figure 16), either N or C-terminal tagged, produced a single band of approximately 280KDa (V5 tagged) or 300kDa (GFP-tagged).

Localization of LRRK2

To determine the cellular localization of LRRK2, COS7 cells were transiently transfected with LRRK2 (mutant, wild type and the appropriate kinase dead) tagged with either GFP or V5 at the N or C terminus. Transfected cells were fixed, stained and imaged using confocal microscopy. Preliminary analysis of LRRK2 localization in COS7 cells suggested the protein was primarily cytoplasmic (Figure 17 and 18; Data not shown for C tagged GFP-LRRK2 and N tagged V5-LRRK2). There was no discernable difference in localization between N and C tagged forms of wild type or mutant forms of LRRK2, and differentially tagged versions of LRRK2 (GFP or V5).

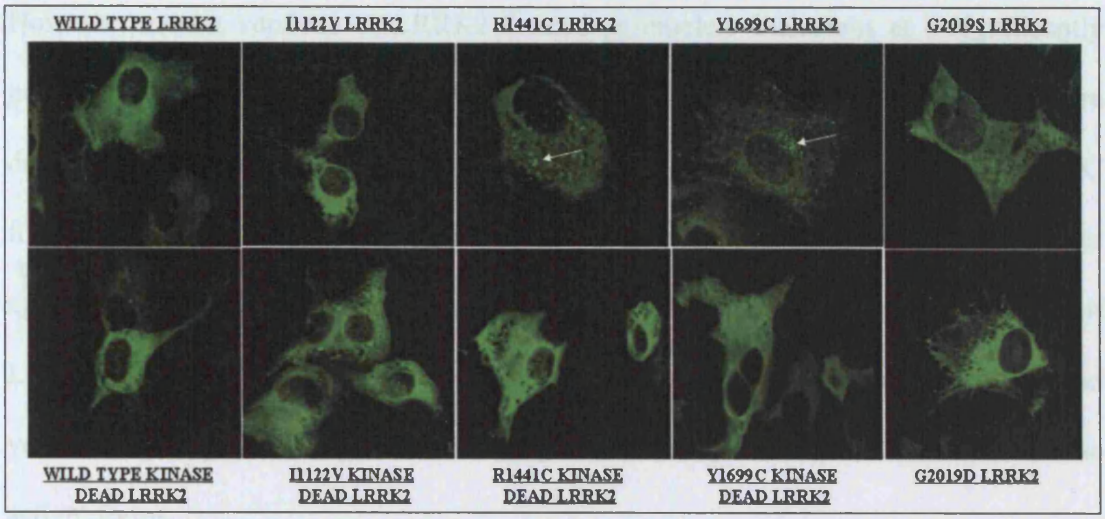

Figure 17: Immuno-staining of COS7 cells transfected with N-terminal GFP tagged LRRK2. Cells were stained with mouse anti-GFP and secondary goat anti mouse IgG AlexaFluor 488. Cells were fixed and analyzed with confocal microscopy. Mutant forms of LRRK2, notably R1441C and Y1699C, formed perinuclear inclusion bodies indicated by white arrows. Magnification x63.

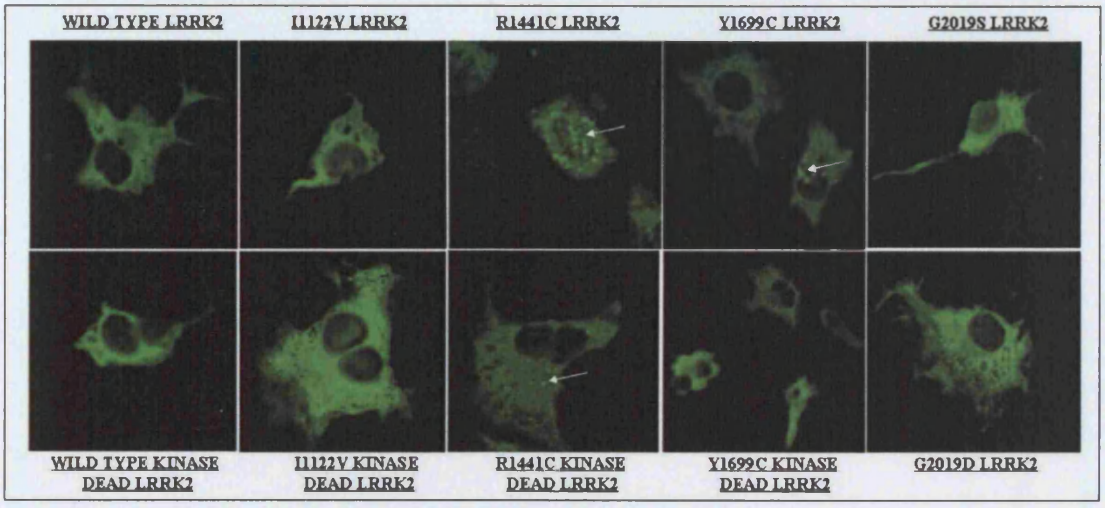

Figure 18: Immunostaining of COS7 cells transfected with C-terminal V5 tagged LRRK2. Cells were fixed and stained with mouse anti αGFP and goat anti mouse IgG AlexaFluor 488. Cells were analyzed with confocal microscopy. Mutant forms of LRRK2 formed perinuclear inclusion bodies indicated by white arrows. Magnification x63

However, mutant versions of LRRK2 formed perinuclear inclusions at a significantly greater rate than wild type (Figure 17 and 18, white arrows). Some mutations were more dramatic in their ability to form inclusion bodies. For example, R1441C and Y1699C formed larger inclusion bodies whereas G2019S and G2019D formed fewer and smaller aggregates. To determine if inclusion body formation required the kinase activity of LRRK2, cells were transfected with the corresponding kinase dead mutant. Kinase-dead versions of the protein formed significantly fewer inclusion bodies than mutant 'kinase active' forms.

Next we wished to determine if LRRK2 mutant aggregate formation was unique to overexpression in COS7 cells or a general property of the protein. The LRRK2 constructs were transfected into HEK 293, SY5Y and primary rat neurons (Figure 19 and 20).

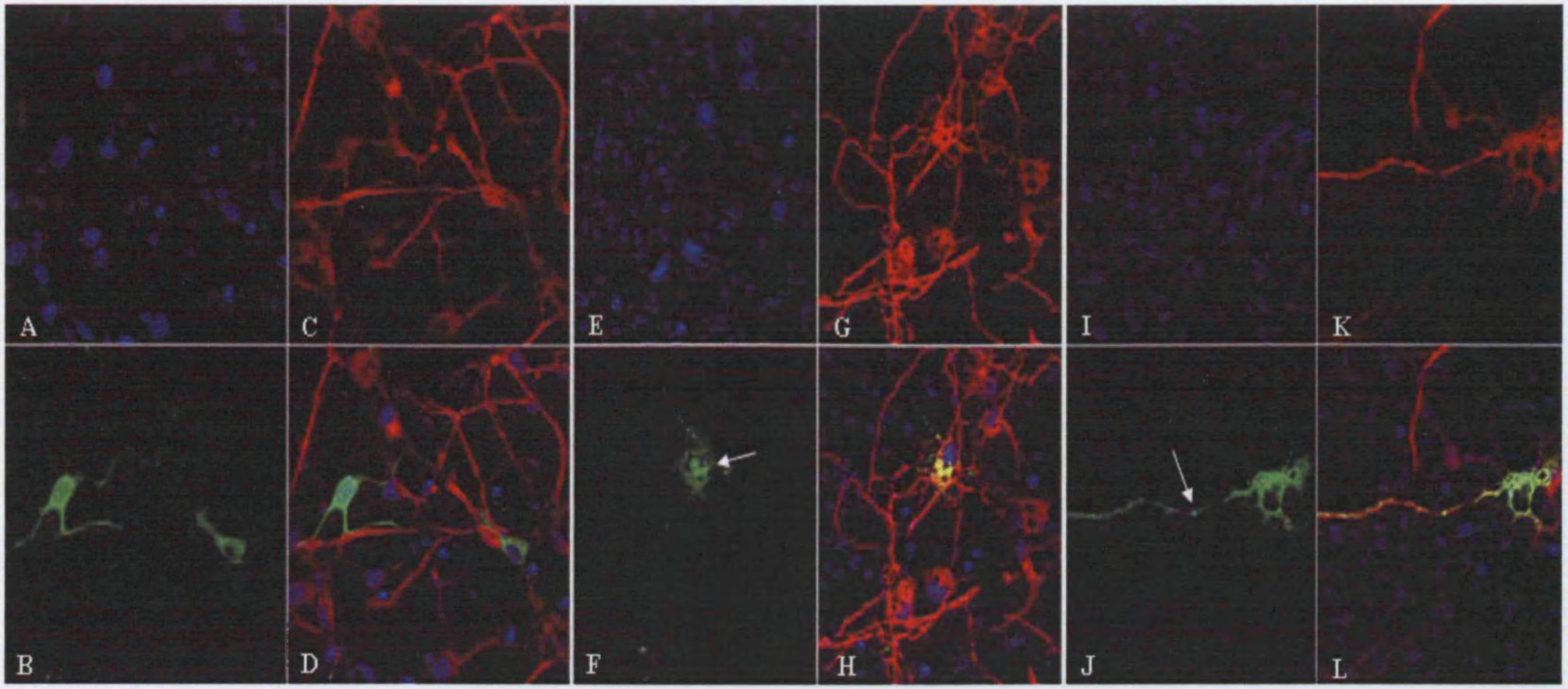

Figure 19: Primary rat E18 rat cortical neurons transfected with N-terminus Myc tagged LRRK2. Cells were stained with mouse-αGFP, rabbit-phospho TAU and counterstained for nuclei using DAPI. Secondary antibodies used were anti-mouse AlexaFluor 488 (green) and anti-rabbit AlexaFluor 568 (red). (A-D) Wild type LRRK2; (E-H) R1441C LRRK2; (I-L) Y1699C LRRK2. Upper left of each quadrant (A, E, I) shows DAPI staining of nuclei. The upper right of each quadrant shows (C, G, K) shows staining for phospho-TAU. Bottom left of each quadrant (B, F, and J) is the staining for LRRK2. Bottom left of each quadrant (D, H, and L) is the merged version of the three channels. LRRK2 inclusion bodies are indicated by white arrows (F, J). Magnification x63.

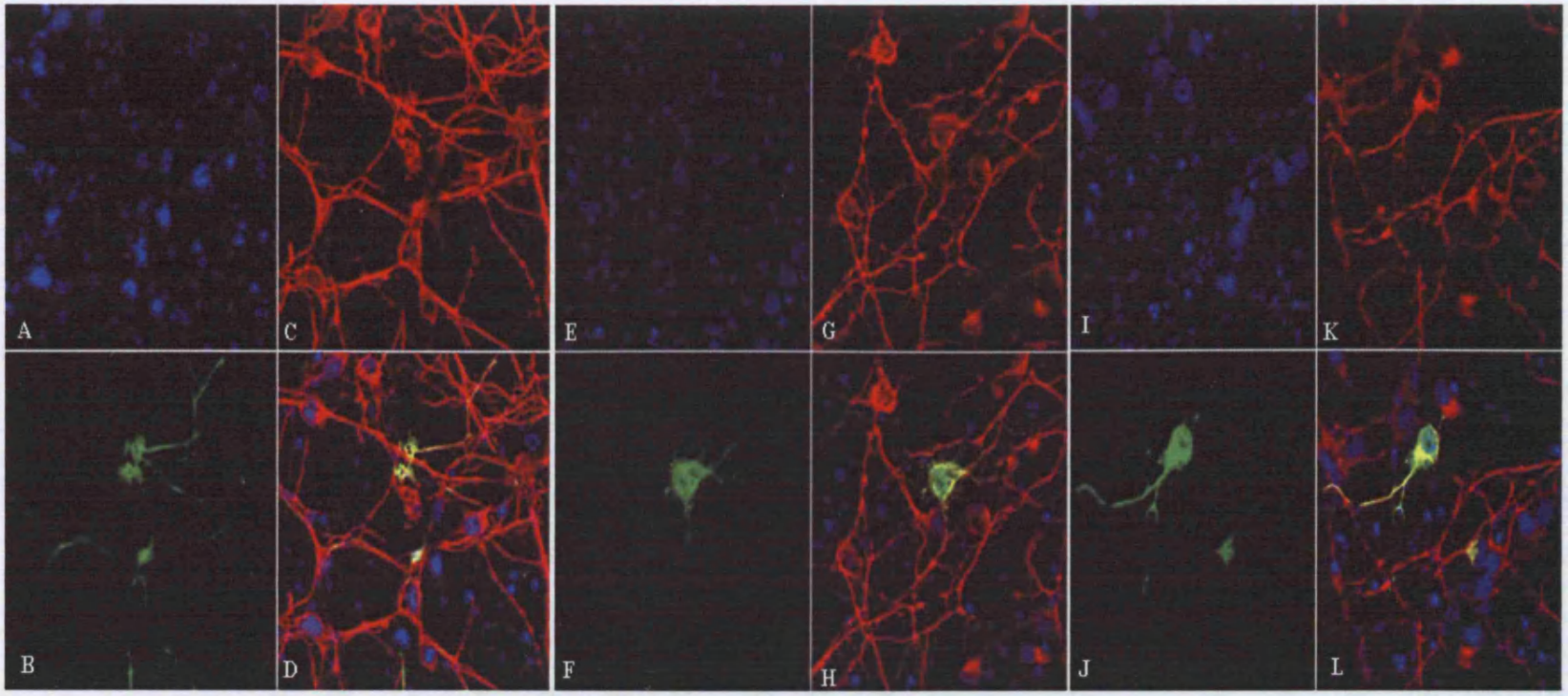

Figure 20: Primary E18 rat cortical neurons transfected with N-terminus Myc tagged LRRK2 kinase dead constructs. Cells were stained for with mouse-anti GFP, rabbit anti-phospho TAU and DAPI for DNA. Secondary antibodies used Ig anti-mouse AlexaFluor 488, anti-rabbit AlexaFluor 568. (A-D) Wild type kinase dead LRRK2; (E-H) R1441C kinase dead LRRK2; (I-L) Y1699C kinase dead LRRK2. Upper left of each quadrant (A, E, I) shows DAPI staining of individual nuclei. The Upper right of each quadrant shows (C, G, K) shows staining for phospho-TAU. Bottom left of each quadrant (B, F, and J) is the staining for LRRK2. Bottom left of each quadrant (D, H, and L) is the merge of all three images. Magnification x63.

Primary rat cortical neurons were transfected and stained for MYC-LRRK2 and the neuronal marker protein, TAU and analyzed by confocal microscopy (Figures 19 and 20). Mutant forms of the protein formed significantly greater number of inclusion bodies compared to wild type LRRK2, which was distributed throughout the cytoplasm and along neuronal processes. Quantification and characterization of the aggregates' formed by LRRK2 were carried out by Dr. Greggio as reported elsewhere (See Manuscripts published during thesis; Greggio et al, 2005) [409].

Self interaction of LRRK2

A yeast two hybrid was performed to identify potential protein interactors of LRRK2 (Chapter 4). A region encompassing LRRK2 RAS domain, bound to three different regions of LRRK2 (18-186aa, 1123-1200aa and 2084-2217aa). To validate the self interaction, differentially tagged versions of LRRK2 were transfected into mammalian cells and immunoprecipitated. DJ-1 was used as a non-specific control for LRRK2 self interactions, as numerous studies have been undertaken to identify DJ-1 interactors [121, 210, 211, 229, 231] and none of the studies have identified LRRK2 as an interactor.

Immunoprecipitation of V5-LRRK2 followed by GFP blotting, detected the presence of GFP-LRRK2 (Figure 21; Lanes 1 and 2). The converse was also true (Figure 21; Lane 3 and 4). V5 or GFP-LRRK2 did not precipitate in absence of the other (lane 5-8) and GFP-LRRK2 did not precipitate in the presence of DJ-1 (Figure 21; 9-12).

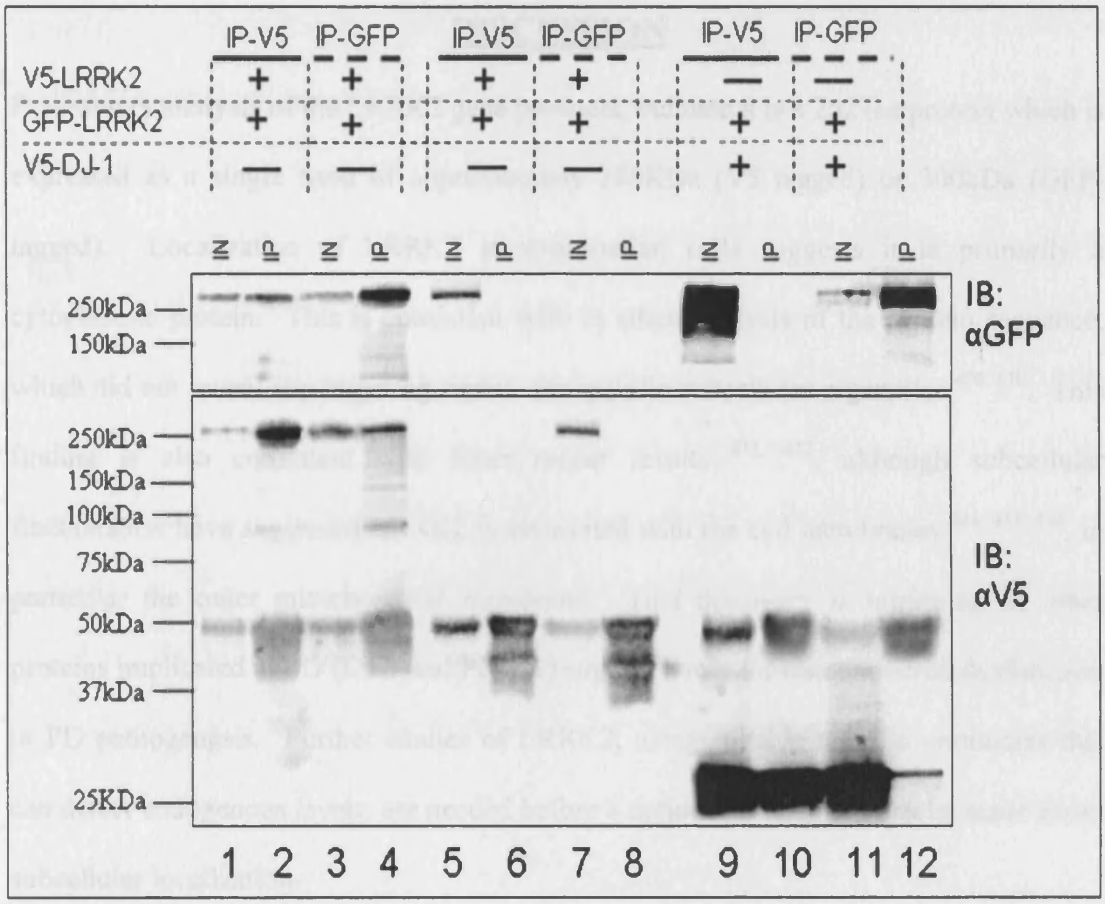

Figure 21: Self interaction of LRRK2. Precipitations were performed as described on pg151-153. Lysis and Wash conditions: 50mM Tris pH7.5, 5mM EDTA, 150mM NaCl, 0.25% NP-40, protease cocktail inhibitor (Roche) and HALT (PIERCE). Monoclonal GFP (Roche) and monoclonal V5 (Invitrogen) were used. Precipitation of V5 or GFP tagged LRRK2 resulted in the immunoprecipitation of either GFP or V5 tagged LRRK2 respectively (Lane 1-4). LRRK2 did not precipitate when transfected in alone (Lane 5-8) or in the presence of V5-DJ-1 (Lane 9-12) demonstrating there is no non-specific binding of LRRK2 to either the antibody or the protein agarose. Abbreviations: IN-Input; IP-immunoprecipitation.

DISCUSSION

Preliminary analysis of the LRRK2 gene products, indicate it is a 2527aa protein which is expressed as a single band of approximately 280KDa (V5 tagged) or 300kDa (GFP-tagged). Localization of LRRK2 in mammalian cells suggests it is primarily a cytoplasmic protein. This is consistent with in silico analysis of the protein sequence, which did not reveal any targeting signals for specific subcellular organelles [400, 410]. This finding is also consistent with other recent results [411, 412], although subcellular fractionation have suggested LRRK2 is associated with the cell membranes [411, 413, 414], in particular the outer mitochondrial membrane. This discovery is intriguing as other proteins implicated in PD (DJ-1 and PINK1) suggest a role for mitochondrial dysfunction in PD pathogenesis. Further studies of LRRK2, using suitable specific antibodies that can detect endogenous levels, are needed before a definitive statement can be made about subcellular localization.

Compared to wild type LRRK2, transient transfections of mutant versions did not change its localization, but did form perinuclear inclusions at a significantly higher frequency than wild type protein [409, 415]. This finding was subsequently replicated in a number of different cell types (HEK293, SY5Y and primary rat cortical neurons) suggesting it is not an artifact associated with over-expression in COS7 cells. As mutations within LRRK2 have been shown to increase kinase activity [409, 411, 414, 416], it was hypothesized that kinase activity was required for the formation of inclusion bodies. Thus 'kinase dead' [244] versions of wild type and mutant LRRK2 were created by replacing the lysine residue that orients the gamma-phosphate of ATP (K1906A), the active site aspartate (D1994A) and the aspartate that chelates divalent metal cations (D2017A) with alanine. Compared

to mutant versions of LRRK2, the 'kinase dead' versions of the mutants formed inclusion bodies at a significantly lower rate [409].

In support of LRRK2 being able to form aggregates, the ROC domain of LRRK2 bound to several regions of LRRK2 (the N-terminus-18-186aa, the LRR domain-1123-1200aa and the WD40 domain-2084-2217aa) in a yeast two hybrid screen (Chapter 4). This interaction was subsequently re-created in mammalian cells and replicated by two other groups [414, 417]. It has been suggested that homo-dimerization may be necessary for the function and/or activation of LRRK2 [414]. Other proteins similar to LRRK2, such as DAP-kinase, MLK-3 or Raf-1 [399, 400, 406, 418], require homodimerization for their function [419]. It remains to be seen if endogenous LRRK2 naturally exists as a dimer and whether this is relevant to the apparent tendency of the protein to form inclusion bodies, as is the case for α-synuclein [133, 420, 421]. Numerous methods can be employed to determine if LRRK2 can form higher order structures [422] such as analysis on non-denaturing western gels [423], various techniques based on light scattering [424, 425] or chromatography (e.g. gel filtration chromatography or fast protein liquid chromatography) [425].

As mutations within LRRK2 increase the formation of inclusion bodies, one might expect individuals with LRRK2 mutations to have LBs that are immunopositive for LRRK2. Very recently, LRRK2-positive dystrophic neurites were seen in nigral neurons from a G2019S mutation case [426]. In idiopathic PD cases, LRRK2 was seen in the cytoplasm of the cell bodies and neuronal processes but also stained the halo of 10-15% of LBs [409]. LRRK2 has subsequently been shown to be a component of LBs with some antibodies [427-429], although not all antibodies may specifically recognize LRRK2. There is, therefore, some in vivo evidence that LRRK2 can accumulate and form aggregates in

both familial and sporadic cases of PD. Additional studies are needed to determine if mutation of LRRK2 increases its propensity to aggregate by affecting its stability and/or degradation.

In addition to increasing the aggregation properties of LRRK2, mutant versions of LRRK2 are significantly more toxic to cells and primary neurons than wild type LRRK2 [409, 412, 415, 416]. Furthermore, the toxic effects of LRRK2 are associated with the kinase activity of LRRK2. Increasing the kinase activity of LRRK2 by introducing pathogenic mutations (Y1699C, G2019S) [409, 411] results in increased toxicity. The converse is also true; decreasing or abolishing kinase activity results in the loss of the toxic affects of mutant LRRK2 [409, 416]. Thus mutations within LRRK2 may lead to neuronal loss via an increase of kinase activity. The caveat with the studies to date is that the assays for kinase activity, autophosphorylation of LRRK2 in vitro, may not reflect a physiological activity and are therefore a limited measure of activity [409, 411, 412, 414]. A more physiological relevant substrate is required to determine if mutations within LRRK2 increase or affect its kinase activity.

CHAPTER 5: IDENTIFICATION OF PROTEIN INTERACTORS FOR LRRK2

INTRODUCTION

LRRK2 encodes a 2527 amino acid protein of unknown function but with multiple domains, as discussed in chapter 3. Sequence analysis indicates that LRRK2 is comprised of two enzymatic domains and several protein-protein interaction domains (Figure 22).

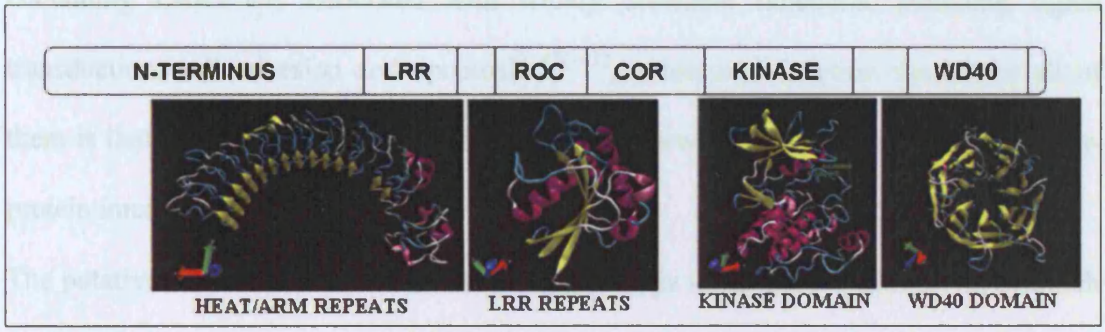

Figure 22: The predicted domains within LRRK2; the N-terminus containing HEAT/ARM repeats, LRR domain, ROC domain, COR domain, kinase domain and WD40 domain. The images below each domain are the predicted structures of that domain. These images were kindly provided by Dr. Jinhui Ding.

The predicted structure of the N-terminal region of LRRK2 (approximately 900aa) is not clearly defined. This region contains potential ARM repeats (residues 180–660) and ankyrin repeats (residues 690–860) [418] although some analyses suggest that this region is

similar to the HEAT repeats [400] which are unique to LRRK2. ARM and HEAT repeats are similar [401, 430] apart from the number of helices present [401]. Therefore, although the N-terminus has repeat units, there are questions about which exact motifs are present and how these are structured. Both ARM/HEAT repeats are involved in mediating protein-protein interactions, including those involved in nuclear transport, vacuolar transport, translation, and cytoskeleton organization, suggesting a range of potential roles for this region [400, 418, 430].

The LRR motif family, consist of 2-42 motifs of 20-30 amino acids in length [431] and are found in a variety of cytoplasmic, membrane and extracellular proteins. LRRK2 is predicted to contain 13 LRRs and based on structural modeling, folds into a horseshoe (or arc) shape with parallel β-strands followed by an α-helix [432]. Although proteins containing LRRs are associated with widely divergent functions, including signal transduction, cell adhesion and apoptosis [430-432], a common function shared for all of them is that they appear to provide a structural framework for the formation of protein-protein interaction [400, 431, 432].

The putative ROC GTPase domain of LRRK2 belongs to the ROCO family [399], in which the predicted GTPase (Roc) is always found in conjunction with a COR domain, the function of which is unknown. GTPases act as switches within the cell, cycling between GTP-bound (generally active conformation) and GDP-bound (inactive conformation) forms. GTPases are involved in a variety of cellular processes including vesicular trafficking and transport [433-435].

The kinase domain of LRRK2 was initially identified as part of the kinome project [396], and is predicted to be a mitogen-activated protein kinase kinase (MAPKKK) [400, 418]. This

signaling cascade activates a downstream MAP kinase kinase via activation-loop phosphorylation. Substrates of activated MAPKs are involved in a diverse range of functions such as transcription, mitochondria protein and cellular trafficking [436].

The C-terminus of LRRK2 contains a potential WD40 domain. WD40 domains have been identified in diverse proteins such as transcriptional regulators, RNA processing complexes and proteins involved in vesicle formation and trafficking proteins [399, 400, 418, 437]. Each WD40 repeat contains a four-stranded, antiparallel β-pleated sheet and, together, these repeats form a circular bladed propeller-like structure. The predicted WD40 domain of LRRK2 comprises seven such repeats. This seven-bladed propeller is thought to form a rigid platform for reversibly interacting with proteins, possibly including those that contain other WD40 domains [437, 438].

As these motifs are involved in numerous and diverse functions, a yeast two hybrid screen was undertaken to identify binding partners of LRRK2, to help elucidate the normal function of LRRK2.

MATERIALS AND METHODS

The yeast two hybrid systems was initially created [439] using the GAL4 protein which is comprised of two domains: the DNA binding domain and the activation domain. Without either of these domains, GAL4 protein is unable to bind to its consensus sequence and activate gene transcription. The bait protein, for which interactors are to be found, is fused to the DNA binding domain of the GAL4 protein. A library of proteins is fused to the activation domain and are referred to as the prey proteins. When the bait and prey protein interact, the DNA binding domain and the activation domain of the GAL4 protein are brought in close proximity and are able to activate the transcription of genes containing the GAL4 consensus sequence (Figure 23). Commonly used selection markers are auxotrophic mutants (histidine and adenine) and chromogenic mutants (LacZ). If the two proteins interact, these genes are transcribed and are able to grow on media lacking histidine and adenine. The β-galactosidase enzyme from the LacZ marker hydrolyzes X-gal to release a blue colored product, allowing for further selection of positively interacting proteins. The overall method used for the yeast two hybrid is displayed in figure 24.

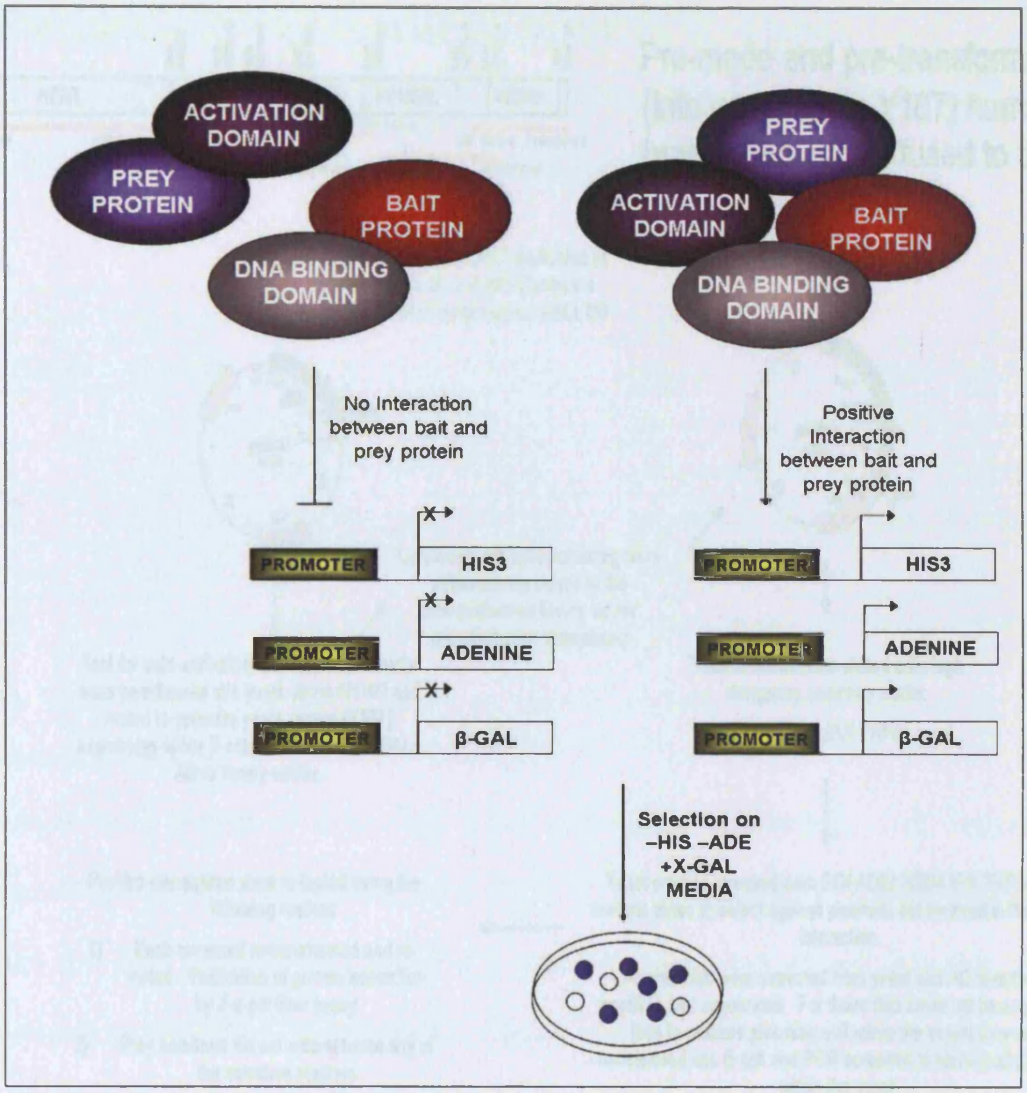

Figure 23: Schematic representation of a yeast two hybrid screen for protein-protein interactions. Only if the bait and prey protein interact can the DNA binding domain and activation domain be brought into close proximity and activate transcription of the various selection genes. Yeast that are able to grow on nutrient deficient media and are able to catalyze the break down of X-gal into a blue color are indicative of a positive interaction.

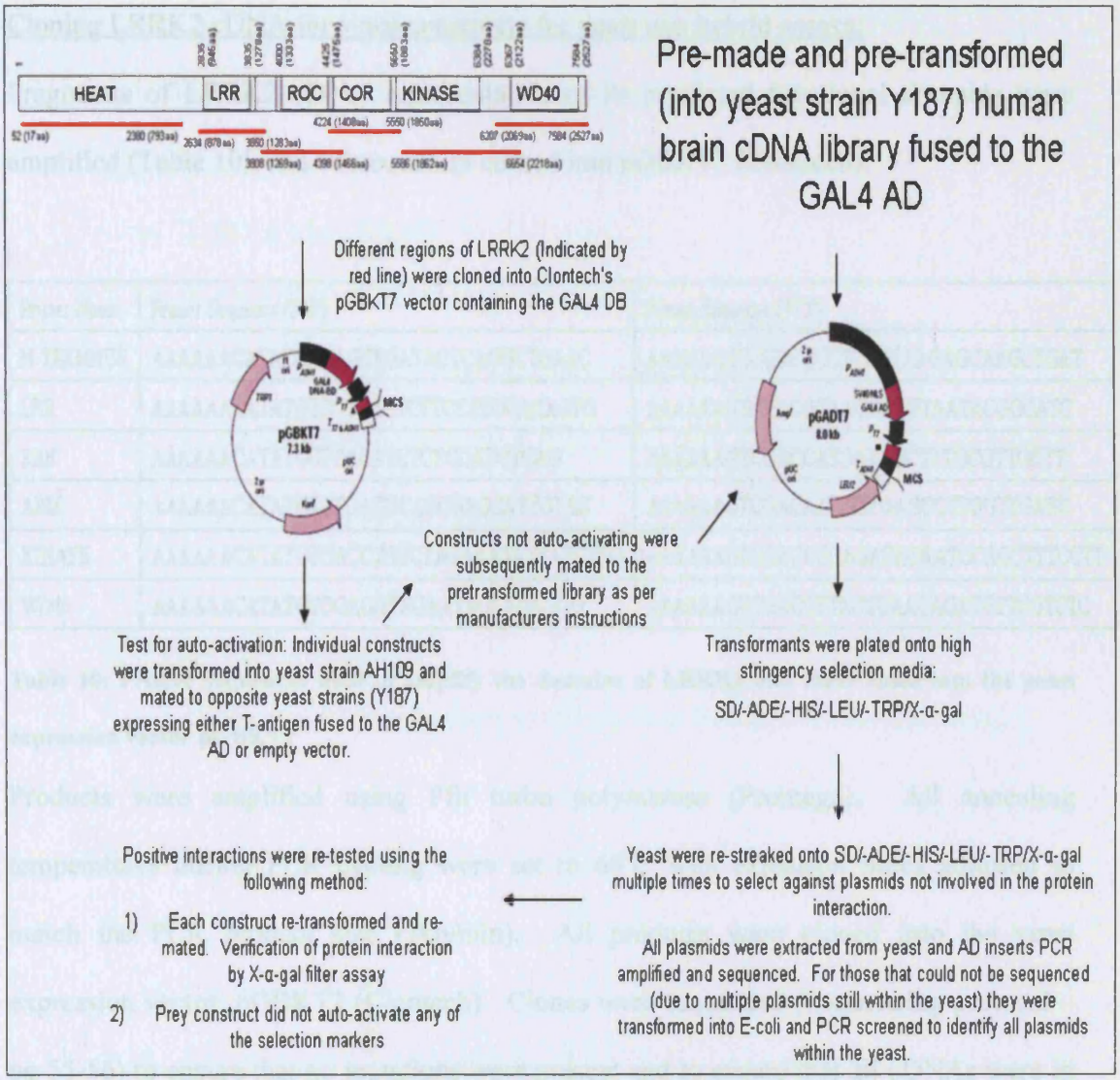

Figure 24: General Methodology followed for yeast two hybrid assay of LRRK2. Regions indicated by red lines under the ideogram of LRRK2 were cloned into yeast expression vector, pGBKT7. Protein expression of individual constructs was verified and auto-activation in yeast was excluded for each construct. All constructs were screened against a human brain cDNA library. Yeast able to grow on nutrient deficient media and catalyze the break down of X-gal, were re-streaked several times. Prey constructs were subsequently isolated and sequenced.

Cloning LRRK2 cDNA for yeast constructs for yeast two hybrid assays:

Fragments of LRRK2 cDNA representative of its predicted functional domains were amplified (Table 10), and subsequently cloned into pGBKT7 (Clontech).

Primer Name	Primer Sequence (5'-3')	Primer Sequence (3'-5')
N-TERMINUS	AAAAAACATATGGAAGTTGATAGTCAGGCTGAAC	AAAAAAGTCGACGCCTCCTTAAGAGCAAGCTGAT
LRR	AAAAAACATATGTCCTGACTCTTCTATGGACAGTG	AAAAAAGTCGACGCAACGCTGTAATACGGCATC
RAS	AAAAAACATATGCTGACATCTCTGGATGTCAG	AAAAAAGTCGACCATGCAGGCTTTGCGTTGCTT
ARM	AAAAAACATATGTATGACGCAGCGAGCATTGTAC	AAAAAAGTCGACAATGGTGAGCCTTGGTTGATC
KINASE	AAAAAACATATGTGACCTGCCTAGAAATATTATGTTG	AAAAAAGTCGACCCCAGACACAATCCAGCTTTCCTT
WD40	AAAAAACATATGTGGAGGTAGAATAGTAGAGGG	AAAAAAGTCGACCTTACTCAACAGATGTTCGTCTC

Table 10: Primer sequences used to amplify the domains of LRRK2 and clone them into the yeast expression vector pGBKT7

Products were amplified using Pfu turbo polymerase (Promega). All annealing temperatures during PCR cycling were set to 60^0C with extension times adjusted to match the PCR product size (1kb/min). All products were cloned into the yeast expression vector, pGBKT7 (Clontech). Clones were sequenced (Sequencing protocol – pg 55-56) to ensure that no mutations were present and to ensure that all cDNAs were in frame with the protein tag (N-MYC) and GAL4 DNA binding domain (DB).

Correct clones (bait vectors) were subsequently transformed into yeast to test for autoactivation of selection markers and protein expression by western blotting using antibodies directed against the MYC tag (Western Blot Protocol, pg 93-95).

Transformation of Yeast (AH109 and Y187)

Solutions:

1x TE/LiAc recipe

- 1.10.2 g LiAc.2 H2O
- 2. 1 ml 1M Tris-HCl stock solution
- 3. 1 ml 0.1M EDTA stock solution + 88 mL distilled water.
- 4. 80 ml distilled water; adjust pH to 7.5 with acetic acid; adjust volume to 100 ml with distilled water

50% PEG stock solution

- 100 g polyethylene glycol 4000; adjust to 200 ml with distilled water.

40% PEG/LiAc Solution

For 50ml

- 40ml of 50% PEG
- 10ml of 1x TE/LiAc solution

YPD medium

- 20g/L Difco peptone
- 10g/L Yeast Extract
- 20g/L Agar
- 15ml/L 0.2% adenine hemisulfate
- Adjust pH to 6.5 and autoclave.

- After cooling to 55 °C, add 50ml/L of sterile 40% stock solution
- Add Kanamycin to final concentration of 10-15mg/L
- Make up volume to 1L

SD dropout media

- 6.7g/L yeast nitrogen base without amino acids
- 20g/L Agar (for plates only)
- 850ml of water
- 100ml of appropriate sterile 10X Dropout solution (e.g. –TRP, -LEU, -TRP/-LEU, -LEU/-TRP/-ADE/-HIS) – recipe and protocol for 10X dropout solution (Clontech, Protocol #PT3024-1, pg 55).

Method:

1. Inoculate 1ml YPDA with 2-3mm colonies. Vortex
2. Incubate at 30°C for 16-18 hr with shaking (250rpm) to stationery phase (OD_{600}>1.5) in 50ml of YPDA
3. Transfer overnight culture into 300ml of YPDA (OD_{600} = 0.2 – 0.3). Incubate for a further 3 hrs (OD_{600} <1)
4. Collect cells by centrifugation at 1000xg for 5mins at room temperature
5. Remove supernatant and re-suspend in sterile TE
6. Pool cells and centrifuge at 1000xg for 5min at room temperature
7. Remove supernatant
8. Resuspend in 1.5ml of sterile 1x TE/LiAC
9. Add 0.1ug of plasmid and 0.1mg of sonicated salmon sperm

10. Add 0.1ml of yeast competent cells and mix well by vortexing
11. Add 0.6ml of freshly prepared PEG/LiAC solution
12. Incubate at 30°C for 30min with shaking (200rpm)
13. Add 70ul of DMSO. Mix by gentle inversion
14. Heat shock at 42°C for 15min.
15. Chill cells on ice 1-2min
16. Centrifuge cells at 14k rpm for 5secs at room temperature.
17. Remove supernatant
18. Re-suspend cells in 500µl of 1xTE
19. Plate on the appropriate drop-out media

Verification of LRRK2 yeast protein expression and suitability as bait proteins

To determine if the constructs were expressing the bait proteins, protein was extracted as per Clontech's instruction manual (Protocol # PT3024-1, Version # PR13103, Pg 12-13). Proteins were run on SDS polyacrylamide gels (Western blot protocol, pg 93-95) and immuno-blotted with anti-MYC antibody (Clone 9E10, Roche Molecular Biology).

All bait vectors were tested for autoactivation of different selection markers (-LEU, -TRP, -ADE, -HIS, X-GAL). Yeast containing the various LRRK2 bait constructs and the control prey (pGADT7 – encoding the T-antigen) were mated (Protocol # PT3024-1, Version # PR13103, Pg 44) and plated onto the following selection medias (Protocol # PT3024-1, Version # PR13103, Pg 21 Table VI):

1. –LEUCINE (-LEU) – selects for prey vector (pGADT7)
2. –TRYPTOPHAN(-TRP) – selects for bait vector (pGBKT7)

3. –LEUCINE/-TYRPTOPHAN(-LEU/-TRP) – selects for prey and bait vectors
4. –LEUCINE/-TRYPTOPHAN/-HISTIDINE/-ADENINE (-4aa) – selects for protein interaction

All plates were incubated for a total of 2 weeks to detect auto-activation of selection markers including X-gal (Protocol # PT3024-1, Version # PR13103, Pg 25).

Library screening with LRRK2 bait constructs

Matings between LRRK2 constructs and pretransformed human brain cDNA libraries were performed as per manufacturer's recommendations (Clontech, protocol manual PT3183-1 pg 37-44). Mating mixtures was plated directly onto quadruple drop out media –LEU/-TRP/-ADE/-HIS. After three weeks, colonies were re-streaked a minimum of three times onto fresh quadruple drop out media, to aid in plasmid segregation (loss of non-interacting plasmids). Colony lift filter assays (Protocol # PT3024-1, Version # PR13103, Pg 25) were performed on final re-streak plates to test for expression of β-galactosidase. Clones able to activate expression of all selection markers were subsequently grown in quadruple drop out media for plasmid extraction.

Mating mixtures were also plated onto control plates, -LEU, -TRP and –LEU/-TRP to determine mating efficiencies and the number of cDNA clones screened. Manufacturer's protocol and calculations were followed (Protocol #PT3183-1 pg 32-33)

Plasmid Extraction from Yeast

Method

1. Pick single yeast colonies (2-3mm in diameter) and grow overnight at 30°C with shaking (230-250rpm) in quadruple (–LEU/-TRP/-ADE/-HIS) dropout media
2. Following day, pellet cells at 5K rpm for 10mins
3. Remove supernatant and resuspend in approx 200µl of water.
4. Add 100µl of glass beads (Sigma) to each well or tube and vortex vigorously for 5 minutes.
5. Freeze (-20 °C)/thaw samples twice. Between each freeze/thaw cycle, vortex samples vigorously for 5 minutes.
6. Add 200µl of phenol:chloroform:isoamyl alcohol (25:24:1)
7. Vortex at high speed for 5 min
8. Spin tubes at 14K rpm for 5 mins. Spin 96 well plates at 5K rpm for 30 mins.
9. Transfer aqueous phase to new tube or plate
10. Add 8µl of 10M ammonium acetate and 500µl of 100% ethanol.
11. Place tubes and plates at -80°C overnight
12. Centrifuge tubes at 14K rpm for 10min at 4°C. Centrifuge plates at 5K rpm for 1 hr at 4°C
13. Discard supernatant and resuspend pellets in 200µl of 70% ethanol.
14. Centrifuge tubes at 14K rpm for 10min at 4°C. Centrifuge plates at 5K rpm for 30min at 4°C.
15. Discard supernatant
16. Air dry and resuspend pellet in 20µl of H_2O.

Amplification and sequencing of inserts in prey vector:

Plasmids extracted from yeast were amplified using (5' and 3' ADY insert PCR primers, Clontech) and run on 1% agarose gels. Plasmids were sequenced using T7 (5'-3') primer. Plasmids were only sequenced in the forward direction as it was not possible to sequence through the polyA-tail. As re-streaking of plasmids did not always remove all non-interacting plasmids, plasmids pools that did not sequence were transformed into XL-gold competent cells (Stratagene) and 10 bacterial colonies were picked to identify all plasmids within the original yeast colony. These were extracted using plasmid extraction kits (Qiagen) per manufacturer's protocol and subsequently sequenced (DNA sequencing reaction, pg 55-56).

PCR cocktail and conditions for amplification of inserts in prey vector:

Component	Amount per reaction
Plasmid from yeast	2µl
Primer 1 (10µM)	1µl
Primer 2 (10µM)	1µl
10x PCR buffer	2.5µl
5x Q solution	5µl
Qiagen Taq (5units/µl)	0.2µl
dNTPS (25mM each dNTP)	0.4µl (Final concentration of each dNTP 200µM)
Distilled H_2O	12.9µl (Total volume 25µl)

PCR cycling conditions

1 cycle:	95°C – 5min
35 cycles:	95 °C – 30 seconds
	60 °C – 30 secs
	72°C – 2min
1 cycle:	72 °C – 5 min
1 cycle:	4 °C – HOLD

PCR products were subsequently analyzed on 0.7% agarose (American Bioanalytical) gels in 1xTAE.

Bioinformatics: Determination of proteins encoded by prey vectors

Once all sequences had been obtained, they were first blasted against the NCBI database (http://www.ncbi.nlm.nih.gov/BLAST/Blast.cgi). If there was no significant similarity to any known genes, the plasmid was not considered for further validation. If the sequence within the prey vector had significant similarity to a known gene, sequence within the prey vector was translated. The prey vector had to be in frame with the GAL4 DB and encode for at least 10 amino acids for further consideration. Having multiple independent clones for the same protein was considered additional evidence for a true interaction.

Confirmation of interaction between LRRK2 and FEZ2.

Of the clones that were identified, the interaction between the N-terminus of LRRK2 and FEZ2 (Fasciculation and elongation factor zeta 2) was chosen for further validation

because multiple independent clones were identified for FEZ2, with yeast colonies containing the interacting proteins appearing during the first week post plating, indicating a relatively strong interaction.

The bait vector, encoding the N-terminus of LRRK2, was retransformed into yeast strain AH109 and the prey vector, encoding a portion of FEZ2, was retransformed into yeast strain Y187 (Transformation of yeast, pg 116-119). The prey vector was tested for auto-activation, just as the initial bait vectors were (pg 120). Both yeast strains were subsequently mated and plated onto quadruple dropout media to re-test the phenotype (Clontech, protocol manual PT3183-1 pg 37-44). The FEZ2 construct isolated from the original yeast two hybrid was mated with the individual domains of LRRK2. The prey vector encoding FEZ2 (pGADT7) and the bait vector encoding LRRK2 (PGBKT7) were swapped into the opposing vectors to ensure the interaction was not being driven by either of the protein tags or GAL4 yeast protein sequences in conjunction with either FEZ2 or LRRK2.

Refinement of interacting region between LRRK2 and FEZ2

In order to identify the key region of interaction between LRRK2 and FEZ2, segments of FEZ1, FEZ2 and the N-terminal region of LRRK2 were amplified and cloned into the appropriate yeast expression (Table 11). The N-terminus of LRRK2 was divided into eight equally sized fragments overlapping by approximately 250bp (Figure 25A). FEZ1 and FEZ2 were divided into 5 fragments, harbouring different portions of the N-terminus, coiled-coil domain and C-terminus (Figure 25B). To determine if LRRK2 specifically bound to FEZ2, a homolog of FEZ2 was used, FEZ1.

PRIMER NAME	PRIMER SEQUENCE (FORWARD)	PRIMER SEQUENCE (REVERSE)
NTER1	AAAAAACATATGATGGCTAGTGGCAGCTGTCA	AAAAAACATATGATGGCATCAAAAATTAACAT
NTER2	AAAAAACATATGGTGCAGCAGGTGGGTTGGTCAC	AAAAAACATATGCACTCATAGGGAATGCTTTC
NTER3	AAAAAACATATGATGCACTCATTTCCAGCCAATG	AAAAAACATATGAACAGGCTTCCAGCCAAAAC
NTER4	AAAAAACATATGTGCTGTTTGCTCCATAGGCT	AAAAAACATATGTTCAGCCACTTCGGGAGAAT
NTER5	AAAAAACATATGTTGTTTTGGCTGGAAGCCTGTT	AAAAAACATATGTATCCTCCCTGGATTCTTCT
NTER6	AAAAAACATATGCAGGCATCTGCGAATGCATTGTCAAC	AAAAAACATATGTCCATAGCACCTTCCAGGGA
NTER7	AAAAAACATATGCATGAGACATCATTACCAGTG	AAAAAACATATGCACGCTCTCTCTAGCATCAC
NTER8	AAAAAACATATGGATCAACAGTTTCTAAACCTCTG	AAAAAACATATGAATTTCCATCGCTGCCTGAG

PRIMER NAME	PRIMER SEQUENCE (FORWARD)	PRIMER SEQUENCE (REVERSE)
FEZ1NTERMINUS	AAAAAA**CATATG**ATGGAGGCCCCACTGGTGAGTCTGGATGA	AAAAAA**CATATG**GGACCAGTTGTTGTTGAAGG
FEZ1COILED COIL	AAAAAA**CATATG**TATGAAGGGCTGAGGCACAT	AAAAAA**CATATG**GCACCGTGATAAAGGAGTTC
FEZ1CTERMINUS	AAAAAA**CATATG**CTTATTGAGGTTCAGAACAAGCAGAAGGAG	AAAAAA**CATATG**TTAGGTAGGGCAGAGCACT
FEZ1cDNA	AAAAAA**CATATG**ATGGAGGCCCCACTGGTGAG	AAAAAA**CATATG**TTAGGTAGGGCAGAGCACTT
FEZ2NTERMINUS	AAAAAA**CATATG**ATGGCGGCGGACGGGGACTGGCAGGATTTC	AAAAAA**GGATCC**CCCGGTACTAGACCTCTTGAG
FEZ2COILED COIL	AAAAAA**CATATG**AGGTCTAGTACCGGCAGTTAT	AAAAAA**GGATCC**CATTCTTCCCATTCTGAGAG
FEZ2CTERMINUS	AAAAAA**GAATTC**TCTCAGAATGGGAAGAATGAG	AAAAAA**GGATCC**CTATGTAGGACACAGAACTTTCAG
FEZ2cDNA	AAAAAA**GAATTC**ATGGCGGCGGACGGGGACTG	AAAAAA**GGATCC**AAGTTCTGTGTCCTACATAG

Table 11: Refinement of interacting region between FEZ1, FEZ2 and LRRK2. FEZ1, FEZ2 and LRRK2 N-terminal (NTER) primer sequences used to create yeast constructs encoding different regions of FEZ1 and FEZ2 and HEAT domain. PCR fragments were digested and cloned into the appropriate yeast expression vector.

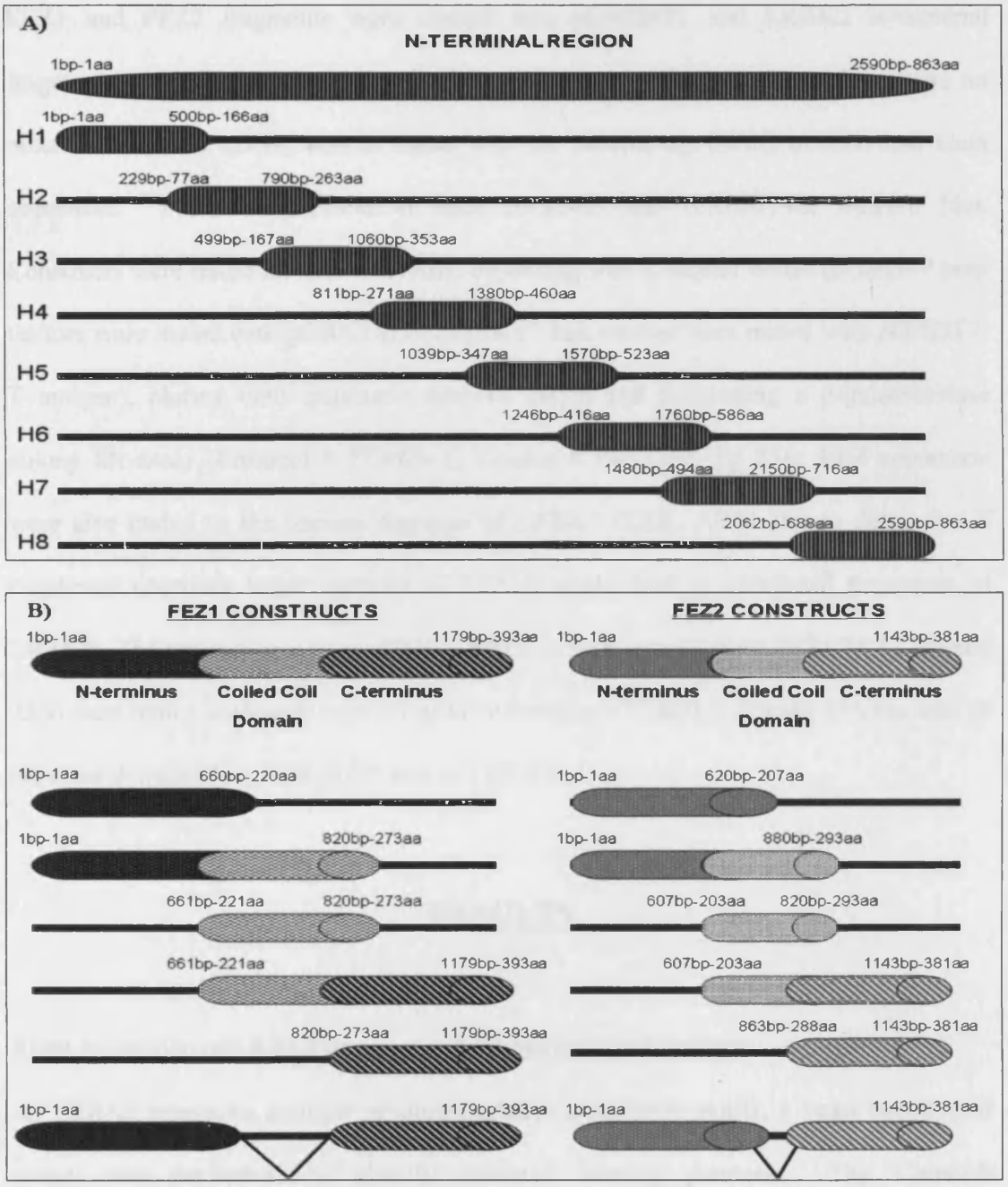

Figure 25: Ideogram of constructs created to refine the interacting region between LRRK2 and FEZ1/2. A) The N-terminal region of LRRK2 (H1-H8) was divided into 8 overlapping fragments. B) Various FEZ1 and FEZ2 constructs were made, containing combinations of the N-terminus, coiled coil region and the c-terminus of each protein. Constructs were sequence verified and tested for auto-activation of selection markers and for protein expression.

FEZ1 and FEZ2 fragments were cloned into pGATDT7 and LRRK2 N-terminal fragments were cloned into pGBKT7. Clones were sequenced to ensure there were no mutations and the cDNA was in frame with the protein tag (MYC or HA) and Gal4 sequences. Protein expression of each construct was verified via western blot. Constructs were tested for auto-activation by mating with a control vector (pGADT7 prey vectors were mated with pGBKT-p53; pGBKT7 bait vectors were mated with pGADT7-T antigen), plating onto quadruple dropout media and performing a β-galactosidase colony lift assay (Protocol # PT3024-1, Version # PR13103, Pg 25). FEZ constructs were also mated to the various domains of LRRK2 (LRR, ARM etc) to determine if constructs encoding larger portions of FEZ1/2 could bind to additional fragments of LRRK2. The various constructs of FEZ1/FEZ2 as well as full length FEZ1/FEZ2 (Figure 25B) were mated with each segment of the n-terminal of LRRK2 (Figure 25A) as well as the other domains (i.e. LRR, ROC etc) of LRRK2.

RESULTS

Yeast expression of LRRK2 domains and suitability as bait vectors

As LRRK2 possesses multiple predicted protein interaction motifs, a yeast two hybrid screen was performed to identify potential binding partners. The Clontech MATCHMAKER system with pre-transformed human brain cDNA library was chosen for these experiments. LRRK2 was divided and cloned as six fragments, encoding each of its predicted domains (Figure 26A). Bait constructs were transformed into yeast and

tested for protein expression (Figure 26B) and autoactivation of selection markers. All constructs expressed the correct size protein.

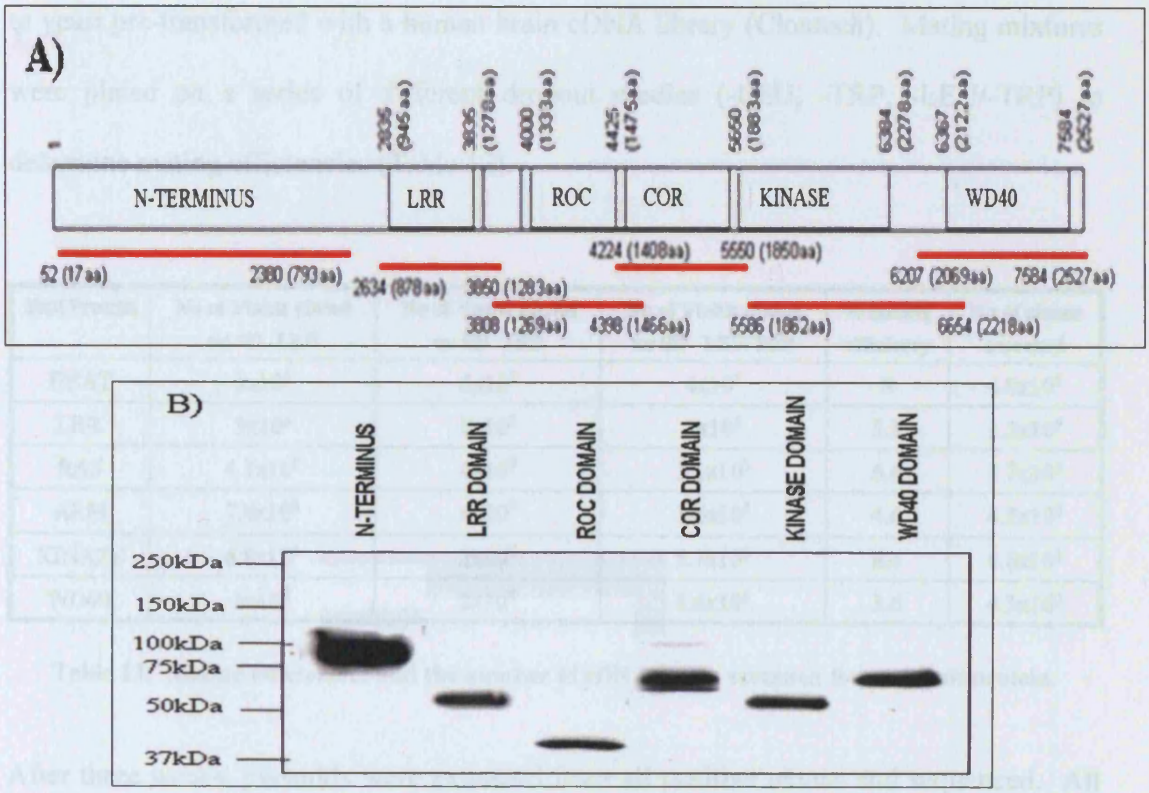

Figure 26: Regions and expression of LRRK2 bait proteins. A) Schematic representation of the predicted domains of LRRK2. Areas underlined in red represent cDNA cloned into the yeast expression vector. B) α-MYC blot of yeast extract demonstrating expression of the different LRRK2 bait vectors.

After two weeks, colonies were not observed on either –LEU/-TRP/-ADE or –LEU/-TRP/-ADE/-HIS agar plates. Colonies on –LEU/-TRP plates were tested for auto-activation of the β-galactosidase selection marker by colony lift filter assay. None of the bait vectors displayed auto activation of the selection markers

Identification of protein interactors for LRRK2

Following confirmation of bait vectors expressing correct size protein and the absence of any auto-activation of the selection markers, yeast expressing the bait vectors were mated to yeast pre-transformed with a human brain cDNA library (Clontech). Mating mixtures were plated on a series of different dropout medias (-LEU, -TRP, -LEU/-TRP) to determine mating efficiencies (Table 12).

Bait Protein	No of Viable cfu/ml on SD -LEU	No of Viable cfu/ml on SD -TRP	No of Viable cfu/ml on SD –LEU/TRP	% mating efficiency	No of clones screened
HEAT	$5x10^6$	$5x10^8$	$4x10^5$	8	$4.8x10^6$
LRR	$3x10^6$	$3x10^8$	$1x10^5$	3.3	$1.2x10^6$
RAS	$4.7x10^6$	$4x10^7$	$3.1x10^5$	6.6	$3.7x10^6$
ARM	$7.8x10^6$	$6x10^7$	$3.6x10^5$	4.6	$4.3x10^6$
KINASE	$6.8x10^6$	$2x10^7$	$5.7x10^5$	8.4	$6.8x10^6$
WD40	$1x10^7$	$2x10^8$	$3.6x10^5$	3.6	$4.3x10^6$

Table 12: Mating efficiencies and the number of cDNA clones screened for each bait protein.

After three weeks, plasmids were extracted from all positive clones and sequenced. All clones encoding a protein fragment of at least ten amino acids and exhibiting significant similarity to a known protein are listed below (Table 13). Common false positives in yeast two hybrids, such as ribosomal and heat shock proteins (http://www.fccc.edu/research/labs/golemis/InteractionTrapInWork), were discounted and not studied further.

INTERACTORS WITH THE N-TERMINUS	
GENE NAME	NO OF CLONES
FASCICULATION AND ELONGATION PROTEIN ZETA 2	27
MKL1 GENE	9
ADENYLATE KINASE 5	8
PROSAPOSIN	8
PROTEASOME (PROSOME, MACROPAIN) SUBUNIT, ALPHA TYPE	6
MRNA FOR SERTA DOMAIN CONTAINING 1 VARIANT	6
CDNA: FLJ20902	5
ZINC FINGER HOMEOBOX 1B	5
PROTEIN PHOSPHATASE 2	5
SEROLOGICALLY DEFINED COLON CANCER ANTIGEN 1	5
SECRETED PROTEIN, ACIDIC, CYSTEINE-RICH (	5
CHROMOSOME 14 OPEN READING FRAME 43, MRNA	4
CDNA CLONE IMAGE:5259272	4
CDNA FLJ34891 FIS	4
CTAGE-5B PROTEIN	4
FULL-LENGTH CDNA CLONE CS0DK008YI09 OF HELA CELLS	3
H.SAPIENS MRNA FOR LON PROTEASE-LIKE PROTEIN	3
CDNA: FLJ22042 FIS	3
FLJ40142 PROTEIN	3
PI-3-KINASE-RELATED KINASE SMG-1,	3
HYPOTHETICAL PROTEIN BC011880	3
MRNA; CDNA DKFZP686H13259	3
MYOSIN, LIGHT POLYPEPTIDE KINASE	3
BROMODOMAIN CONTAINING 4,	3
SOLUTE CARRIER FAMILY 6, MEMBER 17 (SLC6A17	3
ATPASE, H+ TRANSPORTING	3
GENE FOR HIPPOCALCIN	2
KOYT BINDING PROTEIN 2 MRNA	2
STATHMIN-LIKE 2 MRNA	2
CTD	2
GROWTH ASSOCIATED PROTEIN 43	2
DEHYDROGENASE/REDUCTASE	2
CYTOCHROME C OXIDASE SUBUNIT VB, MRNA	2
TRANSLOKIN, MRNA	2
CYCLIC AMP PHOSPHOPROTEIN	2
LIM DOMAIN ONLY 4	2
ANKYRIN REPEAT AND SOCS BOX-CONTAINING 8	2
NHP2 NON-HISTONE CHROMOSOME PROTEIN 2-LIKE	2
PEPTIDYLPROLYL ISOMERASE A	2
KUNIT2-TYPE PROTEASE INHIBITOR	2
K-ALPHA-1 MRNA FOR UBIQUITOUS ALPHA-TUBULIN	2
NEURONAL PENTRAXIN I	2
HUMAN N33 PROTEIN FORM 2 (N33) GENE	2
TUBULIN, ALPHA	2
PROTEASE, SERINE, 15 (PRSS15),	2
GROWTH ASSOCIATED PROTEIN 43	2
BETA III SPECTRIN	2
NEURONATIN	2
PQ LOOP REPEAT CONTAINING 1 (PQLC1	2
CDNA CLONE IMAGE:4513453	1
CHROMOSOME 19 CLONE LLNLR-262C5	1
DNA METHYLTRANSFERASE 1 ASSOCIATED PROTEIN 1	1
HIPK1 HOMEODOMAIN-INTERACTING PROTEIN KINASE-1	1
NEL-LIKE 1	1
BRG1-BINDING PROTEIN ELD/OSA1	1
ARMADILLO REPEAT CONTAINING 8	1
BERNARDINELLI-SEIP CONGENITAL LIPODYSTROPHY	1
PROTEASE, SERINE, 15	1
CDNA FLJ46677 FIS	1
CDNA FLJ46859 FIS	1
MITOGEN-ACTIVATED PROTEIN KINASE 1	1
MRNA; CDNA DKFZP686C195	1
SMALL HISTONE FAMILY CLUSTER	1
TRIPARTITE MOTIF-CONTAINING 2, MR	1
UBIQUITIN B,	1
MRNA FOR ARID4B VARIANT PROTEIN	1
MITOCHONDRIAL CARRIER HOMOLOG 1	1
NUCLEAR PROTEIN LOCALIZATION 4, MRNA	1
MASTL MICROTUBULE SERINE/THREONINE KINASE-LIKE	1
TMED8 TRANSMEMBRANE EMP24 P	1
NEUROENDOCRINE DIFFERENTIATION FACTOR MRNA	1

INTERACTORS WITH THE LRR DOMAIN	
GENE NAME	NO CLONES
MKL1 GENE	9
TACC1-LIKE PROTEIN	8
PROTEASOME (PROSOME, MACROPAIN) SUBUNIT, ALPHA TYPE	7
2',3'-CYCLIC NUCLEOTIDE 3' PHOSPHODIESTERASE	6
HYPOTHETICAL PROTEIN FLJ22175	5
FLJ20902	5
DKFZP686H13259	4
ZINC FINGER HOMEOBOX 1B	3
CLONE PP5644 UNKNOWN	3
FLJ34891 FIS	3
CHROMOSOME X OPEN READING FRAME 53	3
SMALL HISTONE FAMILY CLUSTER	2
PROTOCADHERIN GAMMA SUBFAMILY C	2
PLECKSTRIN HOMOLOGY, SEC7 AND COILED-COIL DOMAINS	2
KINESIN FAMILY MEMBER 4A	2
HIGH-MOBILITY GROUP NUCLEOSOMAL BINDING DOMAIN 2	2
RNA POLYMERASE II 140 KDA SUBUNIT	2
OR2B2	1
UBIQUITIN B	1
PROTEIN TYROSINE PHOSPHATASE, RECEPTOR TYPE	1
PROLIFERATION-INDUCING PROTEIN 8	1
DKFZP686D0249	1
ADAPTER-RELATED PROTEIN COMPLEX 3 DELTA	1
MONOCYTE TO MACROPHAGE DIFFERENTIATION-ASSOCIATED	1
MITOGEN-ACTIVATED PROTEIN KINASE KINASE KINASE 15	1
MITOGEN-ACTIVATED PROTEIN KINASE 1	1
HYPOTHETICAL PROTEIN BC011880	1
HIGH-MOBILITY GROUP NUCLEOSOMAL BINDING DOMAIN 2	1
E2A-PBX1-ASSOCIATED PROTEIN	1
CLUSTERIN	1
FLJ23587 FIS,	1

INTERACTORS WITH THE ROC DOMAIN	
GENE NAME	NO CLONES
LRRK2	9
ZINC FINGER HOMEOBOX 1B,	3
ZINC FINGER PROTEIN, 3115 BP	2
TRANSMEMBRANE AND COILED-COIL DOMAIN FAMILY 2	2
SIALIC ACID-BINDING IG-LIKE LECTIN	1

INTERACTORS WITH THE COR DOMAIN	
GENE NAME	NO CLONES
KCNK3 CHANNEL	5
TRANSFORMATION-RELATED PROTEIN 2	3
BETA-1,3-N-ACETYLGLUCOSAMINYLTRANSFERASE	3
LANC LANTIBIOTIC SYNTHETASE COMPONENT C-LIKE 1	2
LEUCINE RICH REPEAT NEURONAL 5	2
ENOYL COENZYME A HYDRATASE 1	1
GATA ZINC FINGER DOMAIN CONTAINING 2A	1
DKFZP566O134	1
MYOSIN, LIGHT POLYPEPTIDE KINASE (MYLK	1
DIPEPTIDYL PEPTIDASE IV	1
APOLIPOPROTEIN E	1
SERINE PALMITOYLTRANSFERASE	1
AT RICH INTERACTIVE DOMAIN 4B	1

INTERACTORS WITH THE KINASE DOMAIN	
GENE NAME	NO CLONES
CS0DI041YC02 OF PLACENTA COT 25-NORMALIZED	21
NUCLEOSIDE DIPHOSPHATE LINKED MOIETY X-TYPE MOTIF 3	13
SIMILAR TO ATAXIN 2-BINDING PROTEIN 1	11
CALCIUM/CALMODULIN-DEPENDENT PROTEIN KINASE II INHIBITOR	8
MICROTUBULE-ASSOCIATED PROTEIN, RP/EB FAMILY	8
RAB1A, MEMBER RAS ONCOGENE FAMILY	6
RAN GTPASE ACTIVATING PROTEIN 1	6
MODULATOR OF APOPTOSIS 1 (MOAP1)	6
CALMODULIN BINDING TRANSCRIPTION ACTIVATOR 2	6
DKFZP686D12126	5
EIF1ALPHA	7
ENDOTHELIAL DIFFERENTIATION, SPHINGOLIPID G-PROTEIN-COUPLED	4
VISININ-LIKE 1	4
CALCIUM/CALMODULIN-DEPENDENT PROTEIN KINASE II INHIBITOR	4
ZYXIN,	4
MAKORIN, RING FINGER PROTEIN, 1,	3
GLYCOGEN SYNTHASE KINASE 3 ALPHA	3
CDC45 CELL DIVISION CYCLE 45-LIKE	2
FLJ46550 FIS	2
GOLGI REASSEMBLY STACKING PROTEIN 1	2
LOC440752	2
RAN GTPASE ACTIVATING PROTEIN 1	2
TUBULIN, ALPHA, UBIQUITOUS,	2
UBIQUITIN ASSOCIATED PROTEIN 2-LIKE	2
ZINC FINGER PROTEIN 395	2
FOR FIBROBLAST GROWTH FACTOR RECEPTOR 3	2
PROTOCADHERIN GAMMA SUBFAMILY C, 4	2
REGULATING SYNAPTIC MEMBRANE EXOCYTOSIS 4	2
MITOGEN-ACTIVATED PROTEIN KINASE 1	2
L-CABP1	2
NEUROCHONDRIN	2
HETEROGENEOUS NUCLEAR RIBONUCLEOPROTEIN	2
MAP/MICROTUBULE AFFINITY-REGULATING KINASE 3	2
CYTOCHROME C OXIDASE SUB UNIT 3 (COX3)	1
ADP-RIBOSYLATION-LIKE FACTOR 6 INTERACTING PROTEIN	1
AMYLOID BETA PRECURSOR PROTEIN BINDING PROTEIN	1
APEX NUCLEASE	1
FLJ20643 FIS	1
FLJ26635 FIS	1
WD REPEAT AND SOCS BOX-CONTAINING 1	1
PROTEASOME (PROSOME, MACROPAIN) 26S SUBUNIT, NON-ATPASE	1

INTERACTORS WITH THE WD40 DOMAIN	
GENE NAME	NO CLONES
RAN BINDING PROTEIN 9	10
BICAUDAL-D	5
CALSYNTENIN 1	3
PHOSPHODIESTERASE 4D INTERACTING PROTEIN	2
GLUTAMATE RECEPTOR, IONOTROPIC	2
GENE FOR HIPPOCALCIN	1
FIBRONECTIN TYPE III DOMAIN CONTAINING 3A	1

Table 13: List of all proteins identified as potential interactors for LRRK2. Potential interactors are separated by the portion of LRRK2 used as the bait protein and the number of independent clones identified for each interactor are indicated. All proteins listed above were able to transcribe the expression of all selection markers.

Confirmation of interaction between FEZ2 clone and LRRK2:

Of the potential protein interactors identified, FEZ2 was pursued for further analysis as (a) 27 independent clones interacted were recovered, (b) all clones encoded a continuous protein sequence greater than 10 amino acids and (c) all clones activated expression of all selection markers. To ensure the interaction was not a false positive, FEZ2 clones were isolated from yeast and retransformed with the individual domains of LRRK2 and a negative control (pGBKT7-p53). The FEZ2 clone only interacted with the N-terminal region and did not auto-activate any of the selection markers (Figure 27A). To ensure that interaction was being driven by FEZ2 and LRRK2 protein sequences, and not GAL4 protein sequences in a specific conformation with FEZ2 and the N-terminus, the interaction was reversed. FEZ2 was fused with the DNA binding domain (DB) and N-terminal of LRRK2 (NTER) was fused with the activation domain (ADY). NTER-DB and FEZ2-ADY and FEZ2-DB and NTER-DB interacted (Figure 27B), indicating the GAL4 protein sequences were not influencing the conformation of either protein and driving the interaction.

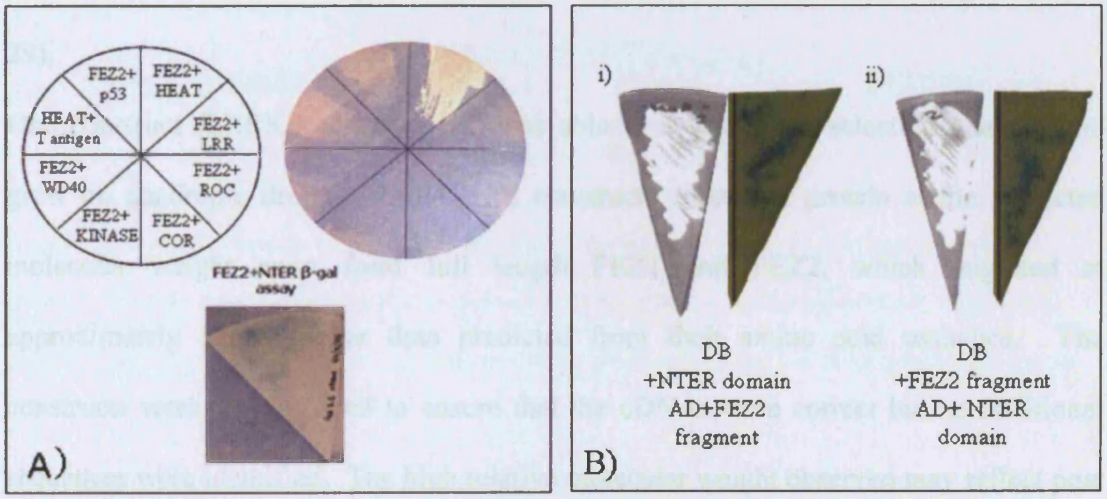

Figure 27: Retest of interaction between FEZ2 and LRRK2 in yeast. A) Retransformation of FEZ2 clone extracted from yeast with all domains of LRRK2 on quadruple dropout media. pGBKT-p53 was used a negative control with FEZ2, to ensure that the FEZ2 clone did not autoactivate selection markers and pTD-1 was used as a negative control to demonstrate the N-terminus of LRRK2 (NTER) construct did not auto-activate any of the selection makers. Only FEZ2 and the NTER construct are able to activate all selection markers including β-galactosidase. B) Fusing the NTER construct to the DNA binding domain (DB) and FEZ2 to the activation domain (AD) and vice versa, maintains the interaction as both proteins in either state are able to activate all selection markers when plated on quadruple dropout media.

Refinement of interacting region between FEZ2 and LRRK2:

From the initial yeast two hybrid screen, an interaction occurred between the N-terminal region of LRRK2 (1aa-793aa) and the coiled coil region of FEZ2 (211aa-306aa). To refine the region of interaction, the N-terminal of LRRK2 was broken down into 8 regions each encoding approx 160aa (Figure 28). FEZ1 and FEZ2 were broken down into a total of 5 constructs encoding different combinations of the N-terminus, coiled coil region and the C-terminus (Figure 29). All proteins were transformed and assessed for protein expression and ability to auto-activate any of the selection markers (Figure 28 and 29).

One construct (LRRK2 construct-H2) was able to auto-activate selection markers and grew on quadruple dropout media. All constructs expressed protein at the predicted molecular weight apart from full length FEZ1 and FEZ2, which migrated at approximately 5kDA higher than predicted from their amino acid sequence. The constructs were re-sequenced to ensure that the cDNAs were correct but no additional sequences were identified. The high relative molecular weight observed may reflect post

translational modification of these proteins, although this statement requires further investigation as no modifications of FEZ proteins have been reported.

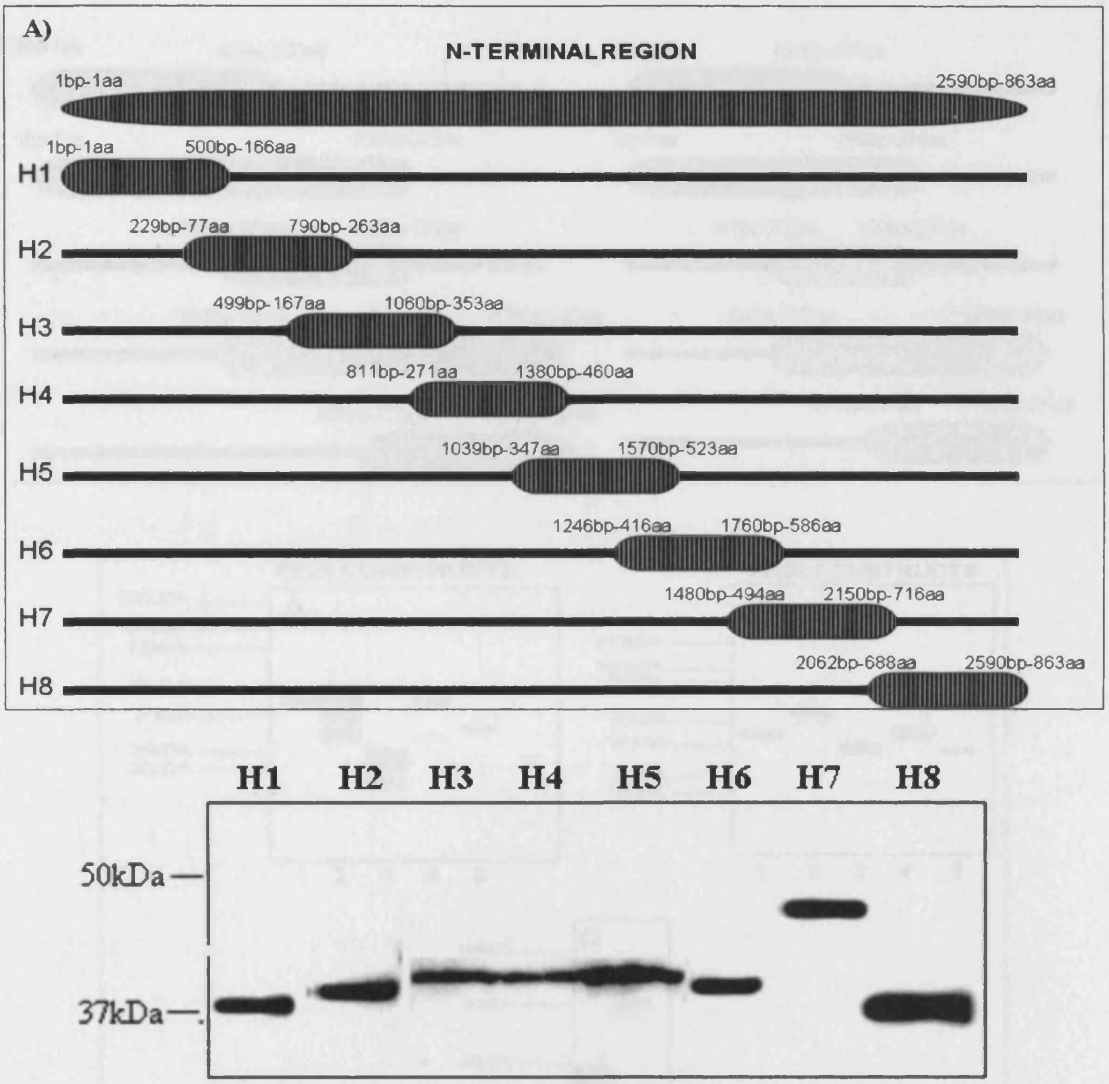

Figure 28: Yeast expression of LRRK2 N-terminal fragments used to refine the interaction with FEZ1/2. Protein extract from yeast transformed with the smaller fragments of the N-terminal of LRRK2 (A). (B) α-MYC western blot demonstrating protein expression of N-terminal bait vectors.

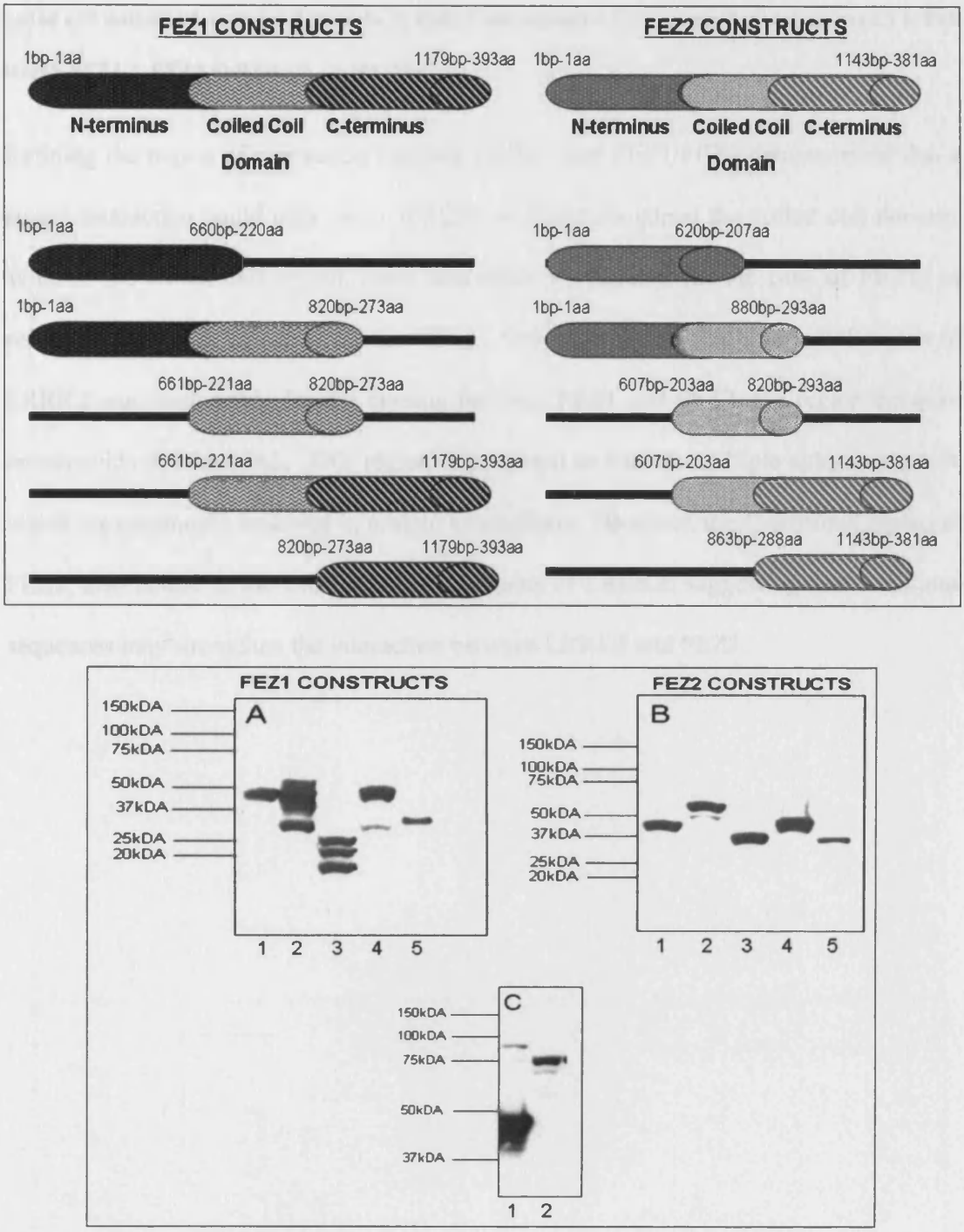

Figure 29: Yeast expression of FEZ1/2 constructs used to refine interaction with LRRK2. Protein extract from yeast transformed with smaller constructs of FEZ1 and FEZ2 (upper diagram). (Lower image) A) FEZ1 constructs (1.N-terminus, 2. N-terminus + coiled coil domain, 3. coiled coil domain, 4. coiled coil domain + C-terminus 5. C-terminus) B) FEZ2 constructs (1.N-terminus, 2. N-terminus +

coiled coil domain, 3. coiled coil domain, 4. coiled coil domain + C-terminus 5. C-terminus) C) 1. Full length FEZ1 2. FEZ2 Full length. α-HA blot.

Refining the region of interaction between LRRK2 and FEZ1/FEZ2 demonstrated that a strong interaction could only occur if FEZ1 or FEZ2 contained the coiled coil domain. Without the coiled coil region, there was either no binding (in the case of FEZ1) or reduced affinity, as was the case for FEZ2. Only one part of the N-terminal region of LRRK2 was responsible for the binding between FEZ1 and FEZ2, the region between amino acids 494 and 863. This region is predicted to contain multiple ankyrin repeats, which are commonly involved in protein interactions. However, the C-terminal region of FEZ2, also bound to the LRR and COR domains of LRRK2, suggesting that additional sequences may strengthen the interaction between LRRK2 and FEZ2.

Prey vector \ Bait vector	NTER H1	NTER H2	NTER H3	NTER H4	NTER H5	NTER H6	NTER H7	NTER H8
FEZ1 N-TERMINUS	-	-	-	-	-	-	-	-
FEZ1 NTERMINUS/COILED COIL	-	-	-	-	-	-	-	-
FEZ1 COILED COIL	-	-	-	-	-	-	++	++
FEZ1 COILED COIL/C-TERMINUS	-	-	-	-	-	-	+	++
FEZ1 C-TERMINUS	-	-	-	-	-	-	-	-
FEZ1 FULL LENGTH	-	-	-	-	-	-	++	++
pGADT7-T antigen	-	+	-	-	-	-	-	-

Prey vector \ Bait vector	NTER	LRR	ROC	COR	KINASE	WD40	Empty pGBKT7
FEZ1 N-TERMINUS	-	-	-	-	-	-	-
FEZ1 NTERMINUS/COILED COIL	+++	-	-	-	-	-	-
FEZ1 COILED COIL	+++	-	-	-	-	-	-
FEZ1 COILED COIL/C-TERMINUS	+++	-	-	-	-	-	-
FEZ1 C-TERMINUS	-	-	-	-	-	-	-
FEZ1 FULL LENGTH	+++	-	-	-	-	-	-
pGADT7-T antigen	-	-	-	-	-	-	-

Prey vector \ Bait vector	NTER H1	NTER H2	NTER H3	NTER H4	NTER H5	NTER H6	NTER H7	NTER H8
FEZ2 N-TERMINUS	-	-	-	-	-	-	-	-
FEZ2 NTERMINUS/COILED COIL	-	-	-	-	-	-	+	++
FEZ2 COILED COIL	-	-	-	-	-	-	+	++
FEZ2 COILED COIL/C-TERMINUS	-	-	-	-	-	-	++	++
FEZ2 C-TERMINUS	-	-	-	-	-	-	-	-
FEZ2 FULL LENGTH	-	-	-	-	-	-	+	++
pGADT7-T antigen	-	+	-	-	-	-	-	-

Prey vector \ Bait vector	NTER	LRR	ROC	COR	KINASE	WD40	Empty pGBKT7
FEZ2 N-TERMINUS	+	-	-	-	-	-	-
FEZ2 NTERMINUS/COILED COIL	+	-	-	-	-	-	-
FEZ2 COILED COIL	++	-	-	-	-	-	-
FEZ2 COILED COIL/C-TERMINUS	++	++	+	-	-	-	-
FEZ2 C-TERMINUS	-	-	-	-	-	-	-
FEZ2 FULL LENGTH	+++	+++	+++	-	-	-	-
pGADT7-T antigen	-	-	-	-	-	-	-

Table 14: Results of matings between FEZ1, FEZ2 and various LRRK2 constructs. The strength of interaction was determined by growth rate and degree of X-gal activity assessed relative to

interaction between p53 and the T antigen (positive control): + weak activation of X-gal, ++ medium activation of X-gal, +++ strong activation of X-gal.

DISCUSSION

In order to conduct large protein-protein interaction screen, a yeast two-hybrid is a logical choice, as one can screen thousands of potential interactors. This method suffers from a high false positive, with some estimates as high as 30%, as well as a false negative rate. There are many reasons for this:

1) Both bait and prey proteins are fused to the GAL4 DNA binding domain and the activation domain respectively and individually, may possess sufficient similarity to the intact GAL4 protein. Consequently, either protein may bind to the GAL4 consensus sequence without requiring the presence of its partner (auto-activation). Auto-activation of the selection markers can be avoided by testing individual bait or prey proteins but this is not possible if one uses a library as there are potentially millions of different protein fragments to test. This can be overcome by re-testing the auto-activation ability of the potential interesting prey proteins chosen for further study as I did during our investigation.
2) All selection markers are encoded by genes in the nucleus, so both the bait and prey protein have a nuclear localization signal (NLS) fused to their N-termini. Furthermore, both proteins are expressed at significantly high levels. A combination of forcing two proteins at high levels into the same compartment of cell can generate artificial protein-protein interactions.
3) The expression of some proteins may either be toxic or beneficial to yeast cells. Proteins that are toxic to yeast cells are unlikely to be identified as potential

protein interactors. Conversely, proteins which promote cell survival may allow yeast to survive more successfully in media lacking certain amino acids and nutrients leading to an over-representation of these proteins in yeast two hybrid screens.

4) Yeast are often maintained on highly selective media for up to 3-4 weeks prior to re-streaking. This can often lead to mutations in the promoter region of the selection markers leading to autoactivation. Yeast with activating mutations do not require an interaction to occur to drive the expression of selection markers. Yeast harbouring such mutations, are at a select advantage to grow. Re-streaking can overcome this false positive but a more effective strategy is to only consider proteins that are represented by multiple clones.

As a result of the inherent drawbacks associated with this technique, the Clontech GAL4 two-hybrid system III was selected for the LRRK2 protein interaction screen. In this system, the AH109, into which the bait construct is transformed, contains several different selection markers under the control of unique promoters. As a result, the likelihood of autoactivation of all selection markers by either bait or prey protein alone, is greatly decreased. Furthermore, premade libraries are pretransformed into a yeast strain allowing screening of a greater number of cDNA clones as mating yeast is a more efficient method than transforming the bait vector into yeast containing a library.

Many potential protein interactors were identified for LRRK2 (Table 13), such as the amyloid β precursor binding protein (APPBP1) and glycogen synthase kinase 3-alpha (GSK3α). As APPBP1 and GSK3α are involved in the control and/or function of the amyloid precursor protein [440, 441] and TAU [442], mutations within LRRK2 could alter TAU

aggregation and deposition [317, 330] via interactions with these two proteins. However not all proteins listed in Table 13 were retransformed into yeast to confirm the interaction and each domain was only screened for protein interactors once. Therefore, further validation of the protein interactors is required. This can be done either by repeating the yeast two hybrid screen for each domain or by the use of alternative methods for protein-protein interactions.

Although the validity of the proteins identified above remain in question, none of the proteins previously identified as LRRK2 interactors, PARKIN [412], HSP90/p50^{cdc37} [414] were identified in the screen apart from LRRK2 itself. This suggests that either previous reports of LRRK2 interactors are not robust or the YTH screen used here has a significant false negative rate. Furthermore, numerous proteins have been shown to bind to proteins mutated in PD [87, 210, 211, 222, 231, 443-446] but these proteins also did not appear in the yeast two hybrid.

Alternative and independent protein interaction screens using the same bait proteins or full length LRRK2 may potentially identify interactors that overlap with the yeast two hybrid hits or aid in the discovery of novel binding partners:

1) Immunoprecipitation: The basic premise allows for the isolation of the bait protein from mammalian cells along with any interacting proteins that form a stable complex. Once the bait protein and interacting proteins are isolated, the protein is digested and analyzed via mass spectrometer, peptide library or protein sequencing. A distinct advantage of immunoprecipitation over YTH is that it allows for the isolation of a complex of proteins as well as single interactors. In addition, post-translational modifications will be present if IPs can be conducted

in mammalian cells. However optimization of the purification procedure is required to enrich the protein interactor over background while maintaining the interaction.

2) Protein affinity purification involves covalently coupling the bait protein to a matrix such as sepharose. Cell extracts are subsequently passed through the column and under appropriate conditions different ligand proteins can be selected for. Weakly bound proteins can washed off using similar strategies employed in co-IP experiments. There are several advantages to this method:
    a. This techniques is potentially sensitive as one can immobilize high levels of bait protein and thus detect relatively weak interactions
    b. As with yeast two hybrid screens, one can test all proteins within a cell extract without bias and the majority of proteins within mammalian cell extracts, will be correctly modified and folded dependent on the solvent conditions.
    c. If the interaction between two proteins actually occurs as either a complex or via a third protein, the accessory proteins will often be present within the cell extract. However, one has to be careful that the interaction is specifically tested between the two proteins and recognize if a third protein is required for the interaction.
3) Protein micro arrays: A relatively recent technology, proteins are spotted onto a nitrocellulose membrane. The bait protein is either tagged in vitro with biotin or purified from cells expressing a tagged version. The bait protein is incubated with the array after blocking, washed to remove non-specific binding and the bait

protein is detected either using antibodies to the tag (fluorescent) or streptavidin conjugated to fluorescent dyes. This is a rapid, although limited (only 5000 proteins present on the array), method for the detection of protein-protein interactions. Once the protein is purified, the whole procedure can be achieved in a day. However as with any array, the entire process is completed in vitro therefore validation of the interaction is required in vivo. The proteins are also immobilized on the membrane and therefore if the protein is not in the correct conformation, there may be a significant false-negative rate.

At present, full length LRRK2 can only be expressed at relatively low levels in mammalian cells, therefore purification is inherently difficult increasing the likelihood of a false positive due to precipitation of non-specific proteins.

4. Mammalian Two hybrids – an extension of the yeast two hybrid system into mammalian cells. If bait and prey protein interact they are able to drive the expression of either the chloramphenicol transacetylase (CAT) gene or another antibiotic resistance gene. The advantage of this method over the yeast system is that, proteins are more likely to be correctly post translational modified and folded. In addition, one could use full length LRRK2 as the bait protein potentially identifying more relevant interactors. Compared to the yeast two hybrid, this method is both more time consuming, expensive and potentially at risk of a greater false positive rate as there is only one selection marker compared to three in the yeast system.

All the methods described above require that the interaction be further investigated by using independent experimental approaches, as many of the methods are extremely

sensitive, and proteins that do not normally co-exist in the same cellular compartment may be inappropriately exposed to one another.

In the current study one specific interaction was selected for validation. FEZ2 was chosen for follow-up as it activated all selection markers and met other criteria for a true interaction including the number of clones recovered, the presence of an open reading frame and the activation of selection markers upon retransformation. A total of 27 clones identified FEZ2 as binding partner of the N-terminal of LRRK2, all of which included the coiled coil region of FEZ2 (211aa-306aa). The interaction could be recapitulated upon re-transformation and swapping the bait and prey proteins into the opposite vector maintained the interaction. A mapping study was undertaking to determine the exact region of binding. As there was considerably homology between the coiled coil domains of FEZ1 and FEZ2, I determined if LRRK2 specifically bound to FEZ2 or if there was a motif common to both proteins.

Initially the interaction had occurred between the N-terminal of LRRK2 and the coiled coil region of FEZ2. This was subsequently mapped to between residues 494 and 863 of LRRK2 and the coiled coil domain (residues 211aa-306aa) of FEZ2. Without the coiled coil domain of FEZ1 and FEZ there was either no interaction (as was the case for FEZ1) or minimal interaction (as was the case for FEZ2) with LRRK2. Upon mating FEZ2 constructs containing the C-terminus and full length FEZ2, an interaction was observed between the LRR and ROC domains suggesting that these motifs may play additional roles in binding FEZ2. To verify this result, constructs expressing FEZ1/2 with/without the coiled coil domain need to be mated with constructs containing residues 494-863aa of LRRK2, or in conjunction with the LRR and/or ROC domains.

Even though and the interaction between LRRK2 and FEZ2 was confirmed in several ways in yeast and mapped to a specific region, it is still possible that the two proteins only bind each other in the yeast nucleus and do not interact in vivo. Thus, alternative methods were explored to verify this interaction in mammalian cells.

CHAPTER 6: CONFIRMATION OF INTERACTION BETWEEN LRRK2 AND FEZ2 IN MAMMALIAN CELLS.

INTRODUCTION

Many proteins operate in conjunction with other proteins as complexes to regulate a variety of processes, such as cell cycle control, differentiation, protein folding, signaling, transcription, translation, and transport. Protein interactions can be stable or transient and can also be either strong or weak [447, 448]. Stable interactions are those associated with proteins that are purified as multi-subunit complexes and are best studied by co-immunoprecipitation, pull-down or far-Western methods. Transient interactions are expected to control the majority of cellular processes and are temporary in nature, typically requiring a set of conditions that promote the interaction. Transient interactions are generally best observed by cross-linking or label transfer methods.

Numerous in vitro techniques have been developed to confirm and study protein interactions, each with their own advantages and the type of information they can impart [447, 448] (Table 15). In vitro affinity-based strategies can be direct, such as those utilized for pull-down assays or far-Western analysis or indirect, such as the typical co-immunoprecipitation experiment that is mediated by an antibody against a target antigen that in turn precipitates an interacting protein. Affinity-based methods can be highly sensitive with some methods capable of detecting weak interactions [448]. In addition, methods such as co-immunoprecipitation, pull-down assays, far-Western analyses and

label transfer methods allow all proteins in the sample to compete equally for the bait protein.

As there were no antibodies that recognized endogenous FEZ2 or LRRK2 and the type of interaction (transient or stable) was unknown, the method chosen to initially investigate the FEZ2/LRRK2 interaction was co-immunoprecipitation. Confocal microscopy was also used to exclude the possibility that the two proteins were normally prevented from interacting by virtue of being in different cellular compartments,

In vitro Methods	*Description*
Co-Immunoprecipitation (Co-IP)	An immunoprecipitation (IP) experiment designed to affinity purify a baitprotein antigen together with its binding partner using a specific antibody against the bait.
Cross-linking Reagents	Strategies involve homo- or heterobifunctional reagents whose chemical cross-links may or may not be reversed. Nearest neighbors (suspected to interact) in vivo or in vitro can be trapped in their complexes for further study.
Far-Western Analysis	The antibody probe in a typical Western blot detection, is substituted with an appropriately labeled bait protein as the probe. Detection can be radioisotopic, chemiluminescent or colorimetric, depending on the probe label.
Label Transfer	Involves a specialized cross-linking agent with several important features. These include heterobifunctionality for stepwise cross-linking, a detectable label and reversibility of the cross-link between binding partners. Upon reduction of the cross-linked complex a binding partner (prey protein) acquires the label from a bait protein that was first modified with the reagent. The label is typically used in the detection process to isolate or identify the unknown prey protein.
Fluorescence Resonance Energy Transfer (FRET)	In this technique, two different fluorescent molecules (fluorophores) are genetically fused the two proteins of interest. When two proteins are extremely close to one another (20-100Å) energy is transferred from the donor fluorophore to the acceptor flurophore.
Protein Interaction Mapping	Utilizes an "artificial protease" on a bait protein to initiate contact-dependent cleavages in the prey protein in the presence of specific reactants. The nonspecific cleavage fragments produced by the artificial protease can be analyzed to map the contact sites or interface of a known protein:protein interaction.
Pull-Down Assays	An affinity chromatography method that involves using a tagged or labeled bait to create a specific affinity matrix that will enable binding and purification of a prey protein from a lysate sample or other protein-containing mixture.
Surface Plasmon Resonance	Relates binding information to small changes in refractive indices of laser light reflected from gold surfaces to which a bait protein has been attached. Changes are proportional to the extent of binding. Special labels and sample purification are not necessary, and analysis occurs in real time.
NMR (Nuclear Magnetic Resonance)	Method that can provide insights into the dynamic interaction of proteins in solution.
Mass Spectroscopy	Used in concert with affinity-based methods, such as co-IPs, to isolate binding partners and complexes and identify the component proteins using standard mass spectral methods, e.g., MALDI-TOF and mass searching of bioinformatics databases.

Table 15: Descriptions of methods commonly used to confirm and analyze protein-protein interactions.

MATERIALS AND METHODS

Cloning of FEZ1 and FEZ2

cDNA primers for FEZ1 and FEZ2 were designed (Table 11) to amplify full length cDNA from human brain cDNA. cDNAs for FEZ1 (NCBI accession number: NM_005103) and FEZ2 (NCBI accession number: NM_001042548) were cloned into pCR8/GW/TOPO to generate a gateway entry clone, verified by sequencing and transferred to mammalian expression vectors with N-terminal V5 or GFP tags (Chapter 3, pg 91). Constructs were transiently transfected into COS7 cells and analyzed by western blotting using antibodies directed against the tags (Western blotting protocol; Chapter 3, pg 93-95).

Colocalisation of FEZ1/2 and LRRK2

COS7 cells were co-transfected with GFP-FEZ1/FEZ2 and V5-LRRK2. FEZ1/FEZ2 were also co-transfected with mutant forms of LRRK2 (mutants and corresponding kinase dead). Transfection protocol was as described above (Chapter 3, pg 92). Transfected cells were stained and fixed as described above (Chapter 3, pg 97-98). The following primary antibodies were used; monoclonal anti-GFP (ROCHE) and polyclonal-V5 (SIGMA) and the appropriate secondary antibody (anti-mouse AlexaFluor 488 and anti rabbit AlexaFluor 568). Slides were imaged using confocal microscopy.

Co-immunoprecipitation of FEZ1/FEZ2 and LRRK2

There are presently no antibodies that recognize the endogenous form of either LRRK2 or FEZ1/2. Therefore, both proteins were tagged with either GFP or V5. FEZ2 was cloned into the gateway expression vectors pcDNA3.1/nV5-dest and pcDNA-DEST53. Co-transfections were carried out as described above (Mammalian cell transfections, pg 92). The total amount of DNA for co-transfections was the same as that used for single plasmid transfections except molar ratios of each vector was used.

CO-IP Method (Fig 30):

1. Remove media from cells and wash twice with ice cold PBS.
2. Scrape cells into ice cold PBS and centrifuge at 5000xg for 10 min.
3. Remove supernatant and resuspend pellet in 250µl of ice cold lysis buffer (see individual co-IP experiments, in results section, for recipe of lysis buffer)
4. Place cells on ice for 30mins
5. After 30mins, add 100µl of 50% slurry of protein G agarose (Amersham).
6. Rotate cells with protein G for two hours at 4°C.
7. Centrifuge lysates with protein G for 10mins at 10000xg
8. Remove supernatant and save an aliquot to run on SDS page and western blotting – precleared input.
9. Incubate remaining lysates with 2µg of the appropriate (Monoclonal anti-GFP (ROCHE) and anti-V5 (Invitrogen)) antibody and 50µl of 50% slurry of protein G agarose.
10. Rotate cells overnight at 4°C.

11. Following day, centrifuge lysates for 1min at 1000xg at 4°C.
12. Remove supernatant and save an aliquot to run on SDS page and western blotting
13. Resuspend agarose pellet with wash buffer, invert 4-5 times and centrifuge for 1min at 1000xg at 4°C. Remove and discard supernatant.
14. Repeat step 13 a total of 5 times
15. Resuspend agarose pellet in Laemmeli loading buffer (Bio-Rad) with 5% β-mercaptoethanol and boil for 15mins at 65°C.
16. Centrifuge samples for 1 min at 1000g.
17. Run supernatant on SDS page and analyze by western blotting (Western blot protocol, Chapter 3; pg 93-95).

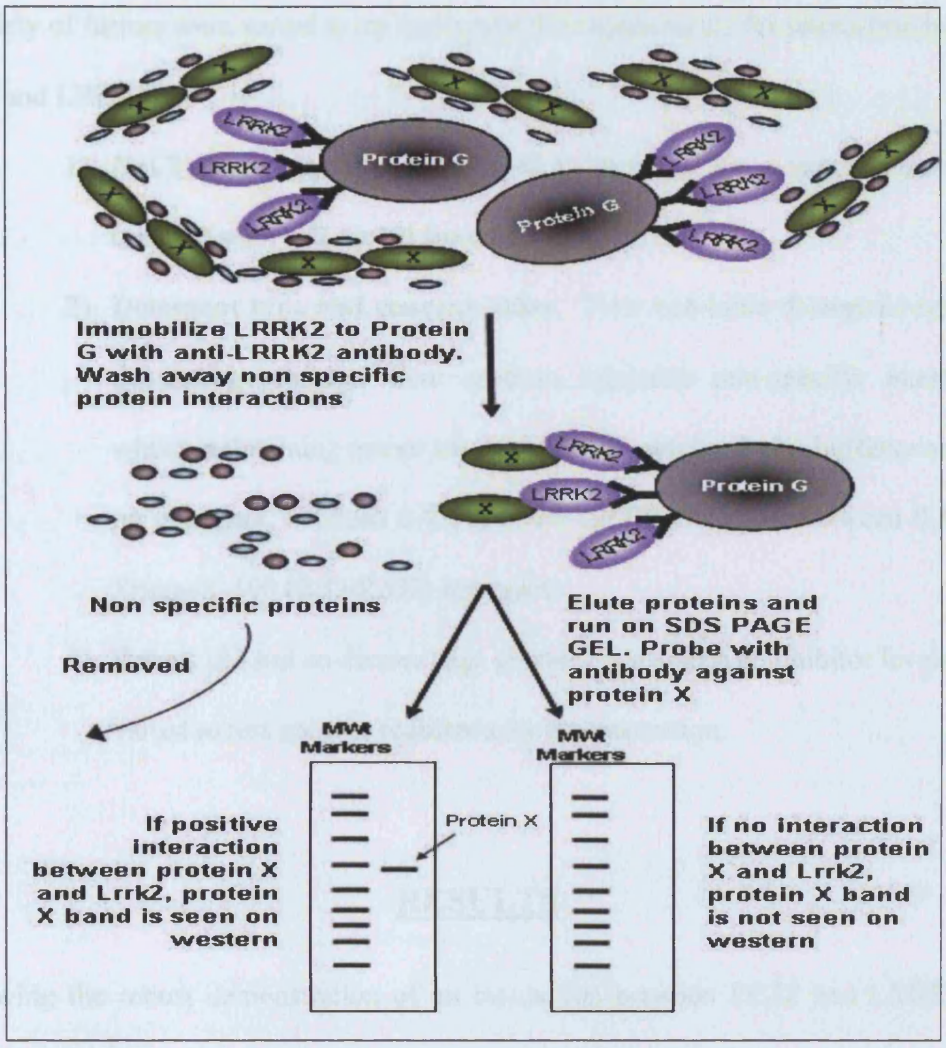

Figure 30: Schematic representation of co-immunoprecipitation protocol. An antibody (monoclonal or polyclonal) against a specific target antigen is allowed to form an immune complex with that target in a sample, such as a cell lysates. The immune complex is then captured on a solid support to which either Protein A or Protein G has been immobilized (Protein A or G binds to the antibody, which is bound to its antigen). Any proteins not co-precipitated on the support are washed away. Finally, components of the bound immune complex (both antigen and antibody) are eluted from the support and analyzed by SDS-PAGE followed by Western blotting to verify the identity of the antigen.

A variety of factors were varied to try and assess the requirements for interaction between FEZ2 and LRRK2:

1) **NaCl concentration**: This is used to break up ionic interactions and its concentration was varied from 50mM to 150mM
2) **Detergent type and concentration**: Two non-ionic detergents with low denaturing potential were used to minimize non-specific interactions whilst maintaining native structure of the protein. Lysis buffers contained no detergent, between 0-0.5% of NP-40 (PIERCE) or between 0.1%-1% Triton-X-100 (BIO-RAD) detergents.
3) **Other**: pH and co-factors (e.g. glycerol, phosphatase inhibitor levels) were varied to test specific requirements for interaction.

RESULTS

Following the robust demonstration of an interaction between FEZ2 and LRRK2 in a yeast two-hybrid model system, verification of the interaction in mammalian cells was attempted.

Expression of FEZ1 and FEZ2

Amplification of FEZ1 (NCBI accession no: NM005103) and FEZ2 (NCBI accession no: NM 001042548) cDNA resulted in amplicon sizes corresponding to published sequences (1179bp and 1143bp respectively; Figure 31). Verified constructs were transiently transfected into COS7 and analyzed by western blot with antibodies directed against the tag (Figure 32).

FEZ1 and FEZ2 have predicted molecular weights of 45kDA and 42kDA respectively. However, both proteins migrate at approximately 5kDA higher than predicted (Figure 32), when tagged with either V5 (expected molecular weight; 46Kda or 44kDA for FEZ1 and FEZ2 respectively) or GFP (expected molecular weight; 72kDA and 69Kda for FEZ1 and FEZ2 respectively). This is consistent with the similar size differences between observed and expected molecular weights in yeast experiments and suggests that FEZ1 and FEZ2 are post-translationally modified, although the nature of this modification is not known.

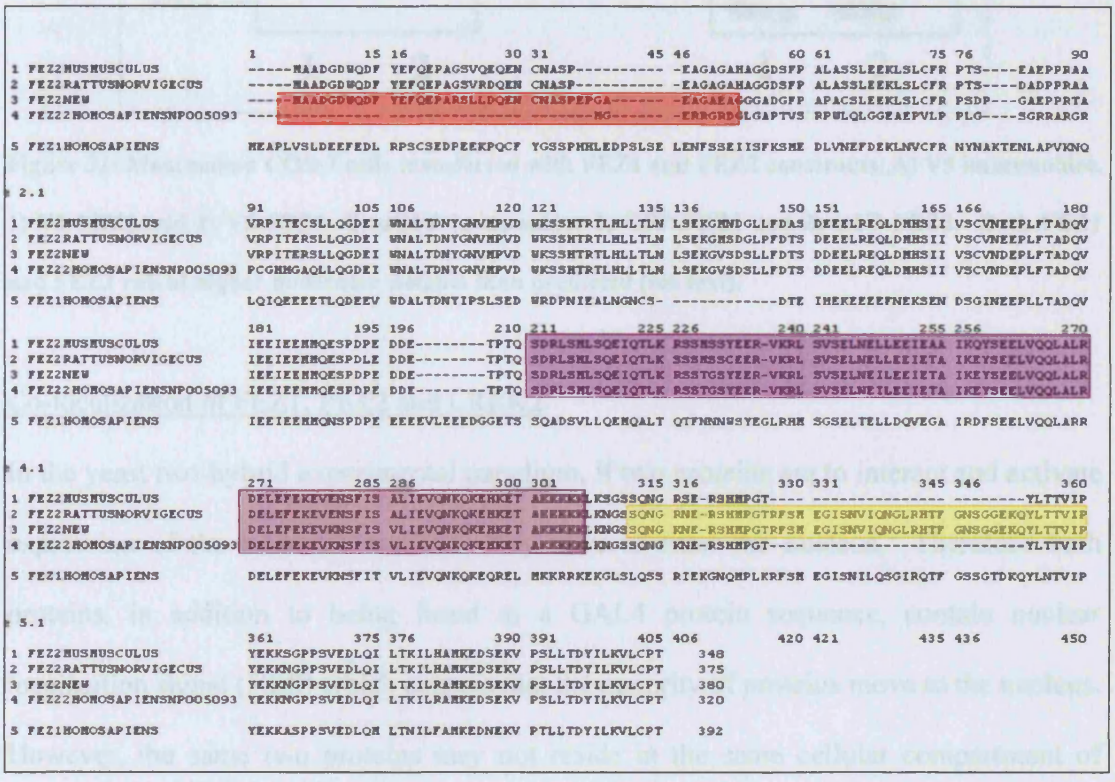

Figure 31: Multiple protein sequence alignment for FEZ2 and its homologous proteins. Region in red represents alternative start codons, purple represents region identified as interacting motif for LRRK2 in initial yeast two hybrid screen and yellow represents an in frame exon identified during

cDNA cloning of FEZ2. 1-mouse FEZ2, 2 rat FEZ2, 3 human FEZ2 isoform 1, 4-human FEZ2 isoform 2, 5-human FEZ1.

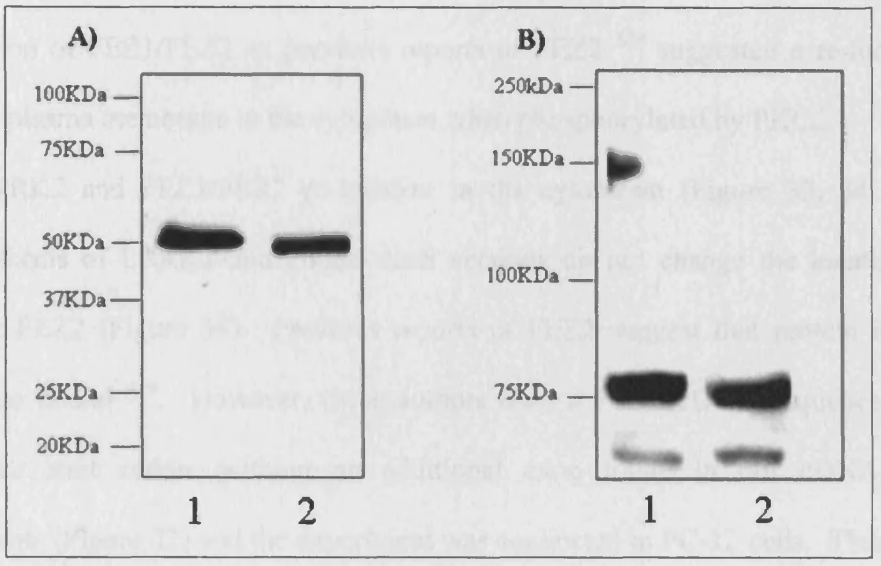

Figure 32: Mammalian COS-7 cells transfected with FEZ1 and FEZ2 constructs. A) V5 immunoblot. 1) V5-FEZ1 and 2) V5-FEZ2. B) αGFP immunoblot 1) GFP-FEZ1 and 2) GFP-FEZ2. Both FEZ1 and FEZ2 run at higher molecular weights than predicted (see text).

Co-localization of FEZ1, FEZ2 and LRRK2

In the yeast two-hybrid experimental paradigm, if two proteins are to interact and activate expression of the selection markers, they have to enter the nucleus. Therefore both proteins, in addition to being fused to a GAL4 protein sequence, contain nuclear localization signal (NLS) which ensures that the majority of proteins move to the nucleus. However, the same two proteins may not reside in the same cellular compartment of mammalian cells. Therefore it is important to assess the subcellular localization of LRRK2 and FEZ1/FEZ2 in mammalian cells.

To address this, COS7 cells were co-transfected with FEZ1/FEZ2 and LRRK2. FEZ1/FEZ2 were also co-transfected with mutants forms of LRRK2 (mutants and corresponding kinase dead) to determine if kinase activity influenced the cellular localization of FEZ1/FEZ2 as previous reports of FEZ2 [449] suggested a re-localization from the plasma membrane to the cytoplasm when phosphorylated by PKCζ.

Both LRRK2 and FEZ1/FEZ2 co-localize in the cytoplasm (Figure 33, 34 and 35). Mutant forms of LRRK2 and kinase dead versions do not change the localization of FEZ1 or FEZ2 (Figure 34). Previous reports of FEZ2 suggest that protein is plasma membrane bound [449]. However, these authors used a FEZ2 cDNA sequence with an alternative start codon, without an additional exon found in our cDNA cloning experiments (Figure 32) and the experiment was conducted in PC-12 cells. Thus, at least in transfected COS7 cells, LRRK2 and FEZ1/FEZ2 reside in the cytoplasm.

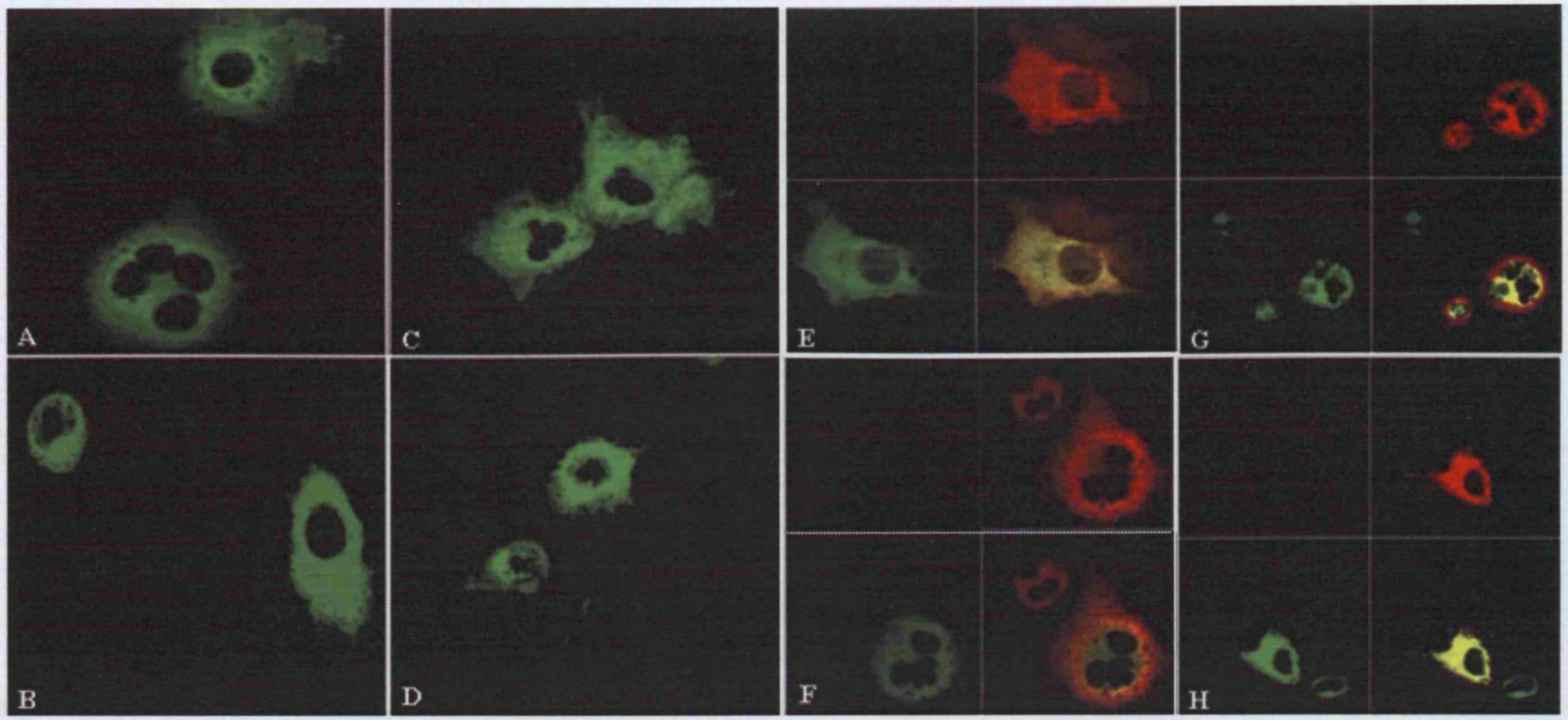

Figure 33: Colocalisation of FEZ1 and FEZ2 with LRRK2 and its mutants in COS7 cells. FEZ1 and FEZ2 are labeled in green (bottom left of quadrants E-H) and LRRK2 in red (Upper right of quadrants E-H). A) N-terminal V5 tagged FEZ1 B) N-terminal GFP V5 tagged FEZ1 C) N-terminal V5 tagged FEZ2 D) N-terminal GFP tagged FEZ2 E) N-terminal V5 FEZ1 and N-terminal MYC wild type LRRK2 F) N-V5 FEZ2 and N-MYC wild type LRRK2 G) N-V5 FEZ1 and N-MYC kinase dead LRRK2 H) N-V5 FEZ2 and N-MYC kinase dead LRRK2. The bottom right of quadrants E-H shows the merged red and green channels. Magnification x63

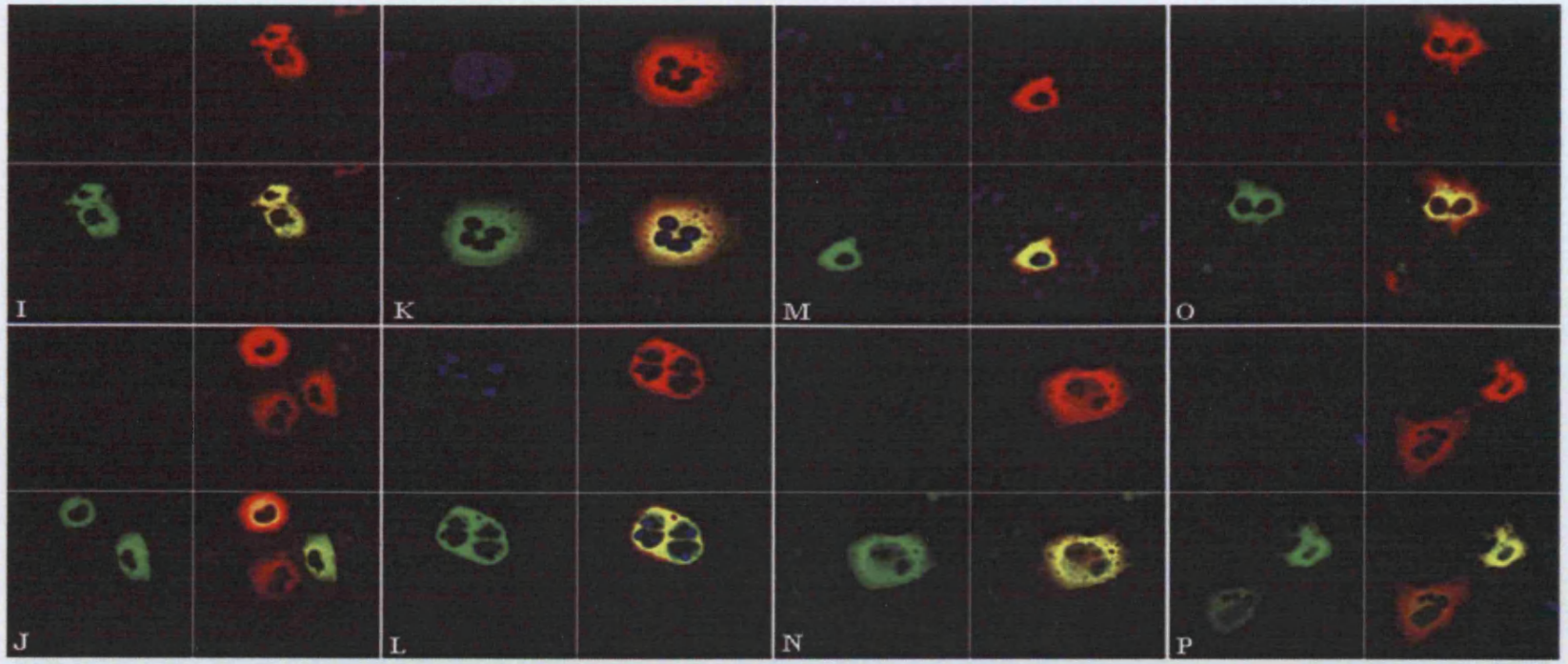

Figure 34: Colocalisation of FEZ1 and FEZ2 with LRRK2 mutants in COS7 cells. I) N-V5 FEZ1 and N-MYC R1441C LRRK2 J) N-V5 FEZ2 and N-MYC R1441C LRRK2 K) N-V5 FEZ1 and N-MYC R1441C kinase dead LRRK2 L) N-V5 FEZ2 and N-MYC R1441C kinase dead LRRK2 M) N-V5 FEZ1 and N-MYC Y1699C LRRK2 N) N-V5 FEZ2 and N-MYC Y1699C LRRK2 O) N-V5 FEZ1 and N-MYC Y1699C kinase dead LRRK2 P) N-V5 FEZ2 and N-MYC Y1699C kinase dead LRRk2. FEZ1 and FEZ2 are labeled in green (bottom left of quadrants) LRRK2 in red (upper right of quadrants), the (bottom right of each quadrant) represents merges between the channels. Nuclei are stained with Hoechst (blue, upper left of each quadrant). Magnification x63

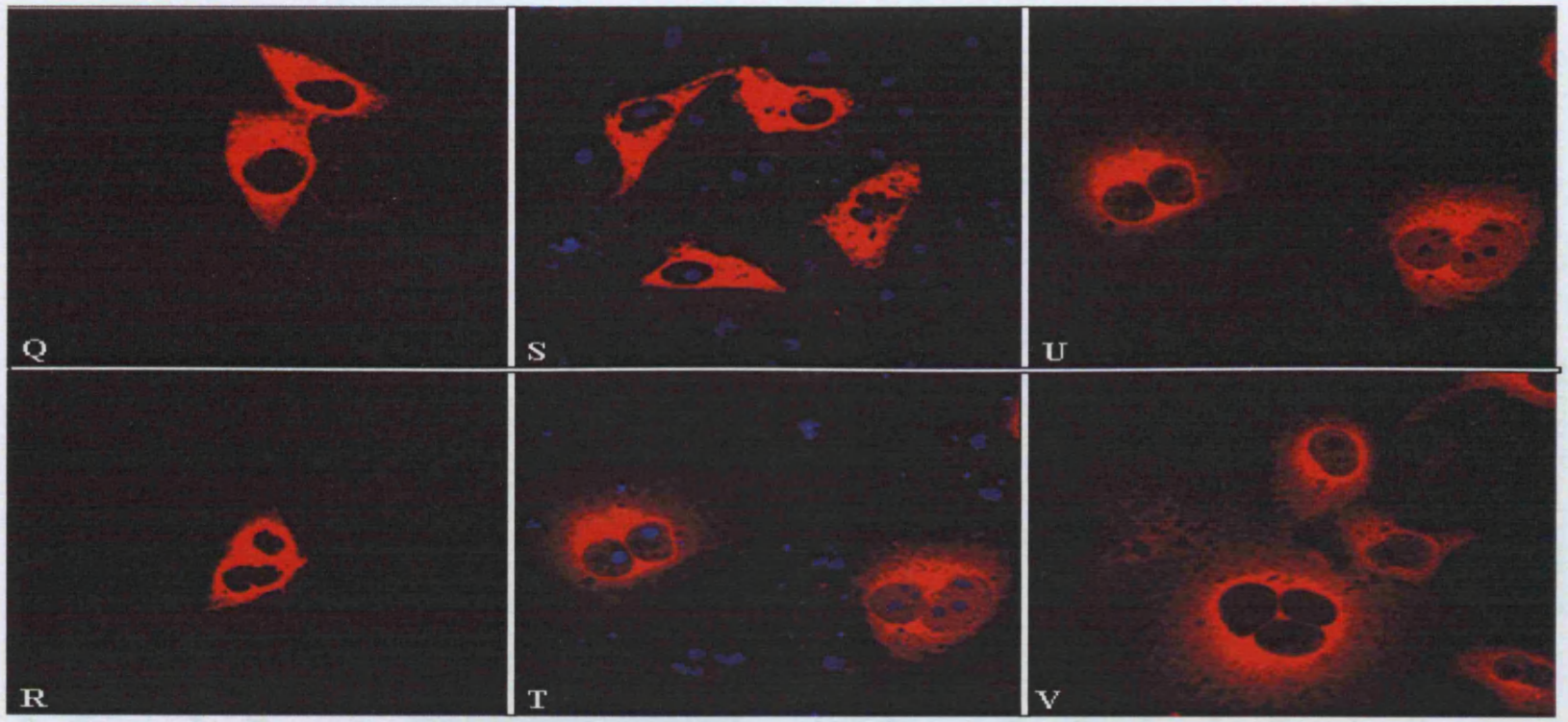

Figure 35: Localization of LRRK2 within COS7 cells: Q) N-MYC wild type LRRK2 R) N-MYC kinase dead LRRK2 S) N-MYC R1441C LRRK2 T) N-MYC R1441C kinase dead LRRK2 U) N-MYC Y1699C LRRK2 V) N-MYC Y1699C kinase dead LRRK2. Nuclei are stained with Hoechst (blue).

Co-immunoprecipitation of FEZ1/2 and LRRK2

As the interaction between FEZ2 and LRRK2 had only been observed in yeast and had not been replicated with full length LRRK2, both proteins were co-expressed in mammalian cells and each of the two proteins immuno-precipitated. If FEZ2 binds to LRRK2, precipitation of one protein would also result in precipitation of the other. Initially, FEZ2 was precipitated and washed in buffers only containing 150mM NaCl. However, the interaction and wash buffer were not sufficiently stringent, as without any FEZ2 present; LRRK2 precipitated suggesting there was no specific binding of LRRK2 either to the antibody or protein G agarose (Figure 36: lane 3 and 4).

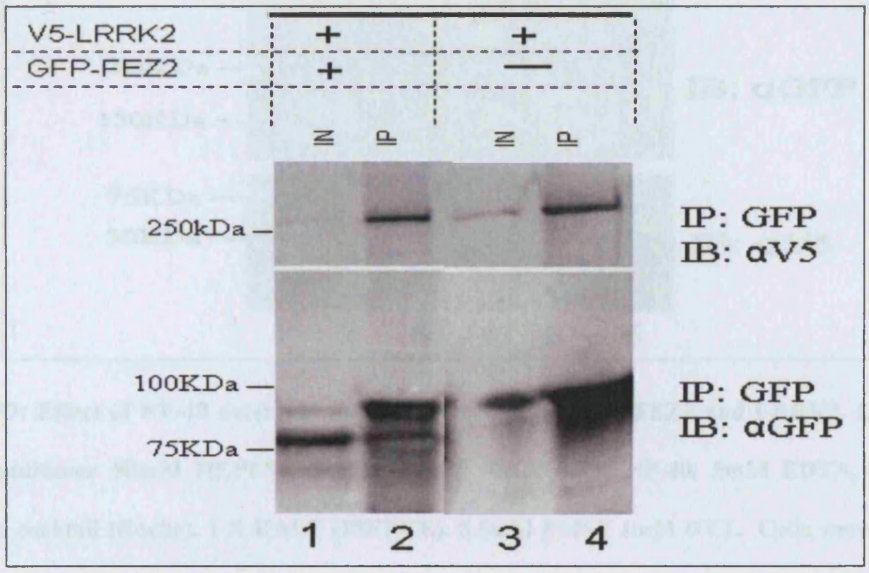

Figure 36: Effect of NaCl on the interaction between FEZ2 and LRRK2. Lysis and wash conditions: 50mM HEPES pH 7.4, 150mM NaCl, 5mM EDTA, protease inhibitor cocktail (Roche), 1 X HALT (PIERCE), 0.5mM PMSF 1mM DTT. Cells were lysed in the above buffer and proteins were precipitated with monoclonal GFP (FEZ2). Proteins and antibody complex were attached to protein G agarose and washed 5 times. Proteins were eluted and analyzed by western blotting with antibodies to GFP and V5. Under these conditions, LRRK2 precipitated in

the presence of FEZ2 (lanes 1 and 2) but LRRK2 also precipitated in the absence of FEZ2 (Lane 3 and 4). Abbreviations: IN-INPUT, IP-IMMUNOPRECIPITANT

The detergent, NP-40 (PIERCE) was subsequently added to reduce and disrupt non-specific interactions. The concentration of NP-40 was systematically raised (0.1%, 0.25% and 0.5%) and eventually increased to 0.5% at which point no interaction was observed between LRRK2 and FEZ2 (Figure 37).

Figure 37: Effect of NP-40 detergent on the interaction between FEZ2 and LRRK2. Lysis and wash conditions: 50mM HEPES pH 7.4, 150mM NaCl, 0.5% NP-40, 5mM EDTA, protease inhibitor cocktail (Roche), 1 X HALT (PIERCE), 0.5mM PMSF 1mM DTT. Cells were lysed in the above buffer and proteins were precipitated with either monoclonal GFP (LRRK2) or V5 (FEZ2). Proteins and antibody complex were attached to protein G agarose and washed 5 times. Proteins were eluted and analyzed by western blotting with antibodies to GFP and V5. Under these conditions, neither FEZ2 nor LRRK2 precipitated when LRRK2 (lane 3) or FEZ2 (lane 6) were precipitated. Abbreviations: IN-INPUT, SUP-SUPPERNATANT, IP-IMMUNOPRECIPITANT

NP-40 is a relatively mild detergent with a low micell count and thus may not lyse the cells very efficiently leading to overall low protein concentrations. As a consequence the detergent was switched to TritonX-100 as this has a higher micelle count and disrupts membranes more efficiently.

The concentration of TritonX-100 was systematically increased to 1%, at which point no interaction was observed between LRRK2 and FEZ2. NaCl levels were decreased to 50mM, in case 150mM was too stringent and broke interaction between FEZ2 and LRRK2. However, no interaction occurred at 50mM NaCl (Figure 38).

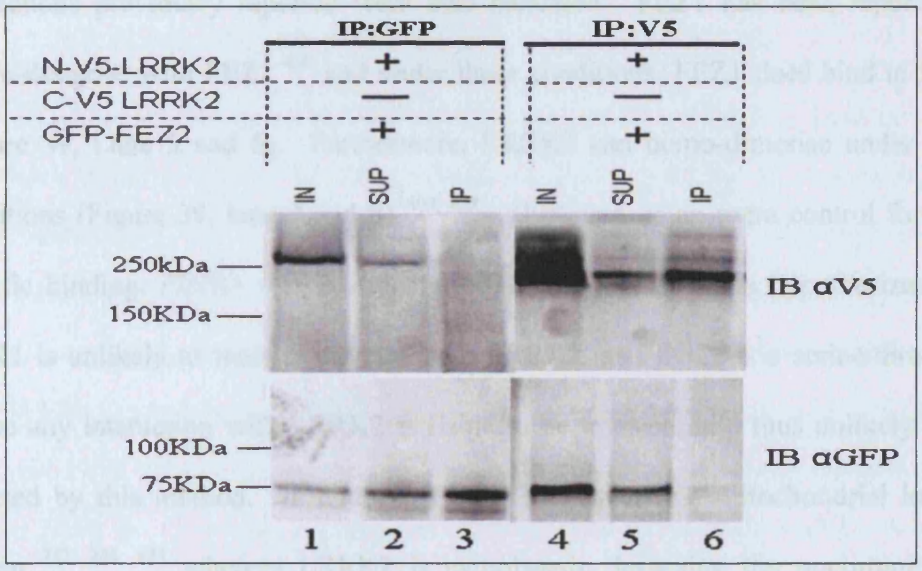

Figure 38: Effect of Triton detergent on the interaction between FEZ2 and LRRK2. Lysis and Wash conditions: 50mM HEPES pH7.4, 50mM NaCl, 1% Triton, 5mM EDTA, protease inhibitor cocktail (Roche), 1xHALT, 0.5mM PMSF, 1mM DTT. Cells were lysed in the above buffer and proteins were precipitated with either mono-clonal GFP (FEZ2) or V5 (LRRK2). Proteins were eluted and analyzed by western blotting with antibodies to GFP and V5. Under these conditions, neither LRRK2 nor FEZ2 precipitated when FEZ2 (lane 3) or LRRK2 (lane 6)

were precipitated respectively. Abbreviations: IN-INPUT, SUP-SUPPERNATANT, IP-IMMUNOPRECIPITANT

As varying the concentration of NaCl or detergent either resulted in no interaction or non-specific binding, additives were included in lysis and wash buffers to try and stabilize the interaction. The first additive used was glycerol as this can stabilize hydrophobic interactions and decrease the protein unfolding rate, thus potentially maintaining the native structure of FEZ2 and LRRK2. In the presence of glycerol, FEZ1/2 bound to LRRK2 (Figure 39, Lane 2 and 4). In addition several other interactions previously reported were also recreated. FEZ1 has been reported to hetero-dimerise with FEZ2 [450] and under these conditions, FEZ1 does bind to FEZ2 (Figure 39, Lane 5 and 6). Furthermore, LRRK2 can homo-dimerise under these conditions (Figure 39, lane 7 and 8) [409, 414]. However, as an extra control for non-specific binding, PINK1 was co-transfected with LRRK2. It is hypothesized that PINK1 is unlikely to interact directly with LRRK2, as PINK1 is a serine/threonine kinase any interaction with LRRK2 is liable to be transient and thus unlikely to be detected by this method. In addition PINK1 is primarily a mitochondrial located protein [232, 244, 451] whereas LRRK2 is cytoplasmic, lessening the opportunity for interaction between the two.

Based on the result below (Figure 39), the addition of glycerol acted to stabilize all protein interactions.

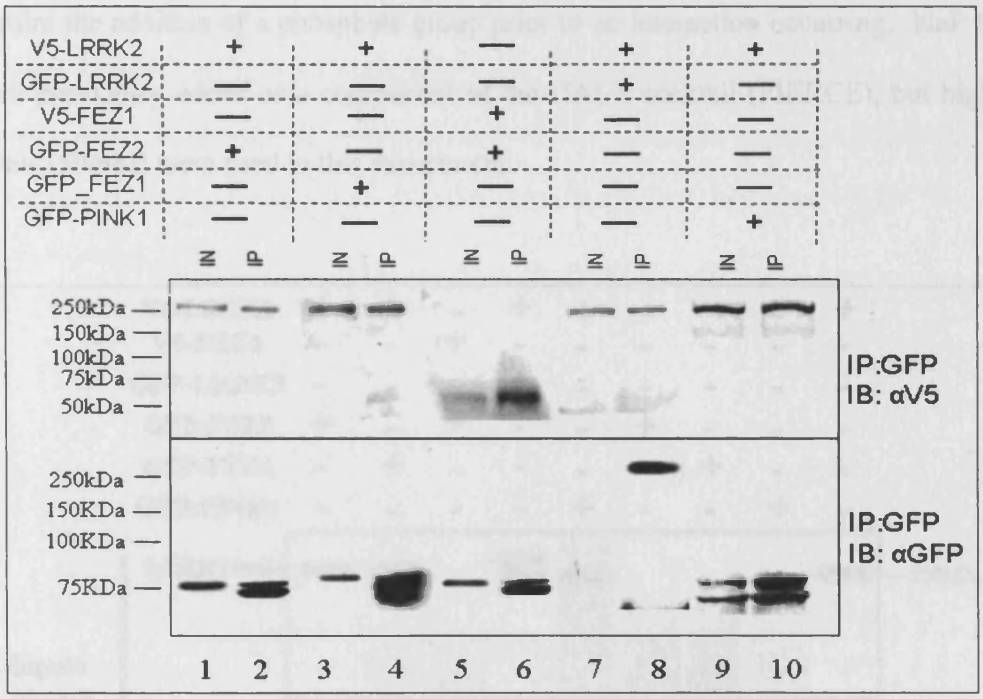

Figure 39: Effect of glycerol on the interaction between FEZ2 and LRRK2. Lysis and Wash conditions: 50mM HEPES pH7.4, 150mM NaCl, 1% Triton, 5mM EDTA, protease inhibitor cocktail (Roche), 1xHALT, 0.5mM PMSF and 7.5% glycerol, 1mM DTT. Cells were lysed in the above buffer and proteins were precipitated with either monoclonal antibodies to GFP or V5. Proteins were eluted and analyzed by western blotting with antibodies to GFP and V5. Under these conditions, precipitation of FEZ2/1 (lanes 2 and 4, respectively) also precipitated LRRK2. FEZ1 and FEZ2 were also able to hetero-dimerise (lane 5) and LRRK2 was also able to self-interact (lane 8). However, precipitation of PINK1 also precipitated LRRK2 (lane 10). Abbreviations: IN-INPUT, IP-IMMUNOPRECIPITANT

Varying the type and concentration of detergent used, as well as varying NaCl levels and the presence of glycerol did not result in a stable interaction between FEZ1/2 and LRRK2 that was specific. As FEZ1/FEZ2 can be phosphorylated but PKZζ [449, 452] and LRRK2 may auto-phosphorylate [409, 411, 414] or be phosphorylated, NaF was added, a serine/threonine phosphatase inhibitor, to determine if one or both the proteins

require the addition of a phosphate group prior to an interaction occurring. NaF had been previously added as a component of the HALT cocktail (PIERCE), but higher levels (50mM) were used in this experiment.

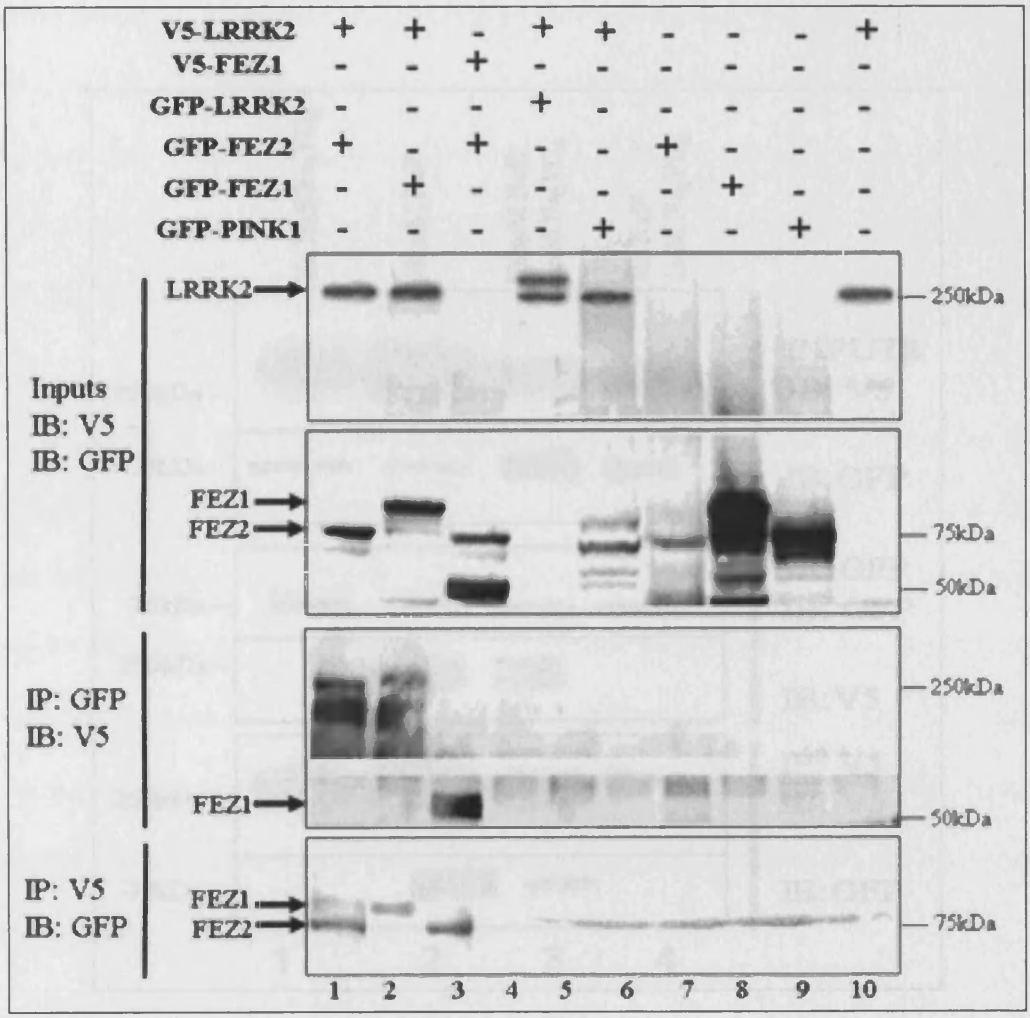

Figure 40: Effect of NaF on the interaction between FEZ2 and LRRK2. Lysis and Wash conditions: 50mM HEPES pH7.4, 150mM NaCl, 1% Triton, 5mM EDTA, protease inhibitor cocktail (Roche), 1xHALT, 0.5mM PMSF and 7.5% glycerol, 1mM DTT, 50mM NaF, 1mM Na_3VO_4. Cells were lysed in the above buffer and proteins were precipitated with either monoclonal GFP or V5. Proteins were eluted and analyzed by western blotting with antibodies to GFP and V5. Under these conditions, precipitation of FEZ2/1 (lanes 1 and 2, respectively)

also precipitated LRRK2. FEZ1 and FEZ2 were also able to hetero-dimerise (lane 3) but LRRK2 was not able to interact with itself (lane 4). FEZ1/2 and LRRK2 did not precipitate in the absence of LRRK2 or FEZ1/2 respectively (lane 7 through 10) and LRRK2 did not precipitate in the presence of PINK1 (lane 5). Abbreviations: IN-INPUT, IP-IMMUNOPRECIPITANT

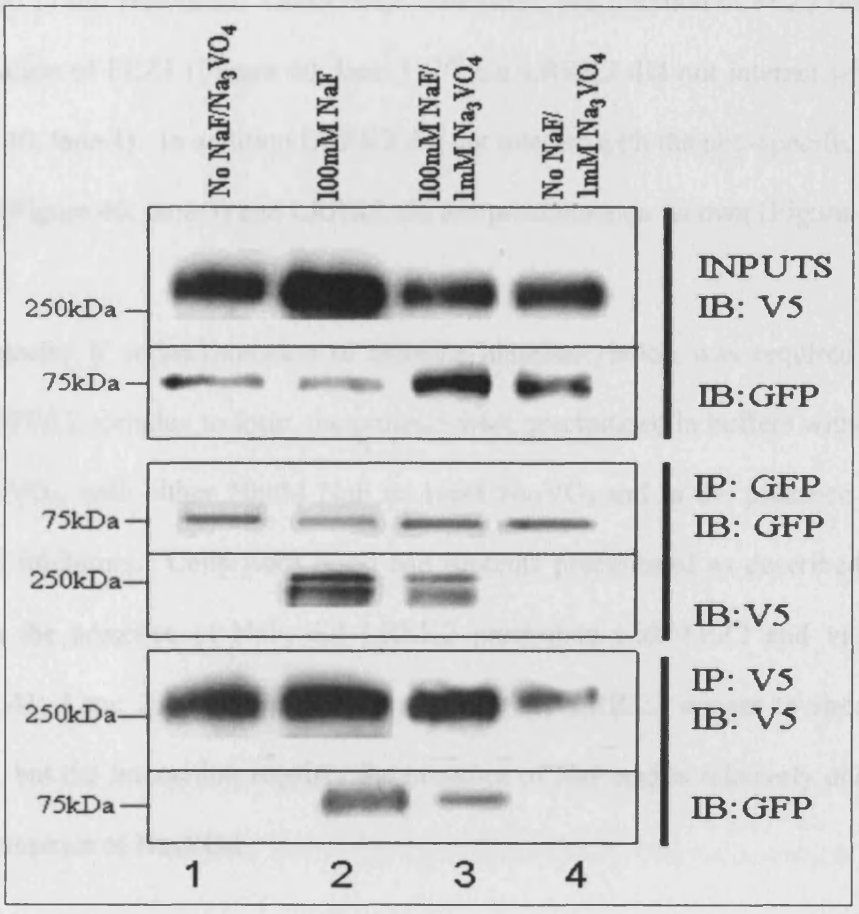

Figure 41: Verification of the interaction between FEZ2 and LRRK2 only in the presence of NaF. Lysis and Wash conditions for lane 1: All buffers contained 50mM HEPES pH7.4, 50mM NaCl, 1% Triton, 5mM EDTA, protease inhibitor cocktail (Roche), 0.5mM PMSF and 7.5% glycerol, 1mM DTT. Lysis and wash buffers for lane 2: as in lane 1 plus 50mM NaF. Lysis and wash buffers for lane 3: as in lane 1 plus 50mM NaF and 1mM Na_3VO_4. Lysis and wash buffers for lane 4: as in lane 1 plus 1mM Na_3VO_4. Cells were lysed in the appropriate buffer and

proteins were precipitated with either mono-clonal GFP (FEZ2) or V5 (LRRK2). Proteins were eluted and analyzed by western blotting with antibodies to GFP and V5. Under these conditions, precipitation of FEZ2 only resulted in the co-IP of LRRK2 and vice versa in the presence of NaF (lanes 3 and 4). Abbreviations: IN-INPUT, IP-IMMUNOPRECIPITANT, IB-IMMUNOBLOT

Precipitation of FEZ1 and FEZ2 resulted in the co-precipitation of LRRK2 (Figure 40 lane1 and 2) and vice versa. Under these conditions, precipitation of FEZ2 resulted in precipitation of FEZ1 (Figure 40; lane 3) [450] but LRRK2 did not interact with itself (Figure 40; lane 4). In addition LRRK2 did not interact with the non-specific control, PINK1 (Figure 40; lane 5) and LRRK2 did not precipitate on its own (Figure 40; lane 10).

To determine if serine/threonine or tyrosine phosphorylation was required for the LRRK2/FEZ2 complex to form, the proteins were precipitated in buffers without NaF and Na_3VO_4, with either 50mM NaF or 1mM Na_3VO_4 and in the presence of both types of inhibitors. Cells were lysed and proteins precipitated as described above. Only in the presence of NaF, did LRRK2 precipitate with FEZ2 and vice versa (Figure 41; Lane 2 and 3). Therefore, FEZ2 and LRRK2 appear to specifically interact, but the interaction requires the presence of NaF and is relatively unaffected by the presence of Na_3VO_4.

DISCUSSION

Currently, very little is known about the function of FEZ2, with the majority of research focused on its homolog, FEZ1. FEZ2 is ubiquitously expressed in mammalian tissues [449]. FEZ1 is exclusively expressed in the brain where it appears to

be involved in neuritogenesis upon phosphorylation by PKCζ [452, 453]. Knockout of the FEZ1 homolog from Drosophila and C-elegans (UNC-76) leads to locomotion and axonal transport defects [452, 454, 455]. The mechanism by which FEZ1 increases axonal outgrowth is not well understood but the UNC-76 appears to form complex with UNC-69 (SOCO-mammalian homolog), which promotes axonal growth and normal presynaptic organization [455]. It has also been shown that FEZ1 is able to homo-dimerise and to hetero-dimerise with FEZ2 but the consequences of this are currently unknown [450]. Given the role of FEZ1 in axonal outgrowth and normal synaptic function, FEZ2 and LRRK2 may co-operate in maintaining SN neuritic length and branching, and makes FEZ2 a good functional interactor for LRRK2. In support of this hypothesis, recent evidence has suggested that LRRK2 plays a role in maintaining neuronal morphology in vitro and in vivo [415].

A variety of factors were varied to try and confirm the interaction between FEZ2 and LRRK2 in mammalian cells. To efficiently detect interactions in these systems, the bait protein concentration should be in excess of the molar K_d of the interaction. The expression levels of LRRK2 were potentially limiting as this protein was more weakly expressed than FEZ1/2, so the type and concentration of the detergent used to lyse the cells were varied to maximize the amount of this protein extracted. Triton-X100 most efficiently released LRRK2 from the cells.

Secondly, to stabilize hydrophobic interactions thus stabilizing protein interactions and promote the re-folding of protein into their native conformation, glycerol was added. With the presence of glycerol the binding between FEZ2/LRRK2 binding as well as LRRK2 self interaction and FEZ1/FEZ2 hetero-dimerisation were recreated.

However, too much glycerol can also increase the possibility of inappropriate protein-protein interactions, which appeared to be the case here as LRRK2 could precipitate with PINK1. Therefore, we considered that these interactions were not physiological under these conditions.

To determine if phosphorylation of FEZ2 and LRRK2 was necessary for the interaction to occur, the concentration of NaF, a serine/threonine phosphatase inhibitor, was increased. Under these conditions, LRRK2 interacted with FEZ1/2, none of the proteins precipitated in the absence of the other and LRRK2 did not interact with PINK1. To confirm the effect of NaF on the interaction between FEZ2 and LRRK2, cells were lysed in various buffers with or without the presence of Na_3VO_4. This demonstrated that FEZ2 and LRRK2 only interact in the presence of NaF.

NaF has two effects, either of which may promote LRRK2 binding to FEZ1/2. Firstly, NaF may prevent the serine/threonine dephosphorylation of either protein and only in there phosphorylated states can the two proteins interact. In support of the hypothesis that phosphorylation is required for the interaction, FEZ1 and FEZ2 can be phosphorylated by PKCζ [449, 452], a serine/threonine kinase, and LRRK2 may be phosphorylated by an upstream kinase [418]. There are no identified phospho-sites of LRRK2, but phosphorylation prediction software (NETPHOS), suggests there is potentially a large region of serine phosphorylation in the LRR domain of LRRK2; an area which has been shown to bind to full length FEZ. If phosphorylation of either protein promotes interaction, the interaction should be inhibited in the presence of serine/threonine phosphatases or serine/threonine kinase inhibitors (e.g.

staurosporine, SIGMA). Na_3VO_4, a tyrosine phosphatase inhibitor, does not promote the interaction suggesting that serine/threonine phosphorylation is important in FEZ2/LRRK2 complex formation or NaF may promote the interaction between the two by a different mechanism.

The second role of NaF is less well understood. As mentioned previously, LRRK2 contains a ROC domain which, in part, can bind to FEZ2. The ROC domain is a GTPase and cycles between GDP-bound and GTP bound states, which are accompanied by large conformational changes [456]. This cycle is partly modulated by guanine nucleotide exchange factors (GEFs) and GTPase-activating proteins (GAPs). In general, GTP binding is thought to promote binding of the GTPase to target or "effector" proteins, whereas hydrolysis of GTP to GDP, in conjunction with GAPs, results in dissociation of these interactions. Exchange factors can then act to remove GDP allowing GTP to bind. Such conditional binding to target proteins allows GTPases to function as molecular switches in a number of cellular processes. NaF has been reported to stabilize other GTP-dependent interactions in mammalian cells and in this case might restrict LRRK2 to a favorable conformation for an interaction with FEZ2, most probably in a GTP 'on' bound state [457]. Although the mechanism of action of NaF is not known, it has been suggested that other fluorides (such as aluminium tetrafluoride) stabilize GDP bound GTPases in their transition states by mimicking the γ-phosphate group of. The hypothesis that NaF affects FEZ2/LRRK2 interactions via altered GTP binding and/or hydrolysis can be tested in multiple ways:

1) Adding excess levels of GTPγS (a non-hydrolyzable form of GTP) or GDPβS (which competes with GTP for GTPase activation) will either

prevent or strengthen the interaction between LRRK2 and FEZ2. If FEZ2 is bound to LRRK2/GTPγS, GTPγS cannot be hydrolyzed and subsequently will stay bound to FEZ2.

2) Mutations can be created within LRRK2 that can either abolish GTPase (e.g. K1347A) activity or make it constitutively active by mutating key residues in one of four loops that interact with GTP (e.g. T1343G or R1398Q) [399, 403, 458].

The effects of NaF on either phosphatase inhibition or altered GTP binding may not be mutually exclusive. Phosphorylation may activate LRRK2, allowing GTP and FEZ2 to bind. Additionally, GTP binding to LRRK2 may cause subsequent auto-phosphorylation of LRRK2 and/or phosphorylation of FEZ2 and might promote an interaction between the two proteins.

Understanding the mechanism behind the FEZ2 and LRRK2 interaction could provide important insights into the pathways and mechanistic control of LRRK2. If LRRK2 phosphorylation is necessary for the interaction with FEZ2, it would be important to understand how LRRK2 phosphorylation is regulated. It was recently shown that PARKIN binds to Eps15, an adaptor protein that is involved in epidermal growth factor (EGF) receptor endocytosis and trafficking. Binding and ubiquitylation of Eps15 by PARKIN required stimulation by EGF [459], thus promoting neuronal survival via the Akt pathway. By analogy to this and many other examples, extracellular signaling may lead to the post translational modifications of LRRK2, allowing the interaction to occur and potentially controlling neuronal outgrowth and survival.

If GTPase function is necessary for the interaction between LRRK2 and FEZ2, clarifying how the ROC domain of LRRK2 affects the interaction may also aid in our understanding of how LRRK2 is controlled. At present, it has only been shown that LRRK2 can bind to GTP [416] and that artificial mutations within the ROC domain [416] appear to decrease kinase activity. However, pathogenic mutations within this region do not appear to directly increase kinase activity [409], thus studying this interaction may help determine the effect of these mutations on the function of the ROC domain and, hence, LRRK2.

The functional consequences of the interaction between FEZ2 and LRRK2 are unknown, but as FEZ1/2 have been reported to increase neuritic outgrowth [449, 452, 454, 460], the effects of co-transfection of LRRK2 and FEZ2 on neuritogenesis may be of interest. Recent evidence suggests that the normal function of LRRK2 is to maintain neuronal length and branching [415]. Mutations within LRRK2 cause progressive reduction in neurite length and branching, while knockdown of LRRK2 leads to increased neurite length and branching [415]. It would be of interest to know if this phenotype is enhanced or suppressed after FEZ2 is knocked out or if such phenotypes can be rescued by over-expression of FEZ2. These experiments would not prove that proteins physically interact but would support a common pathway of action.

In summary, an interaction between LRRK2 and FEZ2 is supported by yeast mapping data, co-localization and CO-IP experiments. Further work is needed to verify the interaction in vivo, investigate the functional consequences of the interaction and if the interaction is significant in the pathogenesis of LRRK2-linked PD.

CONCLUSION

Over the last decade, there have been considerable advances in the discovery of genes responsible for monogenic forms of PD. Together, the known genes account for approximately 2% of all PD cases, while mutations within LRRK2 alone account for approximately 1-2% of sporadic PD and 7-8% of familial PD. As light is shed upon the molecular mechanisms behind the pathogenesis of PD, it is expected that there will be a significant improvements in the treatment of symptoms in PD.

Our discovery of LRRK2 mutations has provided clinical researchers with a large patient pool with a single defined genetic etiology in which to study disease onset, progression and response to treatment. Given that an estimated 10,000 PD patients in North America alone may have the G2019S mutation there are undoubtedly a very large number of subjects who carry this mutation and have not developed disease. Based on current penetrance figures, one would estimate that 30% of these mutation carriers will eventually manifest disease. Large cohorts of asymptomatic subjects will be relatively easy to identify by assessing siblings and children of patients with G2019S linked disease. This group of subjects affords us the opportunity to not only identify signs and symptoms of disease that may be used as specific early indicators of PD, but also provide a cohort of patients in whom the efficacy of neuroprotective agents can be tested.

LRRK2 mutations may also be useful in allowing us to develop novel models of PD in a number of systems. As yet, there is no data available from in vivo models, but from in vitro studies three discernable phenotypes have been associated with LRRK2

mutations: aggregation formation, toxicity and increased kinase activity and it is thought that these three effects are linked. The identification of interactors, such as the self interaction of LRRK2 and the interaction with FEZ2, will hopefully elucidate the normal function of LRRK2 and the mechanisms that underlie its pathogenesis. Understanding what LRRK2 does and how mutations result in PD, will hopefully produce a readily quantifiable endpoint believed to be related to the pathological processes of the disease. This will also allow high throughput screening of molecular libraries of compounds for inhibitors of pathogenic processes.

Even though research on LRRK2 is at an early stage, continued research into and therapies directed towards LRRK2 are likely to have a great clinical impact and may bring us closer to understanding the pathogenic processes underlying PD.

REFERENCES

1. Parkinson, J., An essay on the shaking palsy. 1817. J Neuropsychiatry Clin Neurosci, **14**(2): p. 223-36; discussion 222.2002.

2. Brissaud, E., Lecons sur les Maladies nerveuses, in Masson et Cie. 1985: Paris.

3. Fahn, S., Description of Parkinson's disease as a clinical syndrome. Ann N Y Acad Sci, **991**: p. 1-14.2003.

4. Meynert, T., Ueber Beitrage sur differential Diagnose der paralytischen Irrsinns, in Wiener med. 1871: Germany. p. 645-647.

5. Kapp, W., The history of drugs for the treatment of Parkinson's disease. J Neural Transm Suppl, **38**: p. 1-6.1992.

6. Tretiakoff, C., Contribution a l'etude de l'anatomie pathologique du locus niger de Soemmering avec quelques deductions relatives a la pathogenic des troubles du tonus musculaire et de la maladie de Parkinson. These de Paris.1919.

7. Carlsson, A., M. Lindqvist, and T. Magnusson, 3,4-Dihydroxyphenylalanine and 5-hydroxytryptophan as reserpine antagonists. Nature, **180**(4596): p. 1200.1957.

8. Carlsson, A., et al., On the presence of 3-hydroxytyramine in brain. Science, **127**(3296): p. 471.1958.

9. Carlsson, A., The occurrence, distribution and physiological role of catecholamines in the nervous system. Pharmacol Rev, **11**(2, Part 2): p. 490-3.1959.

10. Sano, I., et al., Distribution of catechol compounds in human brain. Biochim Biophys Acta, **32**: p. 586-7.1959.

11. Ehringer, H. and O. Hornykiewicz, [Distribution of noradrenaline and dopamine (3-hydroxytyramine) in the human brain and their behavior in diseases of the extrapyramidal system.]. Klin Wochenschr, **38**: p. 1236-9.1960.

12. Benmoyal-Segal, L. and H. Soreq, Gene-environment interactions in sporadic Parkinson's disease. J Neurochem, **97**(6): p. 1740-55.2006.

13. Zhang Z-X and Roman G. C, Worldwide occurrence of Parkinson's disease: an updated review. Neuroepidemiology, **12**(4): p. 195-208.1993.

14. de Rijk M. C, et al., Prevalence of parkinsonism and Parkinson's disease in Europe: the EUROPARKINSON Collaborative Study. European Community Concerted Action on the Epidemiology of Parkinson's disease. J Neurol Neurosurg Psychiatry, **62**(1): p. 10-15.1997.

15. de Rijk, M.C., et al., Prevalence of Parkinson's disease in Europe: A collaborative study of population-based cohorts. Neurologic Diseases in the Elderly Research Group. Neurology, **54**(11 Suppl 5): p. S21-3.2000.

16. Elbaz, A., et al., Familial aggregation of Parkinson's disease: a population-based case-control study in Europe. EUROPARKINSON Study Group. Neurology, **52**(9): p. 1876-82.1999.

17. Riederer P and Wuketich S, Time course of nigrostriatal degeneration in parkinson's disease. A detailed study of influential factors in human brain amine analysis. J Neural Transm, **38**(3-4): p. 277-301.1976.

18. Langston J. W and Ballard P. A Jr, Parkinson's disease in a chemist working with 1-methyl-4-phenyl-1,2,5,6-tetrahydropyridine. N Engl J Med., **309**(5): p. 310.1983.

19. Marder K, et al., Environmental risk factors for Parkinson's disease in an urban multiethnic community. Neurology., **50**(1): p. 279-81.1998.

20. Gorell J. M, et al., Occupational exposure to manganese, copper, lead, iron, mercury and zinc and the risk of Parkinson's disease. Neurotoxicology, **20**((2-3)): p. 239-47.1999.

21. Mitra, K., P.K. Gangopadhaya, and S.K. Das, Parkinsonism plus syndrome--a review. Neurol India, **51**(2): p. 183-8.2003.

22. Burn, D.J. and A.J. Lees, Progressive supranuclear palsy: where are we now? Lancet Neurol, **1**(6): p. 359-69.2002.

23. Nath, U. and D.J. Burn, The epidemiology of progressive supranuclear palsy (Steele-Richardson-Olszewski syndrome). Parkinsonism Relat Disord, **6**(3): p. 145-153.2000.

24. Burn, D.J., Update on dementia with Lewy bodies. Curr Neurol Neurosci Rep, **5**(5): p. 339-44.2005.

25. McKeith, I.G. and U.P. Mosimann, Dementia with Lewy bodies and Parkinson's disease. Parkinsonism Relat Disord, **10 Suppl 1**: p. S15-8.2004.

26. Schapira, A.H., MPTP and other Parkinson-inducing agents. Curr Opin Neurol Neurosurg, **5**(3): p. 396-400.1992.

27. Calne D. B, Snow B. J, and Lee C, Criteria for diagnosing Parkinson's disease. Ann Neurol., **32**(Suppl): p. S125-7.1992.

28. Hughes A. J, et al., Accuracy of clinical diagnosis of idiopathic Parkinson's disease: a clinico-pathological study of 100 cases. Journal of Neurology Neurosurgery and Psychiatry., **55**(3): p. 181-184.1992.

29. Hughes A. J, et al., What features improve the accuracy of clinical diagnosis in Parkinson's disease: a clinicopathologic study. Neurology., **42**(6): p. 1142-6.1992.

30. Hughes, A.J., S.E. Daniel, and A.J. Lees, The clinical features of Parkinson's disease in 100 histologically proven cases. Adv Neurol, **60**: p. 595-9.1993.

31. Padovani, A., et al., Parkinson's disease and dementia. Neurol Sci, **27 Suppl 1**: p. S40-3.2006.

32. Braak, H., et al., Staging of brain pathology related to sporadic Parkinson's disease. Neurobiol. Aging, **24**(2): p. 197-211.2003.

33. Braak, H., et al., Idiopathic Parkinson's disease: possible routes by which vulnerable neuronal types may be subject to neuroinvasion by an unknown pathogen. J Neural Transm, **110**(5): p. 517-36.2003.

34. Langston, J.W., The Parkinson's complex: parkinsonism is just the tip of the iceberg. Ann Neurol, **59**(4): p. 591-6.2006.

35. de Lau, L.M., et al., Prognosis of Parkinson disease: risk of dementia and mortality: the Rotterdam Study. Arch Neurol, **62**(8): p. 1265-9.2005.

36. Marras, C., et al., Survival in Parkinson disease: thirteen-year follow-up of the DATATOP cohort. Neurology, **64**(1): p. 87-93.2005.

37. Jellinger, K.A., Mortality in Parkinson's disease. Acta Neurol Scand, **111**(1): p. 71; author reply 72.2005.

38. Carr, J., Tremor in Parkinson's disease. Parkinsonism Relat Disord, **8**(4): p. 223-34.2002.

39. Albin, R.L., Neurobiology of basal ganglia and Tourette syndrome: striatal and dopamine function. Adv Neurol, **99**: p. 99-106.2006.

40. Wichmann, T. and M.R. DeLong, Models of basal ganglia function and pathophysiology of movement disorders. Neurosurg Clin N Am, **9**(2): p. 223-36.1998.

41. Evans, A.H. and A.J. Lees, Dopamine dysregulation syndrome in Parkinson's disease. Curr Opin Neurol, **17**(4): p. 393-8.2004.

42. Obeso, J.A., et al., The origin of motor fluctuations in Parkinson's disease: importance of dopaminergic innervation and basal ganglia circuits. Neurology, **62**(1 Suppl 1): p. S17-30.2004.

43. Vingerhoets, F.J., et al., Longitudinal fluorodopa positron emission tomographic studies of the evolution of idiopathic parkinsonism. Ann Neurol, **36**(5): p. 759-64.1994.

44. Benamer, H.T., et al., Correlation of Parkinson's disease severity and duration with 123I-FP-CIT SPECT striatal uptake. Mov Disord, **15**(4): p. 692-8.2000.

45. Morrish, P.K., G.V. Sawle, and D.J. Brooks, An [18F]dopa-PET and clinical study of the rate of progression in Parkinson's disease. Brain, **119 (Pt 2)**: p. 585-91.1996.

46. Piccini P, et al., Dopaminergic function in familial Parkinson's disease: a clinical and 18F-dopa positron emission tomography study. Ann Neurol, **41**(2): p. 222-9.1997.

47. Piccini P, et al., The role of inheritance in sporadic Parkinson's disease: evidence from a longitudinal study of dopaminergic function in twins. Ann Neurol., **45**(5): p. 577-82.1999.

48. Burn, D.J., et al., Parkinson's disease in twins studied with 18F-dopa and positron emission tomography. Neurology, **42**(10): p. 1894-900.1992.

49. Brooks, D.J., et al., Differing patterns of striatal 18F-dopa uptake in Parkinson's disease, multiple system atrophy, and progressive supranuclear palsy. Ann Neurol, **28**(4): p. 547-55.1990.

50. Lewy, F., Zur pathologischen Anatomie der paralysis agitans, in Dtsch Z. 1914: Nervenheilk. p. 50-55.

51. Spillantini, M.G., et al., Alpha-synuclein in Lewy bodies. Nature, **388**(6645): p. 839-40.1997.

52. Muller, C.M., et al., Staging of sporadic Parkinson disease-related alpha-synuclein pathology: inter- and intra-rater reliability. J Neuropathol Exp Neurol, **64**(7): p. 623-8.2005.

53. Hardy, J. and A.J. Lees, Parkinson's disease: a broken nosology. Mov Disord, **20 Suppl 12**: p. S2-4.2005.

54. Hughes, A.J., et al., Accuracy of clinical diagnosis of idiopathic Parkinson's disease: a clinico-pathological study of 100 cases. J Neurol Neurosurg Psychiatry, **55**(3): p. 181-4.1992.

55. Langston, J.W., et al., Chronic Parkinsonism in humans due to a product of meperidine-analog synthesis. Science, **219**(4587): p. 979-80.1983.

56. Langston, J.W. and P.A. Ballard, Jr., Parkinson's disease in a chemist working with 1-methyl-4-phenyl-1,2,5,6-tetrahydropyridine. N Engl J Med, **309**(5): p. 310.1983.

57. Kolata, G., Monkey model of Parkinson's disease. Science, **220**(4598): p. 705.1983.

58. Blume, E., Street drugs yield primate Parkinson's model. Jama, **250**(1): p. 13-4.1983.

59. Langston, J.W., et al., Evidence of active nerve cell degeneration in the substantia nigra of humans years after 1-methyl-4-phenyl-1,2,3,6-tetrahydropyridine exposure. Ann Neurol, **46**(4): p. 598-605.1999.

60. Davis, G.C., et al., Chronic Parkinsonism secondary to intravenous injection of meperidine analogues. Psychiatry Res, **1**(3): p. 249-54.1979.

61. Dauer, W. and S. Przedborski, Parkinson's disease: mechanisms and models. Neuron, **39**(6): p. 889-909.2003.

62. Asanuma, M., et al., Quinone formation as dopaminergic neuron-specific oxidative stress in the pathogenesis of sporadic Parkinson's disease and neurotoxin-induced parkinsonism. Acta Med Okayama, **58**(5): p. 221-33.2004.

63. Langston, J.W., The etiology of Parkinson's disease with emphasis on the MPTP story. Neurology, **47**(6 Suppl 3): p. S153-60.1996.

64. Muqit, M.M., S. Gandhi, and N.W. Wood, Mitochondria in Parkinson disease: back in fashion with a little help from genetics. Arch Neurol, **63**(5): p. 649-54.2006.

65. Lee, H.C. and Y.H. Wei, Mitochondrial role in life and death of the cell. J Biomed Sci, **7**(1): p. 2-15.2000.

66. Gibson, B.W., The human mitochondrial proteome: oxidative stress, protein modifications and oxidative phosphorylation. Int J Biochem Cell Biol, **37**(5): p. 927-34.2005.

67. Chan, D.C., Mitochondria: dynamic organelles in disease, aging, and development. Cell, **125**(7): p. 1241-52.2006.

68. Cooper, J.M., et al., L-dihydroxyphenylalanine and complex I deficiency in Parkinson's disease brain. Mov Disord, **10**(3): p. 295-7.1995.

69. Schapira, A.H., Mitochondrial complex I deficiency in Parkinson's disease. Adv Neurol, **60**: p. 288-91.1993.

70. Przedborski, S. and M. Vila, The 1-methyl-4-phenyl-1,2,3,6-tetrahydropyridine mouse model: a tool to explore the pathogenesis of Parkinson's disease. Ann N Y Acad Sci, **991**: p. 189-98.2003.

71. Betarbet, R., et al., Chronic systemic pesticide exposure reproduces features of Parkinson's disease. Nat Neurosci, **3**(12): p. 1301-6.2000.

72. Swerdlow, R.H., et al., Matrilineal inheritance of complex I dysfunction in a multigenerational Parkinson's disease family. Ann Neurol, **44**(6): p. 873-81.1998.

73. Keeney, P.M., et al., Parkinson's disease brain mitochondrial complex I has oxidatively damaged subunits and is functionally impaired and misassembled. J Neurosci, **26**(19): p. 5256-64.2006.

74. Sherer, T.B., et al., Mechanism of toxicity in rotenone models of Parkinson's disease. J. Neurosci., **23**(34): p. 10756-64.2003.

75. Lapointe, N., et al., Rotenone induces non-specific central nervous system and systemic toxicity. FASEB J., **18**(6): p. 717-9.2004.

76. Betarbet R, et al., Chronic systemic pesticide exposure reproduces features of Parkinson's disease. Nat Neurosci., **3**(12): p. 1301-6.2000.

77. Swerdlow, R.H., et al., Origin and functional consequences of the complex I defect in Parkinson's disease. Ann Neurol, **40**(4): p. 663-71.1996.

78. Rana, M., et al., An out-of-frame cytochrome b gene deletion from a patient with parkinsonism is associated with impaired complex III assembly and an increase in free radical production. Ann Neurol, **48**(5): p. 774-81.2000.

79. Bender, A., et al., High levels of mitochondrial DNA deletions in substantia nigra neurons in aging and Parkinson disease. Nat Genet, **38**(5): p. 515-7.2006.

80. Kraytsberg, Y., et al., Mitochondrial DNA deletions are abundant and cause functional impairment in aged human substantia nigra neurons. Nat Genet, **38**(5): p. 518-20.2006.

81. Emdadul Haque, M., et al., Apoptosis-inducing neurotoxicity of dopamine and its metabolites via reactive quinone generation in neuroblastoma cells. Biochim Biophys Acta, **1619**(1): p. 39-52.2003.

82. McGowan, C.H. and P. Russell, The DNA damage response: sensing and signaling. Curr Opin Cell Biol, **16**(6): p. 629-33.2004.

83. Ziv I, B.A., Offen D, Nardi N, Melamed E, Nigrostriatal neuronal death in Parkinson's disease --- a passive or an active genetically -controlled process? J Neural Transm Suppl, **49**: p. 69-76.1997.

84. Grimm J, m.A., Hefti F, Rosenthal A, Molecular basis for catecholaminergic neuron diversity. Proc Natl Acad Sci U S A, **101**: p. 13891-13896.2004.

85. Greene JG, D.R., Greenamyre JT, Gene expression profiling of rat midbrain dopamine neurons: implications for selective vulnerability in parkinsonism. Neurobiol Dis, **18**: p. 19-31.2005.

86. Chung CY, S.K., Brooks A, Lin L, Isacson, O, Cell type specific gene expression of midbrain dopaminergic neurons reveals molecules involved in their vulnerability and protection. Human Molecular Genetics, **13**(14): p. 1709-25.2005.

87. Abou-Sleiman, P.M., M.M. Muqit, and N.W. Wood, Expanding insights of mitochondrial dysfunction in Parkinson's disease. Nat Rev Neurosci, **7**(3): p. 207-19.2006.

88. Schapira, A.H., Mitochondrial disease. Lancet, **368**(9529): p. 70-82.2006.

89. Gorell JM, P.E., Rybicki BA, Johnson CC, Multiple risk factors for Parkinson's disease. J Neurol Sci, **217**(2): p. 169-174.2004.

90. Jain, S., N.W. Wood, and D.G. Healy, Molecular genetic pathways in Parkinson's disease: a review. Clin Sci (Lond), **109**(4): p. 355-64.2005.

91. Duvoisin, R.C., et al., Twin study of Parkinson disease. Neurology, **31**(1): p. 77-80.1981.

92. Ward, C.D., et al., Parkinson's disease in 65 pairs of twins and in a set of quadruplets. Neurology, **33**(7): p. 815-24.1983.

93. Tanner, C.M., et al., Parkinson disease in twins: an etiologic study. Jama, **281**(4): p. 341-6.1999.

94. Vieregge, P., et al., Parkinson's disease in twins. Neurology, **42**(8): p. 1453-61.1992.

95. Marsden, C.D., Parkinson's disease in twins. J Neurol Neurosurg Psychiatry, **50**(1): p. 105-6.1987.

96. Marttila, R.J., et al., Parkinson's disease in a nationwide twin cohort. Neurology, **38**(8): p. 1217-9.1988.

97. De Michele, G., et al., A genetic study of Parkinson's disease. J Neural Transm Suppl, **45**: p. 21-5.1995.

98. Tanner C. M, et al., Parkinson disease in twins: an etiologic study. JAMA. 1999 ;, **281**(4): p. 341-6.1999.

99. Wirdefeldt K, et al., No evidence for heritability of Parkinson disease in Swedish twins. Neurology, **63**(2): p. 305-11.2004.

100. Holthoff, V.A., et al., Discordant twins with Parkinson's disease: positron emission tomography and early signs of impaired cognitive circuits. Ann Neurol, **36**(2): p. 176-82.1994.

101. Le Couteur, D.G., et al., Age-environment and gene-environment interactions in the pathogenesis of Parkinson's disease. Rev Environ Health, **17**(1): p. 51-64.2002.

102. Polymeropoulos M. H, et al., Mutation in the alpha-synuclein gene identified in families with Parkinson's disease. Science, **276**(5321): p. 2045-7.1997.

103. Kruger R, et al., Ala30Pro mutation in the gene encoding alpha-synuclein in Parkinson's disease. Nat Genet, **18**(2): p. 106-8.1998.

104. Zarranz, J.J., et al., The new mutation, E46K, of alpha-synuclein causes Parkinson and Lewy body dementia. Ann Neurol, **55**(2): p. 164-73.2004.

105. Ibanez P, et al., Causal relation between alpha-synuclein gene duplication and familial Parkinson's disease. Lancet, **364**(9440): p. 1169-71.2004.

106. Singleton A. B, et al., alpha-Synuclein locus triplication causes Parkinson's disease. Science, **302**(5646): p. 841.2003.

107. Chartier-Harlin M. C, et al., Alpha-synuclein locus duplication as a cause of familial Parkinson's disease. Lancet, **364**(9440): p. 1167-9.2004.

108. Spillantini M. G, et al., Alpha-synuclein in Lewy bodies. Nature, **388**(6645): p. 839-40.1997.

109. Kotzbauer, P.T., et al., Fibrillization of alpha-synuclein and tau in familial Parkinson's disease caused by the A53T alpha-synuclein mutation. Exp Neurol, **187**(2): p. 279-88.2004.

110. Farrer, M., et al., Comparison of kindreds with parkinsonism and alpha-synuclein genomic multiplications. Ann Neurol, **55**(2): p. 174-9.2004.

111. Zarranz J. J, et al., The new mutation, E46K, of alpha-synuclein causes Parkinson and Lewy body dementia. Ann Neurol., **55**(2): p. 164-73.2004.

112. Kruger, R., et al., Familial parkinsonism with synuclein pathology: clinical and PET studies of A30P mutation carriers. Neurology, **56**(10): p. 1355-62.2001.

113. Marti, M.J., E. Tolosa, and J. Campdelacreu, Clinical overview of the synucleinopathies. Mov Disord, **18 Suppl 6**: p. S21-7.2003.

114. Jellinger, K.A., Neuropathological spectrum of synucleinopathies. Mov Disord, **18 Suppl 6**: p. S2-12.2003.

115. Spillantini, M.G. and M. Goedert, The alpha-synucleinopathies: Parkinson's disease, dementia with Lewy bodies, and multiple system atrophy. Ann N Y Acad Sci, **920**: p. 16-27.2000.

116. Mukaetova-Ladinska, E.B. and I.G. McKeith, Pathophysiology of synuclein aggregation in Lewy body disease. Mechanisms of Ageing and Development Dementias and Cognitive Disorders: New Insights and Approaches, **127**(2): p. 188-202.2006.

117. Vekrellis, K., H.J. Rideout, and L. Stefanis, Neurobiology of alpha-synuclein. Mol Neurobiol, **30**(1): p. 1-21.2004.

118. Norris, E.H., B.I. Giasson, and V.M. Lee, Alpha-synuclein: normal function and role in neurodegenerative diseases. Curr Top Dev Biol, **60**: p. 17-54.2004.

119. Clayton, D.F. and J.M. George, The synucleins: a family of proteins involved in synaptic function, plasticity, neurodegeneration and disease. Trends Neurosci, **21**(6): p. 249-54.1998.

120. George, J.M., The synucleins. Genome Biol., **3**(1): p. REVIEWS3002.2002.

121. Cookson, M.R., The biochemistry of Parkinson's disease. Annu Rev Biochem, **74**: p. 29-52.2005.

122. Iwai, A., et al., Non-A beta component of Alzheimer's disease amyloid (NAC) is amyloidogenic. Biochemistry, **34**(32): p. 10139-45.1995.

123. Ueda, K., et al., Molecular cloning of cDNA encoding an unrecognized component of amyloid in Alzheimer disease. Proc. Natl. Acad. Sci. USA, **90**(23): p. 11282-6.1993.

124. George, J.M., et al., Characterization of a novel protein regulated during the critical period for song learning in the zebra finch. Neuron, **15**(2): p. 361-72.1995.

125. Welch, K. and J. Yuan, Alpha-synuclein oligomerization: a role for lipids? Trends Neurosci, **26**(10): p. 517-9.2003.

126. Clayton, D.F. and J.M. George, The synucleins: a family of proteins involved in synaptic function, plasticity, neurodegeneration and disease. Trends Neurosci., **21**(6): p. 249-54.1998.

127. Abeliovich, A., et al., Mice lacking alpha-synuclein display functional deficits in the nigrostriatal dopamine system. Neuron, **25**(1): p. 239-52.2000.

128. Cabin, D.E., et al., Synaptic vesicle depletion correlates with attenuated synaptic responses to prolonged repetitive stimulation in mice lacking alpha-synuclein. J. Neurosci., **22**(20): p. 8797-807.2002.

129. Kaplan, B., V. Ratner, and E. Haas, Alpha-synuclein: its biological function and role in neurodegenerative diseases. J Mol Neurosci, **20**(2): p. 83-92.2003.

130. Singleton, A.B., et al., alpha-Synuclein locus triplication causes Parkinson's disease. Science, **302**(5646): p. 841.2003.

131. Giasson, B.I., et al., A hydrophobic stretch of 12 amino acid residues in the middle of alpha-synuclein is essential for filament assembly. J. Biol. Chem., **276**(4): p. 2380-6.2001.

132. Bodles, A.M., et al., Identification of the region of non-Abeta component (NAC) of Alzheimer's disease amyloid responsible for its aggregation and toxicity. J. Neurochem., **78**(2): p. 384-95.2001.

133. Volles, M.J. and P.T. Lansbury, Jr., Zeroing in on the pathogenic form of alpha-synuclein and its mechanism of neurotoxicity in Parkinson's disease. Biochemistry, **42**(26): p. 7871-8.2003.

134. Crowther, R.A., S.E. Daniel, and M. Goedert, Characterisation of isolated alpha-synuclein filaments from substantia nigra of Parkinson's disease brain. Neurosci. Lett., **292**(2): p. 128-30.2000.

135. Gosavi, N., et al., Golgi fragmentation occurs in the cells with prefibrillar alpha-synuclein aggregates and precedes the formation of fibrillar inclusion. J. Biol. Chem., **277**(50): p. 48984-92.2002.

136. Giasson, B.I., et al., Mutant and wild type human alpha-synucleins assemble into elongated filaments with distinct morphologies in vitro. J. Biol. Chem., **274**(12): p. 7619-22.1999.

137. Conway, K.A., et al., Acceleration of oligomerization, not fibrillization, is a shared property of both alpha-synuclein mutations linked to early-onset Parkinson's disease: implications for pathogenesis and therapy. Proc. Natl. Acad. Sci. USA, **97**(2): p. 571-6.2000.

138. Biere, A.L., et al., Parkinson's disease-associated alpha-synuclein is more fibrillogenic than beta- and gamma-synuclein and cannot cross-seed its homologs. J Biol Chem, **275**(44): p. 34574-9.2000.

139. Cole, N.B., et al., Lipid droplet binding and oligomerization properties of the Parkinson's disease protein alpha-synuclein. J. Biol. Chem., **277**(8): p. 6344-52.2002.

140. Conway, K.A., J.D. Harper, and P.T. Lansbury, Accelerated in vitro fibril formation by a mutant alpha-synuclein linked to early-onset Parkinson disease. Nat Med, **4**(11): p. 1318-20.1998.

141. Volles, M.J. and P.T. Lansbury, Jr., Vesicle permeabilization by protofibrillar alpha-synuclein is sensitive to Parkinson's disease-linked mutations and occurs by a pore-like mechanism. Biochemistry, **41**(14): p. 4595-602.2002.

142. Arrasate, M., et al., Inclusion body formation reduces levels of mutant huntingtin and the risk of neuronal death. Nature, **431**(7010): p. 805-10.2004.

143. Santacruz, K., et al., Tau suppression in a neurodegenerative mouse model improves memory function. Science, **309**(5733): p. 476-81.2005.

144. Goldberg, M.S., Lansbury, P.T, Is there a cause and effect relationship between alpha-synuclein fibrillization and Parkinson's Disease. Nat Cell Biol, **2**(7): p. E115-9.2000.

145. Giasson, B.I., et al., Neuronal alpha-synucleinopathy with severe movement disorder in mice expressing A53T human alpha-synuclein. Neuron, **34**(4): p. 521-33.2002.

146. Lee, M.K., et al., Human alpha-synuclein-harboring familial Parkinson's disease-linked Ala-53 --> Thr mutation causes neurodegenerative disease with alpha-synuclein aggregation in transgenic mice. Proc. Natl. Acad. Sci. USA, **99**(13): p. 8968-73.2002.

147. Auluck, P.K., Chan, H.Y., Trojanowski, J.Q., Lee, V.M., Bonini, N.M., Chaperone suppression of alpha-synuclein in a Drosophila model for Parkinson's disease. Science, **295**(5556): p. 865-8.2002.

148. Feany, M.B. and W.W. Bender, A Drosophila model of Parkinson's disease. Nature, **404**(6776): p. 394-8.2000.

149. Fujiwara, H., et al., alpha-Synuclein is phosphorylated in synucleinopathy lesions. Nat. Cell Biol., **4**(2): p. 160-4.2002.

150. Chen, L. and M.B. Feany, Alpha-synuclein phosphorylation controls neurotoxicity and inclusion formation in a Drosophila model of Parkinson disease. Nat Neurosci, **8**(5): p. 657-63.2005.

151. Oluwatosin-Chigbu, Y., et al., Parkin suppresses wild-type alpha-synuclein-induced toxicity in SHSY-5Y cells. Biochem. Biophys. Res. Commun., **309**(3): p. 679-84.2003.

152. Petrucelli, L., et al., Parkin protects against the toxicity associated with mutant alpha-synuclein: proteasome dysfunction selectively affects catecholaminergic neurons. Neuron, **36**(6): p. 1007-19.2002.

153. Xu J, et al., Dopamine-dependent neurotoxicity of alpha-synuclein: a mechanism for selective neurodegeneration in Parkinson disease. Nat Med, **8**(6): p. 600-6.2002.

154. Hsu, L.J., et al., alpha-synuclein promotes mitochondrial deficit and oxidative stress. Am. J. Pathol., **157**(2): p. 401-10.2000.

155. Cooper, A.A., et al., Alpha-synuclein blocks ER-Golgi traffic and Rab1 rescues neuron loss in Parkinson's models. Science, **313**(5785): p. 324-8.2006.

156. Smith, W.W., et al., Endoplasmic reticulum stress and mitochondrial cell death pathways mediate A53T mutant alpha-synuclein-induced toxicity. Hum Mol Genet, **14**(24): p. 3801-11.2005.

157. Chandra, S., et al., Alpha-synuclein cooperates with CSPalpha in preventing neurodegeneration. Cell, **123**(3): p. 383-96.2005.

158. Chen, L., et al., Proteasome dysfunction in aged human alpha-synuclein transgenic mice. Neurobiol Dis, **23**(1): p. 120-6.2006.

159. Ghee, M., A. Fournier, and J. Mallet, Rat alpha-synuclein interacts with Tat binding protein 1, a component of the 26S proteasomal complex. J Neurochem, **75**(5): p. 2221-4.2000.

160. Nandi, D., et al., The ubiquitin-proteasome system. J Biosci, **31**(1): p. 137-55.2006.

161. McNaught, K.S.P., et al., Systemic exposure to proteasome inhibitors causes a progressive model of Parkinson's disease. Ann. Neurol., **56**: p. 149-162.2004.

162. McNaught, K.S. and C.W. Olanow, Proteolytic stress: a unifying concept for the etiopathogenesis of Parkinson's disease. Ann Neurol, **53 Suppl 3**: p. S73-84; discussion S84-6.2003.

163. Betarbet, R., T.B. Sherer, and J.T. Greenamyre, Ubiquitin-proteasome system and Parkinson's diseases. Exp Neurol, **191 Suppl 1**: p. S17-27.2005.

164. Tanaka, Y., et al., Inducible expression of mutant alpha-synuclein decreases proteasome activity and increases sensitivity to mitochondria-dependent apoptosis. Hum. Mol. Genet., **10**(9): p. 919-26.2001.

165. McNaught, K.S., et al., Proteasomal dysfunction in sporadic Parkinson's disease. Neurology, **66**(10 Suppl 4): p. S37-49.2006.

166. Snyder, H., et al., Aggregated and monomeric alpha-synuclein bind to the S6' proteasomal protein and inhibit proteasomal function. J. Biol. Chem., **278**(14): p. 11753-9.2003.

167. Tatton, N.A., Tatton, W.G., Perl, D.P., Olanow, C.W., A fluorescent double labelling method to detect and confirm apoptotic nuclei in Parkinson's disease. Ann Neurol, **r44**: p. S142-148.2000.

168. Hashimoto, M., et al., Oxidative stress induces amyloid-like aggregate formation of NACP/alpha-synuclein in vitro. Neuroreport, **10**(4): p. 717-21.1999.

169. Giasson, B.I., et al., Oxidative damage linked to neurodegeneration by selective alpha-synuclein nitration in synucleinopathy lesions. Science, **290**(5493): p. 985-9.2000.

170. Uehara, T., et al., S-nitrosylated protein-disulphide isomerase links protein misfolding to neurodegeneration. Nature, **441**(7092): p. 513-7.2006.

171. Hoglinger, G.U., et al., Dysfunction of mitochondrial complex I and the proteasome: interactions between two biochemical deficits in a cellular model of Parkinson's disease. J. Neurochem., **86**(5): p. 1297-307.2003.

172. Sullivan, P.G., et al., Proteasome inhibition alters neural mitochondrial homeostasis and mitochondria turnover. J. Biol. Chem., **279**(20): p. 20699-707.2004.

173. Kitada T, et al., Mutations in the parkin gene cause autosomal recessive juvenile parkinsonism. Nature, **392**(6676): p. 605-8.1998.

174. Abbas N, et al., A wide variety of mutations in the parkin gene are responsible for autosomal recessive parkinsonism in Europe. French Parkinson's Disease Genetics Study Group and the European Consortium on Genetic Susceptibility in Parkinson's Disease. Hum Mol Genet, **8**(4): p. 567-74.1999.

175. Bertoli-Avella, A.M., et al., Novel parkin mutations detected in patients with early-onset Parkinson's disease. Mov Disord, **20**(4): p. 424-31.2005.

176. Klein, C., et al., Parkin deletions in a family with adult-onset, tremor-dominant parkinsonism: expanding the phenotype. Ann. Neurol., **48**(1): p. 65-71.2000.

177. Healy, D.G., P.M. Abou-Sleiman, and N.W. Wood, PINK, PANK, or PARK? A clinicians' guide to familial parkinsonism. Lancet Neurol, **3**(11): p. 652-62.2004.

178. West, A.B. and N.T. Maidment, Genetics of parkin-linked disease. Hum. Genet., **114**(4): p. 327-36.2004.

179. Khan, N.L., Graham, E., Critchley, P., Schraq, A.E., Wood, N.W., Lees, A.J., Bhatia, K.P., Quinn, N.,, Parkin disease: a phenotypic study of a large case series. Brain, (126): p. 1279-92.2003.

180. Lücking C. B, et al., Association between early-onset Parkinson's disease and mutations in the parkin gene. French Parkinson's Disease Genetics Study Group. New Engl J Med, **342**(21): p. 1560–7.2000.

181. Bonifat, V., De Michele, G., Italian PD Genetics Study Group, French PD Genetics Study Group, European Consortium on Genetic Susceptibility in PD, The parkin gene and its phenotype. Neurol Sci, **22**(1): p. 51-2.2001.

182. Lohmann, E., et al., How much phenotypic variation can be attributed to parkin genotype? Ann Neurol, **54**(2): p. 176-85.2003.

183. Yamamura, Y., et al., Autosomal recessive early-onset parkinsonism with diurnal fluctuation: clinicopathologic characteristics and molecular genetic identification. Brain Dev, **22 Suppl 1**: p. S87-91.2000.

184. Pramstaller, P.P., et al., Lewy body Parkinson's disease in a large pedigree with 77 Parkin mutation carriers. Ann Neurol, **58**(3): p. 411-22.2005.

185. Farrer, M., et al., Lewy bodies and parkinsonism in families with parkin mutations. Ann Neurol, **50**(3): p. 293-300.2001.

186. Dawson, T.M., Parkin and defective ubiquitination in Parkinson's disease. J Neural Transm Suppl, (70): p. 209-13.2006.

187. Suzuki, H., Protein-protein interactions in the mammalian brain. J Physiol, **575**(Pt 2): p. 373-7.2006.

188. Zhang, Y., et al., Parkin functions as an E2-dependent ubiquitin- protein ligase and promotes the degradation of the synaptic vesicle-associated protein, CDCrel-1. Proc. Natl. Acad. Sci. USA, **97**(24): p. 13354-9.2000.

189. Shimura, H., et al., Familial Parkinson disease gene product, parkin, is a ubiquitin-protein ligase. Nat. Genet., **25**(3): p. 302-5.2000.

190. Buneeva, O.A. and A.E. Medvedev, Ubiquitin-protein ligase parkin and its role in the development of Parkinson's disease. Biochemistry (Mosc), **71**(8): p. 851-60.2006.

191. Darios, F., et al., Parkin prevents mitochondrial swelling and cytochrome c release in mitochondria-dependent cell death. Hum. Mol. Genet., **12**(5): p. 517-26.2003.

192. Imai Y, et al., An unfolded putative transmembrane polypeptide, which can lead to endoplasmic reticulum stress, is a substrate of Parkin. Cell, **105**(7): p. 891-902.2001.

193. Dong, Z., et al., Dopamine-dependent neurodegeneration in rats induced by viral vector-mediated overexpression of the parkin target protein, CDCrel-1. Proc. Natl. Acad. Sci. USA, **100**(21): p. 12438-43.2003.

194. Yang, Y., et al., Parkin suppresses dopaminergic neuron-selective neurotoxicity induced by Pael-R in Drosophila. Neuron, **37**(6): p. 911-24.2003.

195. Goldberg, M.S., et al., Parkin-deficient mice exhibit nigrostriatal deficits but not loss of dopaminergic neurons. J. Biol. Chem., **278**(44): p. 43628-35.2003.

196. Itier, J.M., et al., Parkin gene inactivation alters behaviour and dopamine neurotransmission in the mouse. Hum. Mol. Genet., **12**(18): p. 2277-91.2003.

197. Kahle, P.J. and C. Haass, How does parkin ligate ubiquitin to Parkinson's disease? EMBO Rep, **5**(7): p. 681-5.2004.

198. Palacino, J.J., et al., Mitochondrial dysfunction and oxidative damage in parkin-deficient mice. J. Biol. Chem., **279**(18): p. 18614-22.2004.

199. Von Coelln, R., V.L. Dawson, and T.M. Dawson, Parkin-associated Parkinson's disease. Cell Tissue Res.2004.

200. Von Coelln, R., et al., Loss of locus coeruleus neurons and reduced startle in parkin null mice. Proc. Natl. Acad. Sci. USA, **101**(29): p. 10744-9.2004.

201. Greene, J.C., et al., Mitochondrial pathology and apoptotic muscle degeneration in Drosophila parkin mutants. Proc. Natl. Acad. Sci. USA, **100**(7): p. 4078-83.2003.

202. Kalia, S.K., et al., BAG5 inhibits parkin and enhances dopaminergic neuron degeneration. Neuron, **44**(6): p. 931-45.2004.

203. Bonifati V, et al., Mutations in the DJ-1 gene associated with autosomal recessive early-onset parkinsonism. Science, **299**(5604): p. 256-9.2003.

204. Clark L. N, et al., Analysis of an early-onset Parkinson's disease cohort for DJ-1 mutations. Mov Disord, **19**(7): p. 796-800.2004.

205. Pankratz, N., et al., Mutations in DJ-1 are rare in familial Parkinson disease. Neurosci Lett.2006.

206. Abou-Sleiman, P.M., D.G. Healy, and N.W. Wood, Causes of Parkinson's disease: genetics of DJ-1. Cell Tissue Res, **318**(1): p. 185-8.2004.

207. Bandopadhyay, R., et al., The expression of DJ-1 (PARK7) in normal human CNS and idiopathic Parkinson's disease. Brain, **127**(Pt 2): p. 420-30.2004.

208. Neumann, M., et al., Pathological properties of the Parkinson's disease-associated protein DJ-1 in alpha-synucleinopathies and tauopathies: relevance for multiple system atrophy and Pick's disease. Acta Neuropathol., **107**(6): p. 489-96.2004.

209. Xu, J., et al., The Parkinson's disease-associated DJ-1 protein is a transcriptional co-activator that protects against neuronal apoptosis. Hum Mol Genet, **14**(9): p. 1231-41.2005.

210. Niki, T., et al., DJBP: a novel DJ-1-binding protein, negatively regulates the androgen receptor by recruiting histone deacetylase complex, and DJ-1

antagonizes this inhibition by abrogation of this complex. Mol. Cancer Res., **1**(4): p. 247-61.2003.

211. Meulener, M.C., et al., DJ-1 is present in a large molecular complex in human brain tissue and interacts with alpha-synuclein. J Neurochem, **93**(6): p. 1524-32.2005.

212. Moore, D.J., et al., A missense mutation (L166P) in DJ-1, linked to familial Parkinson's disease, confers reduced protein stability and impairs homo-oligomerization. J. Neurochem., **87**(6): p. 1558-67.2003.

213. Macedo, M.G., et al., The DJ-1L166P mutant protein associated with early onset Parkinson's disease is unstable and forms higher-order protein complexes. Hum. Mol. Genet., **12**(21): p. 2807-16.2003.

214. Gorner, K., et al., Differential effects of Parkinson's disease-associated mutations on stability and folding of DJ-1. J. Biol. Chem., **279**(8): p. 6943-51.2004.

215. Canet-Aviles, R.M., et al., The Parkinson's disease protein DJ-1 is neuroprotective due to cysteine-sulfinic acid-driven mitochondrial localization. Proc. Natl. Acad. Sci. USA, **101**(24): p. 9103-8.2004.

216. Miller, D.W., et al., L166P mutant DJ-1, causative for recessive Parkinson's disease, is degraded through the ubiquitin-proteasome system. J. Biol. Chem., **278**(38): p. 36588-95.2003.

217. Olzmann, J.A., et al., Familial Parkinson's disease-associated L166P mutation disrupts DJ-1 protein folding and function. J. Biol. Chem., **279**(9): p. 8506-15.2004.

218. Yang, Y., et al., Mitochondrial pathology and muscle and dopaminergic neuron degeneration caused by inactivation of Drosophila Pink1 is rescued by Parkin. Proc Natl Acad Sci U S A, **103**(28): p. 10793-8.2006.

219. Meulener, M.C., et al., Mutational analysis of DJ-1 in Drosophila implicates functional inactivation by oxidative damage and aging. Proc Natl Acad Sci U S A, **103**(33): p. 12517-22.2006.

220. Taira, T., et al., DJ-1 has a role in antioxidative stress to prevent cell death. EMBO Rep., **5**(2): p. 213-8.2004.

221. Abou-Sleiman P. M, et al., The role of pathogenic DJ-1 mutations in Parkinson's disease. Ann Neurol, **54**(3): p. 283-6.2003.

222. Bandyopadhyay, S. and M.R. Cookson, Evolutionary and functional relationships within the DJ1 superfamily. BMC Evol. Biol., **4**(1): p. 6.2004.

223. Bonifati, V., et al., Mutations in the DJ-1 gene associated with autosomal recessive early-onset parkinsonism. Science, **299**(5604): p. 256-9.2003.

224. Kinumi, T., et al., Cysteine-106 of DJ-1 is the most sensitive cysteine residue to hydrogen peroxide-mediated oxidation in vivo in human umbilical vein endothelial cells. Biochem. Biophys. Res. Commun., **317**(3): p. 722-8.2004.

225. Shen, J. and M.R. Cookson, Mitochondria and dopamine: new insights into recessive parkinsonism. Neuron, **43**(3): p. 301-4.2004.

226. Takahashi-Niki, K., et al., Reduced anti-oxidative stress activities of DJ-1 mutants found in Parkinson's disease patients. Biochem. Biophys. Res. Commun., **320**(2): p. 389-97.2004.

227. Mitsumoto, A., et al., Oxidized forms of peroxiredoxins and DJ-1 on two-dimensional gels increased in response to sublethal levels of paraquat. Free Radic. Res., **35**(3): p. 301-10.2001.

228. Choi, J., et al., Oxidative damage of DJ-1 is linked to sporadic Parkinson and Alzheimer diseases. J Biol Chem, **281**(16): p. 10816-24.2006.

229. Hod, Y., et al., Identification and characterization of a novel protein that regulates RNA-protein interaction. J. Cell. Biochem., **72**(3): p. 435-44.1999.

230. Zhong, N., et al., DJ-1 transcriptionally up-regulates the human tyrosine hydroxylase by inhibiting the sumoylation of pyrimidine tract-binding protein-associated splicing factor. J Biol Chem, **281**(30): p. 20940-8.2006.

231. Junn, E., et al., Interaction of DJ-1 with Daxx inhibits apoptosis signal-regulating kinase 1 activity and cell death. Proc Natl Acad Sci U S A, **102**(27): p. 9691-6.2005.

232. Valente E. M, et al., Hereditary early-onset Parkinson's disease caused by mutations in PINK1. Science, **304**(5674): p. 1158-60.2004.

233. Valente E. M, et al., PINK1 mutations are associated with sporadic early-onset parkinsonism. Ann Neurol, **56**(3): p. 336-41.2004.

234. Hatano Y, et al., Novel PINK1 mutations in early-onset parkinsonism. Ann Neurol, **56**(3): p. 424-7.2004.

235. Rogaeva, E., et al., Analysis of the PINK1 gene in a large cohort of cases with Parkinson disease. Arch Neurol, **61**(12): p. 1898-904.2004.

236. Li, Y., et al., Clinicogenetic study of PINK1 mutations in autosomal recessive early-onset parkinsonism. Neurology, **64**(11): p. 1955-7.2005.

237. Bonifati, V., et al., Early-onset parkinsonism associated with PINK1 mutations: frequency, genotypes, and phenotypes. Neurology, **65**(1): p. 87-95.2005.

238. Ibanez, P., et al., Mutational analysis of the PINK1 gene in early-onset parkinsonism in Europe and North Africa. Brain, **129**(Pt 3): p. 686-94.2006.

239. Klein, C., A. Grunewald, and K. Hedrich, Early-onset parkinsonism associated with PINK1 mutations: frequency, genotypes, and phenotypes. Neurology, **66**(7): p. 1129-30; author reply 1129-30.2006.

240. Hedrich, K., et al., Clinical spectrum of homozygous and heterozygous PINK1 mutations in a large German family with Parkinson disease: role of a single hit? Arch Neurol, **63**(6): p. 833-8.2006.

241. Zadikoff, C., et al., Homozygous and heterozygous PINK1 mutations: considerations for diagnosis and care of Parkinson's disease patients. Mov Disord, **21**(6): p. 875-9.2006.

242. Tan, E.K., et al., PINK1 mutations in sporadic early-onset Parkinson's disease. Mov Disord, **21**(6): p. 789-93.2006.

243. Gandhi, S., et al., PINK1 protein in normal human brain and Parkinson's disease. Brain, **129**(Pt 7): p. 1720-31.2006.

244. Beilina, A., et al., Mutations in PTEN-induced putative kinase 1 associated with recessive parkinsonism have differential effects on protein stability. Proc Natl Acad Sci U S A, **102**(16): p. 5703-8.2005.

245. Sim, C.H., et al., C-terminal truncation and Parkinson's disease-associated mutations down-regulate the protein serine/threonine kinase activity of PTEN-induced kinase-1. Hum Mol Genet.2006.

246. Clark, I.E., et al., Drosophila pink1 is required for mitochondrial function and interacts genetically with parkin. Nature, **441**(7097): p. 1162-6.2006.

247. Park, J., et al., Mitochondrial dysfunction in Drosophila PINK1 mutants is complemented by parkin. Nature, **441**(7097): p. 1157-61.2006.

248. Pallanck, L. and J.T. Greenamyre, Neurodegenerative disease: pink, parkin and the brain. Nature, **441**(7097): p. 1058.2006.

249. Reich, T., et al., Genetic studies fo alcoholism and substance dependence. American Journal of Human Genetics, **65**: p. 599-605.1999.

250. St George-Hyslop, P., Molecular Genetics of Alzheimer's Disease. Biological Psychiatry, **47**: p. 183-199.2000.

251. Zimran, A., et al., Prediction of severity of Gaucher's disease by identification of mutations at DNA level. Lancet, **2**(8659): p. 349-52.1989.

252. Bembi, B., et al., Gaucher's disease with Parkinson's disease: clinical and pathological aspects. Neurology, **61**(1): p. 99-101.2003.

253. Spitz, M., et al., Parkinsonism in type 1 Gaucher's disease. J Neurol Neurosurg Psychiatry, **77**(5): p. 709-10.2006.

254. Goker-Alpan, O., et al., Glucocerebrosidase mutations are an important risk factor for Lewy body disorders. Neurology.2006.

255. Cuervo, A.M., et al., Impaired degradation of mutant alpha-synuclein by chaperone-mediated autophagy. Science, **305**(5688): p. 1292-5.2004.

256. Zimran, A., O. Neudorfer, and D. Elstein, The glucocerebrosidase gene and Parkinson's disease in Ashkenazi Jews. N Engl J Med, **352**(7): p. 728-31; author reply 728-31.2005.

257. Schlossmacher, M.G., V. Cullen, and J. Muthing, The glucocerebrosidase gene and Parkinson's disease in Ashkenazi Jews. N Engl J Med, **352**(7): p. 728-31; author reply 728-31.2005.

258. Aharon-Peretz, J., H. Rosenbaum, and R. Gershoni-Baruch, Mutations in the glucocerebrosidase gene and Parkinson's disease in Ashkenazi Jews. N Engl J Med, **351**(19): p. 1972-7.2004.

259. Eblan, M.J., J.M. Walker, and E. Sidransky, The glucocerebrosidase gene and Parkinson's disease in Ashkenazi Jews. N Engl J Med, **352**(7): p. 728-31; author reply 728-31.2005.

260. Sato, C., et al., Analysis of the glucocerebrosidase gene in Parkinson's disease. Mov Disord, **20**(3): p. 367-70.2005.

261. Clark, L.N., et al., Pilot association study of the beta-glucocerebrosidase N370S allele and Parkinson's disease in subjects of Jewish ethnicity. Mov Disord, **20**(1): p. 100-3.2005.

262. Zondervan, K.T. and L.R. Cardon, The complex interplay among factors that influence allelic association. Nat Rev Genet, **5**(2): p. 89-100.2004.

263. Leroy, E., et al., The ubiquitin pathway in Parkinson's disease. Nature, **395**(6701): p. 451-2.1998.

264. Healy, D.G., P.M. Abou-Sleiman, and N.W. Wood, Genetic causes of Parkinson's disease: UCHL-1. Cell Tissue Res.2004.

265. Barrachina, M., et al., Reduced ubiquitin C-terminal hydrolase-1 expression levels in dementia with Lewy bodies. Neurobiol Dis, **22**(2): p. 265-73.2006.

266. Osaka, H., et al., Ubiquitin carboxy-terminal hydrolase L1 binds to and stabilizes monoubiquitin in neuron. Hum Mol Genet, **12**(16): p. 1945-58.2003.

267. Lincoln, S., et al., Low frequency of pathogenic mutations in the ubiquitin carboxy-terminal hydrolase gene in familial Parkinson's disease. Neuroreport, **10**(2): p. 427-9.1999.

268. Shi, Q. and E. Tao, An Ile93Met substitution in the UCH-L1 gene is not a disease-causing mutation for idiopathic Parkinson's disease. Chin Med J (Engl), **116**(2): p. 312-3.2003.

269. Wintermeyer, P., et al., Mutation analysis and association studies of the UCHL1 gene in German Parkinson's disease patients. Neuroreport, **11**(10): p. 2079-82.2000.

270. Zhang, J., et al., Failure to find mutations in ubiquitin carboxy-terminal hydrolase L1 gene in familial Parkinson's disease. Parkinsonism Relat Disord, **6**(4): p. 199-200.2000.

271. Harhangi, B.S., et al., The Ile93Met mutation in the ubiquitin carboxy-terminal-hydrolase-L1 gene is not observed in European cases with familial Parkinson's disease. Neurosci Lett, **270**(1): p. 1-4.1999.

272. Maraganore, D.M., et al., UCHL1 is a Parkinson's disease susceptibility gene. Ann Neurol, **55**(4): p. 512-21.2004.

273. Liu, Y., et al., The UCH-L1 gene encodes two opposing enzymatic activities that affect alpha-synuclein degradation and Parkinson's disease susceptibility. Cell, **111**(2): p. 209-18.2002.

274. Maraganore, D.M., et al., Case-control study of the ubiquitin carboxy-terminal hydrolase L1 gene in Parkinson's disease. Neurology, **53**(8): p. 1858-60.1999.

275. Mellick, G.D. and P.A. Silburn, The ubiquitin carboxy-terminal hydrolase-L1 gene S18Y polymorphism does not confer protection against idiopathic Parkinson's disease. Neurosci Lett, **293**(2): p. 127-30.2000.

276. Savettieri, G., et al., Lack of association between ubiquitin carboxy-terminal hydrolase L1 gene polymorphism and PD. Neurology, **57**(3): p. 560-1.2001.

277. Levecque, C., et al., No genetic association of the ubiquitin carboxy-terminal hydrolase-L1 gene S18Y polymorphism with familial Parkinson's disease. J Neural Transm, **108**(8-9): p. 979-84.2001.

278. Wang, J., et al., ACT and UCH-L1 polymorphisms in Parkinson's disease and age of onset. Mov Disord, **17**(4): p. 767-71.2002.

279. Xue, S. and J. Jia, Genetic association between Ubiquitin Carboxy-terminal Hydrolase-L1 gene S18Y polymorphism and sporadic Alzheimer's disease in a Chinese Han population. Brain Res, **1087**(1): p. 28-32.2006.

280. Nishikawa, K., et al., Alterations of structure and hydrolase activity of parkinsonism-associated human ubiquitin carboxyl-terminal hydrolase L1 variants. Biochem Biophys Res Commun, **304**(1): p. 176-83.2003.

281. Strauss, K.M., et al., Loss of function mutations in the gene encoding Omi/HtrA2 in Parkinson's disease. Hum Mol Genet, **14**(15): p. 2099-111.2005.

282. Hegde, R., et al., Identification of Omi/HtrA2 as a mitochondrial apoptotic serine protease that disrupts inhibitor of apoptosis protein-caspase interaction. J Biol Chem, **277**(1): p. 432-8.2002.

283. Suzuki, Y., et al., Mitochondrial protease Omi/HtrA2 enhances caspase activation through multiple pathways. Cell Death Differ, **11**(2): p. 208-16.2004.

284. Martins, L.M., et al., Neuroprotective role of the Reaper-related serine protease HtrA2/Omi revealed by targeted deletion in mice. Mol Cell Biol, **24**(22): p. 9848-62.2004.

285. Jones, J.M., et al., Loss of Omi mitochondrial protease activity causes the neuromuscular disorder of mnd2 mutant mice. Nature, **425**(6959): p. 721-7.2003.

286. Le, W.D., et al., Mutations in NR4A2 associated with familial Parkinson disease. Nat Genet, **33**(1): p. 85-9.2003.

287. Marx, F.P., et al., Identification and functional characterization of a novel R621C mutation in the synphilin-1 gene in Parkinson's disease. Hum Mol Genet, **12**(11): p. 1223-31.2003.

288. Wallen, A. and T. Perlmann, Transcriptional control of dopamine neuron development. Ann N Y Acad Sci, **991**: p. 48-60.2003.

289. Engelender, S., et al., Synphilin-1 associates with alpha-synuclein and promotes the formation of cytosolic inclusions. Nat Genet, **22**(1): p. 110-4.1999.

290. Chung K. K, et al., Parkin ubiquitinates the alpha-synuclein-interacting protein, synphilin-1: implications for Lewy-body formation in Parkinson disease. Nat Med. 2001 ;:. **7**(10): p. 1144-50.2001.

291. Najim, a.-D.A.S., Wriekat, A., Mubaidin, A., Dasouki, M., Hiari, M.,, Pallido-pyramidal degeneration, supranuclear upgaze paresis and dementia: Kufor-Rakeb syndrome. Acta Neurol Scand, **89**(5): p. 347-52.1994.

292. Hampshire D. J, et al., Kufor-Rakeb syndrome, pallido-pyramidal degeneration with supranuclear upgaze paresis and dementia, maps to 1p36. J Med Genet., **38(10):**(10): p. 680-2.2001.

293. Williams, D.R., Hadeed, A., al-Din, A.S., Wreikat, A.L., Lees, A.J.,, Kufor Rakeb disease:autosomal recessive, levodopa-responsive parkinsonism with pyramidal degeneration, supranuclear gaze palsy, and dementia. Mov Disord, **20**(10): p. 1264-71.2005.

294. Ramirez, A., Heimbach, A., Grundermann, J., Stiller, B., Hampshire, D., Cid, L.P., Woods, C.G., Behrens, M.L., Kubisch, C.,, Hereditary parkinsonism with dementia is caused by mutations in ATP13A2, encoding a lysosomal type 5 P-type ATPase. Nat Genet, **38**(10): p. 1184-91.2006.

295. Holmans, P., Affected Sib-pair methods for detecting linkage to dichotomous traits:review of methodology. Hum Biol, **70**(6): p. 1025-40.1998.

296. Freimer, N., Sabatti, C.,, The use of pedigree, sib-pair and association studies of common diseases for genetic mapping and epidemiology. Nat Genet, **36**(10): p. 1045-51.2004.

297. Li, Y.J., et al., Age at onset in two common neurodegenerative diseases is genetically controlled. Am J Hum Genet, **70**(4): p. 985-93.2002.

298. Klein, C., et al., Search for the PARK3 founder haplotype in a large cohort of patients with Parkinson's disease from northern Germany. Ann Hum Genet, **63 (Pt 4)**: p. 285-91.1999.

299. West A. B, et al., Refinement of the PARK3 locus on chromosome 2p13 and the analysis of 14 candidate genes. Europ. J. Hum. Genet., **9**: p. 659-666.2001.

300. Pankratz, N., et al., Genome screen to identify susceptibility genes for Parkinson disease in a sample without parkin mutations. Am J Hum Genet, **71**(1): p. 124-35.2002.

301. Scott, W.K., et al., Complete genomic screen in Parkinson disease: evidence for multiple genes. Jama, **286**(18): p. 2239-44.2001.

302. Martinez, M., et al., Genome-wide scan linkage analysis for Parkinson's disease: the European genetic study of Parkinson's disease. J Med Genet, **41**(12): p. 900-7.2004.

303. Foroud, T., N. Pankratz, and M. Martinez, Chromosome 5 and Parkinson disease. Eur J Hum Genet.2006.

304. Pankratz N, et al., Significant linkage of Parkinson disease to chromosome 2q36-37. Am. J. Hum Genet 2003, 72: 1053-57), **72**(4): p. 1053-57.2003.

305. Prestel J, S.M., Leitner P, Zimprich A, Vaughan JR, Durr A, Bonifati V, De Michele G, Hanagasi HA, Farrer M, Hofer A, Asmus F, Volpe G, Meco G, Brice A, Wood NW, Muller-Myhsok B, Gasser T; European Consortium on Genetic Susceptibility in Parkinson's Disease (GSPD). PARK11 is not linked with Parkinson's disease in European families.2005.

306. Maraganore, D.M., et al., High-resolution whole-genome association study of Parkinson disease. Am J Hum Genet, **77**(5): p. 685-93.2005.

307. Hicks, A.A., et al., A susceptibility gene for late-onset idiopathic Parkinson's disease. Ann Neurol, **52**(5): p. 549-55.2002.

308. Payami H, et al., Familial aggregation of Parkinson disease: a comparative study of early-onset and late-onset disease. Arch Neurol., **59**(5): p. 848-50.2002.

309. Oliveira, S.A., et al., Identification of risk and age-at-onset genes on chromosome 1p in Parkinson disease. Am J Hum Genet, **77**(2): p. 252-64.2005.

310. Farrer, M.J., et al., Genomewide association, Parkinson disease, and PARK10. Am J Hum Genet, **78**(6): p. 1084-8; author reply 1092-4.2006.

311. Funayama, M., et al., A new locus for Parkinson's disease (PARK8) maps to chromosome 12p11.2-q13.1. Ann Neurol, **51**(3): p. 296-301.2002.

312. Zimprich A, et al., The PARK8 locus in autosomal dominant parkinsonism: confirmation of linkage and further delineation of the disease-containing interval. Am J Hum Genet, **74**(1): p. 11-9.2004.

313. Khan NL, et al., Mutations in the gene LRRK2 encoding dardarin (PARK8) cause familial

Parkinson's disease: clinical, pathological, olfactory and functional imaging

and genetic data. Brain., **128**(12): p. 2786-96.2005.

314. Zimprich A, et al., Erratum: The PARK8 locus in autosomal dominant parkinsonism: confirmation of linkage and further delineation of the disease-containing interval. Am J Hum Genet, **75**: p. 534.2004.

315. Hasegawa, K., Kowa, H.,, Autosomal dominant familial Parkinson's disease:older age of onset and good response to levodopa therapy. Europ. Neurol, **38**(Suppl 1): p. 39-43.1997.

316. Wszolek, Z.K., Pfeiffer, B., Fulgham, J., Parisi, J., Thompson, B., Uitti, R., Calne, D., Pfeiffer,R.,, Western Nebraska family (Family D) with autosomal dominant parkinsonism. Neurology, **45**: p. 502-505.1995.

317. Wszolek Z. K, et al., Autosomal dominant parkinsonism associated with variable synuclein and tau pathology. Neurology, **62**(9): p. 1619-22.2004.

318. Gibb W.R and Lees A.J, The relevance of the Lewy body to the pathogenesis of idiopathic Parkinson's disease. J Neurol Neurosurg Psychiatry., **51**(6): p. 745-52.1988.

319. Nicholl, D.J., et al., Two large British kindreds with familial Parkinson's disease: a clinico-pathological and genetic study. Brain, **125**(Pt 1): p. 44-57.2002.

320. Cottingham Jr. R. W, Idury R. M, and Schaffer A. A, Faster Sequential Genetic Linkage Computations. American Journal of Human Genetics, **53**: p. 252-263.1993.

321. Lathrop G. M and Lalouel J. M, Easy Calculations of LOD Scores and Genetic Risks on Small Computers. American Journal of Human Genetics, **36**: p. 460-465.1984.

322. Lathrop G. M, Lalouel J. M, and White R. L, Construction of Human Genetic Linkage Maps: Likelihood Calculations for Multilocus Analysis. Genetic Epidemiology, **3**(1986): p. 39-52.1986.

323. Lathrop G. M, et al., Strategies for multilocus linkage analysis in humans. Proc Natl Acad Sci U S A., **81**(11): p. 3443-6.1984.

324. Schaffer A. A, et al., Avoiding Recomputation in Genetic Linkage Analysis. Hum Hered., **44**(4): p. 225-37.1994.

325. Sobel E and Lange K, Descent graphs in pedigree analysis: applications to haplotyping, location scores, and marker-sharing statistics. Am J Hum Genet., **58**(6): p. 1323-37.1996.

326. Cann H. M, et al., A human genome diversity cell line panel. Science, **296**(5566): p. 261-2.2002.

327. Bernheimer H, et al., Brain dopamine and the syndromes of Parkinson and Huntington. Clinical, morphological and neurochemical correlations. J Neurol Sci, **20**(4): p. 415-55.1973.

328. Paisan-Ruiz C, et al., Familial Parkinson's disease: clinical and genetic analysis of four Basque families. Ann Neurol, **57**(3): p. 365-72.2005.

329. Funayama M, et al., An LRRK2 mutation as a cause for the parkinsonism in the original PARK8 family. Ann Neurol, **57**(6): p. 918-21.2005.

330. Zimprich A, et al., Mutations in LRRK2 cause autosomal-dominant parkinsonism with pleomorphic pathology. Neuron, **44**(4): p. 601-7.2004.

331. Zabetian C. P, et al., A clinic-based study of the LRRK2 gene in Parkinson disease yields new mutations. Neurology, **65**(5): p. 741-4.2005.

332. Brice, A., Genetics of Parkinson's disease: LRRK2 on the rise. Brain, **128**(Pt 12): p. 2760-2.2005.

333. Toft M, et al., LRRK2 mutations and Parkinsonism. Lancet, **365**(9466): p. 1229-30.2005.

334. Gilks, W.P., et al., A common LRRK2 mutation in idiopathic Parkinson's disease. Lancet, **365**(9457): p. 415-6.2005.

335. Ozelius, L.J., et al., LRRK2 G2019S as a cause of Parkinson's disease in Ashkenazi Jews. N Engl J Med, **354**(4): p. 424-5.2006.

336. Bialecka M, et al., Analysis of LRRK2 G2019S and I2020T mutations in Parkinson's disease. Neurosci Lett.2005.

337. Nichols W. C, et al., Genetic screening for a single common LRRK2 mutation in familial Parkinson's disease. Lancet, **365**(9457): p. 410-2.2005.

338. Bras J. M, et al., G2019S dardarin substitution is a common cause of Parkinson's disease in a Portuguese cohort. Movement Disorders, **in press**.2005.

339. Lesage S, et al., LRRK2 Haplotype Analyses in European and North African Families with Parkinson Disease: A Common Founder for the G2019S Mutation Dating from the 13th Century. Am J Hum Genet, **77**(2): p. 330-2.2005.

340. Aasly J. O, et al., Clinical features of LRRK2-associated Parkinson's disease in central Norway. Ann Neurol, **57**(5): p. 762-5.2005.

341. Gosal D, R.O., Wiley J, Irvine GB, Johnston JA, Toft M, Mata IF, Kachergus J, Hulihan M, Taylor JP, Lincoln SJ, Farrer MJ, Lynch T, Mark Gibson J., Clinical traits of LRRK2-associated Parkinson's disease in Ireland: A link between familial and idiopathic PD. Parkinsonism Relat Disord.2005.

342. Di Fonzo A, et al., A frequent LRRK2 gene mutation associated with autosomal dominant Parkinson's disease. Lancet, **365**(9457): p. 412-5.2005.

343. Kachergus J, et al., Identification of a Novel LRRK2 Mutation Linked to Autosomal Dominant Parkinsonism: Evidence of a Common Founder across European Populations. Am J Hum Genet, **76**(4): p. 672-80.2005.

344. Hernandez D, et al., The dardarin G2019S mutation is a common cause of Parkinson's disease but not other neurodegenerative diseases. Neurosci Lett.;.2005.

345. Cookson, M.R., G. Xiromerisiou, and A. Singleton, How genetics research in Parkinson's disease is enhancing understanding of the common idiopathic forms of the disease. Curr Opin Neurol, **18**(6): p. 706-11.2005.

346. Kay D. M, et al., Escaping Parkinson's disease: A neurologically healthy octogenarian with the LRRK2 G2019S mutation. Mov Disord, **20**(8): p. 1077-1078.2005.

347. Funayama M, et al., A new locus for Parkinson's disease (PARK8) maps to chromosome 12p11.2-q13.1. Ann Neurol, **51**(3): p. 296-301.2002.

348. Singleton, A.B., Altered alpha-synuclein homeostasis causing Parkinson's disease: the potential roles of dardarin. Trends Neurosci, **28**(8): p. 416-21.2005.

349. Botstein, D. and N. Risch, Discovering genotypes underlying human phenotypes: past successes for mendelian disease, future approaches for complex disease. Nat Genet, **33 Suppl**: p. 228-37.2003.

350. Cardon, L.R. and L.J. Palmer, Population stratification and spurious allelic association. Lancet, **361**(9357): p. 598-604.2003.

351. Tan, E.K., et al., Variability and validity of polymorphism association studies in Parkinson's disease. Neurology, **55**(4): p. 533-8.2000.

352. Riess, O., R. Kruger, and J.B. Schulz, Spectrum of phenotypes and genotypes in Parkinson's disease. J Neurol, **249 Suppl 3**: p. III/15-20.2002.

353. Storey, J.D. and R. Tibshirani, Statistical significance for genomewide studies. Proc Natl Acad Sci U S A, **100**(16): p. 9440-5.2003.

354. Carlson, C.S., et al., Mapping complex disease loci in whole-genome association studies. Nature, **429**(6990): p. 446-52.2004.

355. Maniatis, N., et al., Positional cloning by linkage disequilibrium. Am J Hum Genet, **74**(5): p. 846-55.2004.

356. Maniatis, N., et al., The optimal measure of linkage disequilibrium reduces error in association mapping of affection status. Hum Mol Genet, **14**(1): p. 145-53.2005.

357. Altmuller, J., et al., Genomewide scans of complex human diseases: true linkage is hard to find. Am J Hum Genet, **69**(5): p. 936-50.2001.

358. Kruger, R., et al., Increased susceptibility to sporadic Parkinson's disease by a certain combined alpha-synuclein/apolipoprotein E genotype. Ann Neurol, **45**(5): p. 611-7.1999.

359. Farrer M, et al., alpha-Synuclein gene haplotypes are associated with Parkinson's disease. Hum Mol Genet, **10**(17): p. 1847-51.2001.

360. Tan E. K, et al., Alpha synuclein promoter and risk of Parkinson's disease: microsatellite and allelic size variability. Neurosci Lett, **336**(1): p. 70-2.2003.

361. Tan E. K, et al., Alpha-synuclein haplotypes implicated in risk of Parkinson's disease. Neurology, **62**(1): p. 128-31.2004.

362. Mizuta, I., et al., Meta-analysis of alpha synuclein/ NACP polymorphism in Parkinson's disease in Japan. J Neurol Neurosurg Psychiatry, **73**(3): p. 350.2002.

363. Maraganore, D.M., et al., Collaborative analysis of alpha-synuclein gene promoter variability and Parkinson disease. Jama, **296**(6): p. 661-70.2006.

364. Hutton, M., et al., Association of missense and 5'-splice-site mutations in tau with the inherited dementia FTDP-17. Nature, **393**(6686): p. 702-5.1998.

365. Rademakers, R., M. Cruts, and C. van Broeckhoven, The role of tau (MAPT) in frontotemporal dementia and related tauopathies. Hum Mutat, **24**(4): p. 277-95.2004.

366. Hutton, M., Molecular genetics of chromosome 17 tauopathies. Ann N Y Acad Sci, **920**: p. 63-73.2000.

367. Conrad, C., et al., Genetic evidence for the involvement of tau in progressive supranuclear palsy. Ann Neurol, **41**(2): p. 277-81.1997.

368. Bennett, P., et al., Direct genetic evidence for involvement of tau in progressive supranuclear palsy. European Study Group on Atypical Parkinsonism Consortium. Neurology, **51**(4): p. 982-5.1998.

369. Houlden, H., et al., Corticobasal degeneration and progressive supranuclear palsy share a common tau haplotype. Neurology, **56**(12): p. 1702-6.2001.

370. Hughes, A.J., et al., The accuracy of diagnosis of parkinsonian syndromes in a specialist movement disorder service. Brain, **125**(Pt 4): p. 861-70.2002.

371. van de Warrenburg, B.P., et al., Clinical and pathologic abnormalities in a family with parkinsonism and parkin gene mutations. Neurology, **56**(4): p. 555-7.2001.

372. Farrall, M. and A.P. Morris, Gearing up for genome-wide gene-association studies. Hum Mol Genet, **14 Spec No. 2**: p. R157-62.2005.

373. Khan, N.L., et al., Parkin disease in a Brazilian kindred: Manifesting heterozygotes and clinical follow-up over 10 years. Mov Disord, **20**(4): p. 479-84.2005.

374. Djarmati, A., et al., Heterozygous PINK1 mutations: a susceptibility factor for Parkinson disease? Mov Disord, **21**(9): p. 1526-30.2006.

375. Abou-Sleiman, P.M., et al., A heterozygous effect for PINK1 mutations in Parkinson's disease? Ann Neurol, **60**(4): p. 414-9.2006.

376. Khan, N.L., et al., Dopaminergic dysfunction in unrelated, asymptomatic carriers of a single parkin mutation. Neurology, **64**(1): p. 134-6.2005.

377. Khan, N.L., et al., Clinical and subclinical dopaminergic dysfunction in PARK6-linked parkinsonism: an 18F-dopa PET study. Ann. Neurol., **52**(6): p. 849-53.2002.

378. Hu, M.T., et al., Nigral degeneration and striatal dopaminergic dysfunction in idiopathic and Parkin-linked Parkinson's disease. Mov Disord, **21**(3): p. 299-305.2006.

379. Oliveira, S.A., et al., Association study of Parkin gene polymorphisms with idiopathic Parkinson disease. Arch. Neurol., **60**(7): p. 975-80.2003.

380. Satoh J and Kuroda Y, Association of codon 167 Ser/Asn heterozygosity in the parkin gene with sporadic Parkinson's disease. Neuroreport, **10**(13): p. 2735-9.1999.

381. Lucking C. B, et al., Coding polymorphisms in the parkin gene and susceptibility to Parkinson disease. Arch Neurol., **60**(9): p. 1253-6.2003.

382. Lewontin, R.C., The Interaction of Selection and Linkage. Ii. Optimum Models. Genetics, **50**: p. 757-82.1964.

383. Pritchard, J.K. and M. Przeworski, Linkage disequilibrium in humans: models and data. Am J Hum Genet, **69**(1): p. 1-14.2001.

384. Weale M. E, et al., Selection and evaluation of tagging SNPs in the neuronal-sodium-channel gene SCN1A: implications for linkage-disequilibrium gene mapping. Am J Hum Genet, **73**(3): p. 551-65.2003.

385. Zhao J. H, et al., GENECOUNTING: haplotype analysis with missing genotypes. Bioinformatics, **18**(12): p. 1694-5.2002.

386. Paisan-Ruiz C, et al., LRRK2 gene in Parkinson disease: mutation analysis and case control association study. Neurology, **65**(5): p. 696-700.2005.

387. Paisan-Ruiz, C., et al., Testing association between LRRK2 and Parkinson's disease and investigating linkage disequilibrium. J Med Genet, **43**(2): p. e9.2006.

388. Biskup, S., et al., Common variants of LRRK2 are not associated with sporadic Parkinson's disease. Ann Neurol, **58**(6): p. 905-8.2005.

389. Skipper, L., et al., Comprehensive evaluation of common genetic variation within LRRK2 reveals evidence for association with sporadic Parkinson's disease. Hum Mol Genet, **14**(23): p. 3549-56.2005.

390. Aharon-Peretz, J., H. Rosenbaum, and R. Gershoni-Baruch, Mutations in the glucocerebrosidase gene and Parkinson's disease in Ashkenazi Jews. New Eng. J. Med, **351**(19): p. 1972-1977.2004.

391. Tan, E.K., et al., The LRRK2 Gly2385Arg variant is associated with Parkinson's disease: genetic and functional evidence. Hum Genet.2006.

392. Fung, H.C., et al., A common genetic factor for Parkinson disease in ethnic Chinese population in Taiwan. BMC Neurol, **6**(1): p. 47.2006.

393. Di Fonzo, A., et al., A common missense variant in the LRRK2 gene, Gly2385Arg, associated with Parkinson's disease risk in Taiwan. Neurogenetics, **7**(3): p. 133-8.2006.

394. Tan, E.K., et al., LRRK2 G2019S founder haplotype in the Chinese population. Mov Disord.2006.

395. Mahley, R.W., K.H. Weisgraber, and Y. Huang, Apolipoprotein E4: a causative factor and therapeutic target in neuropathology, including Alzheimer's disease. Proc Natl Acad Sci U S A, **103**(15): p. 5644-51.2006.

396. Manning, G., et al., The protein kinase complement of the human genome. Science, **298**(5600): p. 1912-34.2002.

397. Paisan-Ruiz, C., et al., Cloning of the gene containing mutations that cause PARK8-linked Parkinson's disease. Neuron, **44**(4): p. 595-600.2004.

398. Zimprich, A., et al., Mutations in LRRK2 cause autosomal-dominant parkinsonism with pleomorphic pathology. Neuron, **44**(4): p. 601-7.2004.

399. Bosgraaf, L. and P.J. Van Haastert, Roc, a Ras/GTPase domain in complex proteins. Biochim Biophys Acta, **1643**(1-3): p. 5-10.2003.

400. Marin, I., The Parkinson Disease gene LRRK2: Evolutionary and structural insights. Mol Biol Evol, **23**(12): p. 2423-33.2006.

401. Andrade, M.A., et al., Comparison of ARM and HEAT protein repeats. J Mol Biol, **309**(1): p. 1-18.2001.

402. Chen, S., et al., Interaction of Gbetagamma with RACK1 and other WD40 repeat proteins. J Mol Cell Cardiol, **37**(2): p. 399-406.2004.

403. Korr, D., et al., LRRK1 protein kinase activity is stimulated upon binding of GTP to its Roc domain. Cell Signal, **18**(6): p. 910-20.2006.

404. Kobe, B. and J. Deisenhofer, The leucine-rich repeat: a versatile binding motif. Trends Biochem Sci, **19**(10): p. 415-21.1994.

405. Cohen, O., E. Feinstein, and A. Kimchi, DAP-kinase is a Ca2+/calmodulin-dependent, cytoskeletal-associated protein kinase, with cell death-inducing

functions that depend on its catalytic activity. Embo J, **16**(5): p. 998-1008.1997.

406. Bosgraaf, L., et al., A novel cGMP signalling pathway mediating myosin phosphorylation and chemotaxis in Dictyostelium. Embo J, **21**(17): p. 4560-70.2002.

407. Abysalh, J.C., L.L. Kuchnicki, and D.A. Larochelle, The identification of pats1, a novel gene locus required for cytokinesis in Dictyostelium discoideum. Mol Biol Cell, **14**(1): p. 14-25.2003.

408. Brice A, How much does dardarin contribute to Parkinson's disease? Lancet, **365**(9457): p. 363-4.2005.

409. Greggio, E., et al., Kinase activity is required for the toxic effects of mutant LRRK2/dardarin. Neurobiol Dis, **23**(2): p. 329-41.2006.

410. Emanuelsson, O. and G. von Heijne, Prediction of organellar targeting signals. Biochim Biophys Acta, **1541**(1-2): p. 114-9.2001.

411. West A B, et al., Parkinson's disease-associated mutations in leucine-rich repeat kinase 2 augment kinase activity. Proc Natl Acad Sci U S A., **102**(46): p. 16842-7.2005.

412. Smith WW, et al., Leucine-rich repeat kinase 2 (LRRK2) interacts with parkin, and mutant LRRK2 induces neuronal degeneration. Proc Natl Acad Sci U S A, **102**(51): p. 18676-81.2005.

413. Biskup, S., et al., Localization of LRRK2 to membranous and vesicular structures in mammalian brain. Ann Neurol, **60**(5): p. 557-569.2006.

414. Gloeckner CJ, et al., The Parkinson disease causing LRRK2 mutation I2020T is associated with increased kinase activity. Hum Mol Genet, **15**(2): p. 223-32.2006.

415. Macleod, D., et al., The Familial Parkinsonism Gene LRRK2 Regulates Neurite Process Morphology. Neuron, **52**(4): p. 587-93.2006.

416. Smith, W.W., et al., Kinase activity of mutant LRRK2 mediates neuronal toxicity. Nat Neurosci, **9**(10): p. 1231-3.2006.

417. Dachsel, J.C., et al., Digenic parkinsonism: Investigation of the synergistic effects of PRKN and LRRK2. Neurosci Lett, **410**(2): p. 80-4.2006.

418. Mata, I.F., et al., LRRK2 in Parkinson's disease: protein domains and functional insights. Trends Neurosci, **29**(5): p. 286-93.2006.

419. Leung, I.W. and N. Lassam, The kinase activation loop is the key to mixed lineage kinase-3 activation via both autophosphorylation and hematopoietic progenitor kinase 1 phosphorylation. J Biol Chem, **276**(3): p. 1961-7.2001.

420. Uversky, V.N., A protein-chameleon: conformational plasticity of alpha-synuclein, a disordered protein involved in neurodegenerative disorders. J. Biomol. Struct. Dyn., **21**(2): p. 211-34.2003.

421. Uversky, V.N., et al., Accelerated alpha-synuclein fibrillation in crowded milieu. FEBS Lett., **515**(1-3): p. 99-103.2002.

422. Caughey, B. and P.T. Lansbury, Protofibrils, pores, fibrils, and neurodegeneration: separating the responsible protein aggregates from the innocent bystanders. Annu Rev Neurosci, **26**: p. 267-98.2003.

423. Krause, F., Detection and analysis of protein-protein interactions in organellar and prokaryotic proteomes by native gel electrophoresis: (Membrane) protein complexes and supercomplexes. Electrophoresis, **27**(13): p. 2759-81.2006.

424. Mogridge, J., Using light scattering to determine the stoichiometry of protein complexes. Methods Mol Biol, **261**: p. 113-8.2004.

425. Ye, H., Simultaneous determination of protein aggregation, degradation, and absolute molecular weight by size exclusion chromatography-multiangle laser light scattering. Anal Biochem, **356**(1): p. 76-85.2006.

426. Giasson, B.I., et al., Biochemical and pathological characterization of Lrrk2. Ann Neurol, **59**(2): p. 315-22.2006.

427. Miklossy, J., et al., LRRK2 expression in normal and pathologic human brain and in human cell lines. J Neuropathol Exp Neurol, **65**(10): p. 953-63.2006.

428. Zhu, X., et al., LRRK2 protein is a component of lewy bodies. Ann Neurol.2006.

429. Giasson BI, et al., Biochemical and pathological characterization of Lrrk2. Ann Neurol, **59**(2): p. 315-322.2006.

430. Andrade, M.A., C. Perez-Iratxeta, and C.P. Ponting, Protein repeats: structures, functions, and evolution. J Struct Biol, **134**(2-3): p. 117-31.2001.

431. Kobe, B. and A.V. Kajava, The leucine-rich repeat as a protein recognition motif. Curr Opin Struct Biol, **11**(6): p. 725-32.2001.

432. Enkhbayar, P., et al., Structural principles of leucine-rich repeat (LRR) proteins. Proteins, **54**(3): p. 394-403.2004.

433. Pfeffer, S. and D. Aivazian, Targeting Rab GTPases to distinct membrane compartments. Nat Rev Mol Cell Biol, **5**(11): p. 886-96.2004.

434. Pfeffer, S.R., Structural clues to Rab GTPase functional diversity. J Biol Chem, **280**(16): p. 15485-8.2005.

435. Grosshans, B.L., D. Ortiz, and P. Novick, Rabs and their effectors: achieving specificity in membrane traffic. Proc Natl Acad Sci U S A, **103**(32): p. 11821-7.2006.

436. Gaestel, M., MAPKAP kinases - MKs - two's company, three's a crowd. Nat Rev Mol Cell Biol, **7**(2): p. 120-30.2006.

437. Rybakin, V. and C.S. Clemen, Coronin proteins as multifunctional regulators of the cytoskeleton and membrane trafficking. Bioessays, **27**(6): p. 625-32.2005.

438. Li, D. and R. Roberts, WD-repeat proteins: structure characteristics, biological function, and their involvement in human diseases. Cell Mol Life Sci, **58**(14): p. 2085-97.2001.

439. Fields, S. and O. Song, A novel genetic system to detect protein-protein interactions. Nature, **340**(6230): p. 245-6.1989.

440. Chow, N., et al., APP-BP1, a novel protein that binds to the carboxyl-terminal region of the amyloid precursor protein. J Biol Chem, **271**(19): p. 11339-46.1996.

441. Phiel, C.J., et al., GSK-3alpha regulates production of Alzheimer's disease amyloid-beta peptides. Nature, **423**(6938): p. 435-9.2003.

442. Takashima, A., GSK-3 is essential in the pathogenesis of Alzheimer's disease. J Alzheimers Dis, **9**(3 Suppl): p. 309-17.2006.

443. Dev, K.K., et al., Part I: parkin-associated proteins and Parkinson's disease. Neuropharmacology, **45**(1): p. 1-13.2003.

444. Dawson, T.M. and V.L. Dawson, Molecular pathways of neurodegeneration in Parkinson's disease. Science, **302**(5646): p. 819-22.2003.

445. Giasson, B.I., V.M. Lee, and J.Q. Trojanowski, Interactions of amyloidogenic proteins. Neuromolecular Med, **4**(1-2): p. 49-58.2003.

446. Giasson, B.I. and V.M. Lee, Are ubiquitination pathways central to Parkinson's disease? Cell, **114**(1): p. 1-8.2003.

447. Golemis, E., Toward an Understanding of Protein Interactrions. In Protein-Protein Interactions-A molecular Cloning Manual, ed. Golemis E. Vol. pp1-5. 2002: Cold Spring Harbor Laboratory Press.

448. Phizicky, E.M. and S. Fields, Protein-protein interactions: methods for detection and analysis. Microbiol Rev, **59**(1): p. 94-123.1995.

449. Fujita, T., et al., Identification of a tissue-non-specific homologue of axonal fasciculation and elongation protein zeta-1. Biochem Biophys Res Commun, **313**(3): p. 738-44.2004.

450. Assmann, E.M., et al., FEZ1 dimerization and interaction with transcription regulatory proteins involves its coiled-coil region. J Biol Chem, **281**(15): p. 9869-81.2006.

451. Muqit, M.M., et al., Altered cleavage and localization of PINK1 to aggresomes in the presence of proteasomal stress. J Neurochem, **98**(1): p. 156-69.2006.

452. Kuroda, S., et al., Mammalian homologue of the Caenorhabditis elegans UNC-76 protein involved in axonal outgrowth is a protein kinase C zeta-interacting protein. J Cell Biol, **144**(3): p. 403-11.1999.

453. Wooten, M.W., et al., Transport of protein kinase C isoforms to the nucleus of PC12 cells by nerve growth factor: association of atypical zeta-PKC with the nuclear matrix. J Neurosci Res, **49**(4): p. 393-403.1997.

454. Gindhart, J.G., et al., The kinesin-associated protein UNC-76 is required for axonal transport in the Drosophila nervous system. Mol Biol Cell, **14**(8): p. 3356-65.2003.

455. Su, C.W., et al., The short coiled-coil domain-containing protein UNC-69 cooperates with UNC-76 to regulate axonal outgrowth and normal presynaptic organization in Caenorhabditis elegans. J Biol, **5**(4): p. 9.2006.

456. Bourne, H.R., D.A. Sanders, and F. McCormick, The GTPase superfamily: conserved structure and molecular mechanism. Nature, **349**(6305): p. 117-27.1991.

457. Mittal, R., et al., Formation of a transition-state analog of the Ras GTPase reaction by Ras-GDP, tetrafluoroaluminate, and GTPase-activating proteins. Science, **273**(5271): p. 115-7.1996.

458. Heo, W.D. and T. Meyer, Switch-of-function mutants based on morphology classification of Ras superfamily small GTPases. Cell, **113**(3): p. 315-28.2003.

459. Fallon, L., et al., A regulated interaction with the UIM protein Eps15 implicates parkin in EGF receptor trafficking and PI(3)K-Akt signalling. Nat Cell Biol, **8**(8): p. 834-42.2006.

460. Okumura, F., et al., Functional regulation of FEZ1 by the U-box-type ubiquitin ligase E4B contributes to neuritogenesis. J Biol Chem, **279**(51): p. 53533-43.2004.

MANUSCRIPTS PUBLISHED DURING THESIS

Healy, D.G., Abou-Sleiman, P.M., Gibson, J.M., Ross, O.A., **Jain, S.**, Gandhi, S., Gosal, D., Muqit, M.M., Wood, N.W. and Lynch, T. (2004a) PINK1 (PARK6) associated Parkinson disease in Ireland. Neurology, 63, 1486-1488.

Healy, D.G., Abou-Sleiman, P.M., **Jain, S.**, Ahmadi, K.R. and Wood, N.W. (2004b) Assessment of a DJ-1 (PARK7) polymorphism in Finnish PD. Neurology, 62, 2335.

Paisan-Ruiz, C., **Jain, S.**, Evans, E.W., Gilks, W.P., Simon, J., van der Brug, M., Lopez de Munain, A., Aparicio, S., Gil, A.M., Khan, N., Johnson, J., Martinez, J.R., Nicholl, D., Carrera, I.M., Pena, A.S., de Silva, R., Lees, A., Marti-Masso, J.F., Perez-Tur, J., Wood, N.W. and Singleton, A.B. (2004) Cloning of the gene containing mutations that cause PARK8-linked Parkinson's disease. Neuron, 44, 595-600.***CO-FIRST AUTHORS**

Gilks, W.P., Abou-Sleiman, P.M., Gandhi, S., **Jain, S.**, Singleton, A., Lees, A.J., Shaw, K., Bhatia, K.P., Bonifati, V., Quinn, N.P., Lynch, J., Healy, D.G., Holton, J.L., Revesz, T. and Wood, N.W. (2005) A common LRRK2 mutation in idiopathic Parkinson's disease. Lancet, 365, 415-416.

Hernandez, D.G., Paisan-Ruiz, C., McInerney-Leo, A., **Jain, S.**, Meyer-Lindenberg, A., Evans, E.W., Berman, K.F., Johnson, J., Auburger, G., Schaffer, A.A., Lopez, G.J., Nussbaum, R.L. and Singleton, A.B. (2005) Clinical and positron emission tomography of Parkinson's disease caused by LRRK2. Ann Neurol, 57, 453-456.

Jain, S., Wood, N.W. and Healy, D.G. (2005) Molecular genetic pathways in Parkinson's disease: a review. Clin Sci (Lond), 109, 355-364.

Khan, N.L., **Jain, S.**, Lynch, J.M., Pavese, N., Abou-Sleiman, P., Holton, J.L., Healy, D.G., Gilks, W.P., Sweeney, M.G., Ganguly, M., Gibbons, V., Gandhi, S., Vaughan, J., Eunson, L.H., Katzenschlager, R., Gayton, J., Lennox, G., Revesz, T., Nicholl, D., Bhatia, K.P., Quinn, N., Brooks, D., Lees, A.J., Davis, M.B., Piccini, P., Singleton, A.B. and Wood, N.W. (2005) Mutations in the gene LRRK2 encoding LRRK2 (PARK8) cause familial Parkinson's disease: clinical, pathological, olfactory and functional imaging and genetic data. Brain, 128, 2786-2796.

Nichols, W.C., Pankratz, N., Hernandez, D., Paisan-Ruiz, C., **Jain, S.**, Halter, C.A., Michaels, V.E., Reed, T., Rudolph, A., Shults, C.W., Singleton, A. and Foroud, T. (2005) Genetic screening for a single common LRRK2 mutation in familial Parkinson's disease. Lancet, 365, 410-412

Greggio, E., **Jain, S.**, Kingsbury, A., Bandopadhyay, R., Lewis, P., Kaganovich, A., van der Brug, M.P., Beilina, A., Blackinton, J., Thomas, K.J., Ahmad, R., Miller, D.W., Kesavapany, S., Singleton, A., Lees, A., Harvey, R.J., Harvey, K. and Cookson, M.R. (2006) Kinase activity is required for the toxic effects of mutant LRRK2/LRRK2. Neurobiol Dis.***CO-FIRST AUTHORS**

Paisan-Ruiz, C., Evans, E.W., **Jain, S.**, Xiromerisiou, G., Gibbs, J.R., Eerola, J., Gourbali, V., Hellstrom, O., Duckworth, J., Papadimitriou, A., Tienari, P.J., Hadjigeorgiou, G.M. and Singleton, A.B. (2006) Testing association between LRRK2

and Parkinson's disease and investigating linkage disequilibrium. J Med Genet, 43, e9.

Jain, S and Singleton, AB (2006). Genomics and Medicine: Parkinson's Disease: Current Hopes and Perspectives. Elsevier Publishing (In Press).

Momeni P., Schymick JC., **Jain S.**, Cookson MR., Cairns NJ., Greggio E., Greenway MJ., Berger S., Pickering-Brown S., Chio A., Fung HC., Holtzman DM., Huey ED., Wassermann EM., Adamson J., Hutton ML., Rogaeva E., St George-Hyslop P., Rothstein JD., Hardiman O., Grafman J., Singleton A., Hardy J., Traynor BJ. (2006) Analysis of IFT74 as a candidate gene for chromosome 9p-linked ALS-FTD. BMC Neurol. Dec **13**; 6(1):44